

https://dspace.org/

The impact of binge alcohol consumption on the developing humerus of adolescent Sprague Dawley rats

Rakgoathe, Rethabile

2025
University of the Witwatersrand, Johannesburg
https://hdl.handle.net/10539/49869

Rakgoathe, Rethabile. (2025). The impact of binge alcohol consumption on the developing humerus of adolescent Sprague Dawley rats [Master's dissertation, University of the Witwatersrand, Johannesburg]. WIReDSpace. https://hdl.handle.net/10539/49869

Downloaded from a DSpace repository. https://dspace.org/

The impact of binge alcohol consumption on the developing humerus of adolescent Sprague Dawley rats

Student name: Rethabile Rakgoathe

Student number: 2091064

Registered degree: Master of Science in Medicine

Faculty of Health Sciences, University of Witwatersrand, Johannesburg

Supervisor 1:

Dr Akaashni Bhika (BChD)

Lecturer (Morphological Anatomy)

School of Anatomical Sciences

Medical School

7 York Road Parktown

Faculty of Health Sciences

Tel: +27 11 717 2136

Email: akaashni.bhika@wits.ac.za

Supervisor 2:

Dr Illke Malungo (PhD)

Lecturer (Morphological Anatomy)

School of Anatomical Sciences

Medical School

7 York Road Parktown

Faculty of Health Sciences

Tel: +27 11 717 2104

Email: illke.malungo@wits.ac.za

UNIVERSITY OF THE WITWATERSRAND, JOHANNESBURG

FACULTY OF HEALTH SCIENCES

100 YEARS OF TEACHING EXCELLENCE

Anatomical Sciences

A Dissertation submitted to the Faculty of Health Sciences, University of the Witwatersrand, Johannesburg, in fulfilment of the requirements for the degree of Master of Science in Medicine.

Declaration

I, Rethabile Rakgoathe, declare that this Dissertation is my own, unaided work. It is being submitted for the Degree of Master of Science in Medicine at the University of the Witwatersrand, Johannesburg. It has not been submitted before for any degree or examination at any other University.



(Signature of candidate)

13 October 2025 in Parktown

Abstract:

Binge drinking is the ingestion of alcohol in high volumes during a short period, raising blood alcohol concentration to ≥80 mg/dL. It is common among adolescents, which is concerning since this is a critical period for skeletal growth and development, processes that binge drinking may impair. Moreover, the question of whether alcohol abstinence can reverse any damage inflicted by binge drinking is also contemplated. Therefore, this study investigated how binge drinking affects bone structure, strength, and development in the adolescent humerus and whether these effects can be reversed through alcohol abstinence. The study included 48 adolescent Sprague Dawley rats (24 males and 24 females) aged 7 weeks (49 postnatal days) as the age corresponds to 14.5 human years which represents the human adolescent period (ages 10-19). They were divided into two major groups where Group 1 was the chronic binge consumption model, (four-week alcohol exposure) and Group 2 was the binge alcohol recovery model (four-week alcohol exposure followed by a 26-day abstinent period). Each group had an alcohol-exposed (A) and control (B) group resulting in a total of four groups (1A,1B,2A,2B) where each of the four groups consisted of n =12 rats (6 males and 6 females). A 20% (vol/vol) alcohol solution at a dose of 3g/kg was administered to the study animals, as a single dose via oral gavage. An isocaloric equivalent of maltose dextrin, via oral gavage, was given to the control animals. Alcohol/maltose dextrin was administered 3 days/week (on every alternative day) and no further administration was done during the remaining 4 days of the week. Humeral osteometry was performed and humeral weights were recorded to investigate the impact of binge drinking on the external structure. Following this, we used 3D micro-focus X-ray tomography (3D-μCT) allowing for detailed examination of humeral morphometry. To assess humeral strength, we performed a three-point bending test. Finally, we evaluated humeral development using Haematoxylin and Eosin (H&E) staining and immunohistochemistry (IHC). H&E staining facilitated a qualitative assessment of growth plate chondrocytes (cartilage cells) and IHC provided a quantitative measure of chondrocyte proliferation, using the anti-Ki-67 antibody. Statistical analysis included normality tests (such as the Shapiro Wilk test), T-tests and the Mann Whitney test (for non-parametric data). In the chronic binge consumption model, four weeks of alcohol exposure caused reduced humeral weight in females. In the binge alcohol recovery model, trabecular number (Tb.N), spacing (Tb.Sp), and fracture times remained significantly affected. Overall, the findings indicate that four weeks of binge alcohol exposure did not cause severe structural damage to the humeri in either sex, as most parameters showed minimal or no change across both models. The results of the binge alcohol recovery model suggest that recovery may be possible and that male humeri respond

better to alcohol exposure than female humeri. However, significant alterations in select measures, such as reduced humeral weights in females (Group 1); delayed fracture times in females (Group 2) and changes in trabecular architecture in males (Group 2), suggest that alcohol exposure, while not overtly damaging, did exert measurable adverse effects. The research also showcased evidence of site-specific heterogeneity as the proximal and distal regions of the humeri had a differential response to alcohol exposure. Lastly, the research underscored the influence of sexual dimorphism, as both male and female humeri exhibited distinct responses to alcohol exposure. The findings of this study are relevant in the clinical setting, indicating that binge drinking in adolescents has an impact on the developing skeleton, more so in males than in females, and can lead to growth and skeletal complications including an increase in fracture rates in this vulnerable population.

Acknowledgements

A heartfelt thanks to my supervisors, Dr. A. Bhika and Dr. I. Malungo for the support, guidance, and compassion they expressed throughout my research journey. The lessons they imparted, both academic and personal, will stay with me far beyond this project, shaping my future in ways I deeply cherish.

I am profoundly grateful to the School of Anatomical Sciences of the University of Witwatersrand for providing an excellent research environment along with the National Research Foundation (NRF) for their support through the NRF Thuthuka Fund, which made this research financially viable.

A special thank you to Mr. G. Chinamatira, from the Evolutionary Studies Institute (ESI) at the University of the Witwatersrand, for graciously allowing us access to the Nikon Metrology XTH 225 LC X-ray dual-source microtomography. His assistance in scanning and reconstructing the rat humeri for this study was invaluable. I also wish to thank Mr. B. Khoza and Mrs. T. Mulaudzi for their support in providing access to essential reagents and other inventory required for this research. A heartfelt thanks to Mrs. Ali, not only for granting access to reagents and inventory but for her kindness, support, wisdom, and compassion. Your presence was a source of strength, especially during the more challenging moments of this journey.

I would also like to thank Dr. Nura, Dr. Hassan, Ms. T. Mwila, Ms. Y. Peya, Mr. R. Mngoma, Ms. X. Mhlathi, Ms. M. Sahib, Ms. G. Govender, and Ms. T. Rathokane. Whether through academic advice, listening to my thoughts, or offering a helping hand in any way they could, they always went above and beyond. Each of them created a warm, welcoming environment that fostered both personal and academic growth. I deeply appreciate the kindness and camaraderie they shared with me throughout my research journey.

To my family and friends, I express my deepest gratitude to you for your unwavering support that means more than words can convey. You kept me strong through challenging times, and your prayers and encouragement were instrumental in helping me reach this milestone. I owe a special debt of gratitude to my parents, Mr Pule Rakgoathe and Mrs Malebo Rakgoathe. I consider myself incredibly fortunate, as unlike many students, I have been blessed with parents

who were able to fund my tertiary education, even in the absence of bursaries or scholarships. They have faced countless challenges, yet they continuously overcame adversity to ensure that my brother and I had the opportunity to pursue our dreams. Their emotional and financial sacrifices have been the foundation upon which I have built my success. May this acknowledgment serve as a small reflection of how much they mean to me. I am where I am today because of the love, sacrifices, and endless support they have given me. Thank you for everything.

Lastly to God be all the glory for everything! For his mercy and grace follows me all the days of my life. His strength pushed me to persevere till the end and this work is a testament of His power.

CONTENTS

Declaration	i
Abstract	ii
Acknowledgements	iv
Table of Contents	vi
List of abbreviations	ix
List of figures	xii
List of tables	xv

Chapter 1: Introduction, Literature review, Aims and Objectives

1.1 Introduction	2
1.2 Literature review	3
1.2.1. Binge drinking and alcohol use	3
1.2.2. Adolescence: Skeletal growth and development	5
1.2.3. Biomechanics	7
1.2.4. Alcohol and metabolism and the resting cellular impacts	10
1.2.5. Sexual dimorphism	15
1.2.6. Animal models in science and alcohol administration techniques	16
1.3 Aims and objectives	17
1.3.1. Aim	17
1.3.2. Objectives	17

Chapter 2: Methodology

2.1 Ethical Clearance	20
2.2 Study animals	20
2.3 Group allocation and administration	20
2.4 Skeletal Harvesting	22
2.5 Bone weight and osteometric measurements	22
2.6 Three-dimensional Micro-Focus X-ray Computed Tomography (3D-μCT)	23
2.7 Humeral osteometry and trabecular morphometry	23
2.8 Biomechanics: Three-point bending test	24
2.9 Tissue processing for histology and immunohistochemical techniques (IHC)	26

2.10 Photography and quantification of chondrocytes 27
2.11 Measurement Reliability 28
2.12 Data Analysis 28

Chapter 3: Results
3.1 Bone weight and osteometric measurements 32
3.1.1. Humeral weight 32
3.1.2 Maximum humeral length 33
3.1.3 Bicondylar breadth 35
3.2 Humeral osteometry and trabecular morphometry 37
3.2.1 Bone to total volume ratio (BV/TV) 37
3.2.2 Trabecular thickness (Tb.Th) 39
3.2.3 Trabecular Number (Tb.N) 41
3.2.4 Trabecular Spacing (Tb.Sp) 43
3.3 Biomechanics: Three-point bending test 46
3.3.1 Maximum force 46
3.3.2 Maximum displacement 47
3.3.3 Fracture time 49
3.3.4 Break force 50
3.4 Morphological assessment of the humeral epiphyseal growth plate through Haematoxylin and Eosin (H&E) staining 52
3.5 Quantitative assessment of the humeral epiphyseal growth plate chondrocytes through Immunohistochemistry (IHC) using the anti-Ki-67 antibody 57

Chapter 4: General discussion and conclusion
Discussion 66
Conclusion 77
References 78
Appendices
Appendix 1: Turnitin report and Similarity index letter 93
Appendix 2: Ethical clearance certificate 95
Appendix 3: Reagents used 97
Appendix 4: Equipment used 98

Appendix 5: Software used 98
Appendix 6: Calculation of the Alcohol (alcohol 20%) dosage administered 98
Appendix 7: Calculation of the Maltose dextrin (isocaloric) dosage administered 99
Appendix 8: Preparation of 10% Neutral Buffered Formalin (1000 ml) 99
Appendix 9: Measuring trabecular morphometry of humerus using VG studio software 100
Appendix 10: EDTA solution (14%) for bone decalcification 101
Appendix 11: Silane coated slides 101
Appendix 12: Tissue processing using the Thermo Scientific Citadel 2000 automatic tissue processor 102
Appendix 13: Silane coated slides 103
Appendix 14: Immunohistochemistry 106

NOMENCLATURE/LIST OF ABBREVIATIONS AND SYMBOLS

% :	percent
µa :	microampere
µm :	micrometre
3D -µCT :	three-dimensional micro-focus X-ray computed tomography
dl :	decilitre
g :	grams
kg :	kilogram
kV :	kilovolts
mg :	milligram
ml :	millilitre
mm :	millimetre
mm^{-1} :	per 1 millimetre unit
mm^2 :	area in millimetres
min:	minute
nm:	nanometres
N :	Newton
^{o} C :	degree Celsius
sec :	second
vol/vol :	volume per volume
w/v :	weight per volume
1A :	4-week alcohol-exposed rats
1B :	4-week pair-fed control rats
2A :	Binge-alcohol recovery rats
2B :	Binge-alcohol recovery pair-control rats
ADH :	Alcohol dehydrogenase
ALDH :	Acetaldehyde dehydrogenase
APES :	3-aminopropyltriexothysilan
AREC:	Animal Research Ethics Committee of the University of the Witwatersrand
BAC :	Blood alcohol concentration
BT/TV :	Bone volume to total volume
DAB :	3-3’ diaminobenzidine
DNA:	Deoxyribonucleic acid

EDTA :	Ethylenediamine tetra acetic acid
ESR1:	Oestrogen receptor 1
ESR2:	Oestrogen receptor 2
FGF23:	Fibroblast growth factor 23
Fig :	Figure
GH:	Growth hormone
GPER:	G protein-coupled oestrogen receptor
H&E :	Haematoxylin and Eosin
H2O2 :	Hydrogen peroxide
HDL :	High density lipoprotein
HIV:	Human immunodeficiency virus
HZ :	Hypertrophic zone
IBM:	International business machine corporation
IHC :	Immunohistochemistry
IHH:	Indian Hedgehog
IP:	Intraperitoneal
NIAAA :	National institute on alcohol abuse and alcoholism
PBS :	Phosphate buffer solution
PTH :	Parathyroid hormone
pH :	Potential of hydrogen
PTHrP:	Parathyroid related protein
PZ :	Proliferative zone
RANK	Receptor Activator of NF-κB
RANKL	Receptor Activator of NF-κB Ligand
ROI:	Region of interest
ROS:	Reactive oxidative species
RZ :	Resting zone
SACENDU:	South African Community Epidemiology Network on Drug Use
SD :	Standard deviation
SPSS :	Statistical package for social services
Tb.N :	Trabecular number
Tb.Th :	Trabecular thickness
Tb.Sp :	Trabecular Space

TGF-β:	Transforming growth factor
USA:	United States of America
VDR	Vitamin D receptor
VEGF	Vascular Endothelial Growth Factor
WHO:	World Health Organisation
WRAF :	University of the Witwatersrand research animal facility

List of figures:

Figure	Description	Page
Figure 2.1	Three-point bending test using the Shimadzu 3-point bending machine	25
Figure 2.2	An illustration of a load displacement curve showing the various parameters describing bone strength	26
Figure 3.1.1	Humeral weight of the chronic binge consumption model and the binge alcohol recovery model	33
Figure 3.1.2	Maximum humeral length of the chronic binge consumption model and the binge alcohol recovery model	35
Figure 3.1.3	Bicondylar breadth of the chronic binge consumption model and the binge alcohol recovery model	36
Figure 3.2.1	Humeral bone volume to total volume ratio (BV/TV) of the proximal and distal epiphyses for the chronic binge consumption model and binge alcohol recovery model	39
Figure 3.2.2	Humeral trabecular thickness of the proximal and distal epiphyses for the chronic binge consumption model and binge alcohol recovery model	41
Figure 3.2.3	Humeral trabecular number of the proximal and distal epiphyses for the chronic binge consumption model and binge alcohol recovery model	43
Figure 3.2.4	Humeral trabecular space of the proximal and distal epiphyses for the chronic binge consumption model and binge alcohol recovery model	45
Figure 3.3.1	Maximum force of the chronic binge consumption model and the binge alcohol recovery model	47
Figure 3.3.2	Maximum displacement of the chronic binge consumption model and the binge alcohol recovery model	48
Figure 3.3.3	Fracture time of the chronic binge consumption model and the binge alcohol recovery model	50

Figure 3.3.4	Break force of the chronic binge consumption model and the binge alcohol recovery model	51
Figure 3.4.1	Reference illustrations of the humeral proximal (A) and distal epiphysis (B) showing the growth plate chondrocyte zones in progressive order namely: the resting zone (RZ), proliferative zone (PZ) and hypertrophic zone (HZ).	52
Figure 3.4.2	Haematoxylin and Eosin-stained sections of the proximal and distal epiphyseal growth plates of the humeri for the pair-fed control and alcohol-exposed groups in female rats of the chronic binge consumption model.	53
Figure 3.4.3	Haematoxylin and Eosin-stained sections of the proximal and distal epiphyseal growth plates of the humeri for the pair-fed control and alcohol-exposed groups in male rats of the chronic binge consumption model.	54
Figure 3.4.4	Haematoxylin and Eosin-stained sections of the proximal and distal epiphyseal growth plates of the humeri for the pair-fed control and alcohol-exposed groups in female rats of the binge alcohol recovery model.	55
Figure 3.4.5	Haematoxylin and Eosin-stained sections of the proximal and distal epiphyseal growth plates of the humeri for the pair-fed control and alcohol-exposed groups in male rats of the binge alcohol recovery model.	56
Figure 3.5.1	Reference illustrations of the humeral proximal (A) and distal epiphysis (B) showing the active chondrocytes in the resting zone (RZ), proliferative zone (PZ) and hypertrophic zone (HZ).	57
Figure 3.5.2	Chondrocyte numbers of the proximal epiphysis (A) and distal epiphysis (B) of the chronic binge consumption model.	58
Figure 3.5.3	Immunolabeled humeral chondrocytes using the anti-Ki-67 antibody. Images are representative sections of the proximal and distal epiphyseal growth plates for the pair-fed control and alcohol-exposed groups in female rats of the chronic binge consumption model.	59

Figure 3.5.4	Figure 3.5.4: Immunolabeled humeral chondrocytes using the anti-Ki-67 antibody. Images are representative sections of the proximal and distal epiphyseal growth plates for the pair-fed control and alcohol-exposed groups in male rats of the chronic binge consumption model.	60
Figure 3.5.5	Chondrocyte numbers of the proximal epiphysis (A) and distal epiphysis (B) of the binge alcohol recovery model. The mean values for this parameter are represented for both pair-fed control and alcohol-exposed groups in male and female animals and the error bars represent the standard deviation. Significant differences are indicated by connecting brackets.	62
Figure 3.5.6	Immunolabeled humeral chondrocytes using the anti-Ki-67 antibody. Images are representative sections of the proximal and distal epiphyseal growth plates for the pair-fed control and alcohol-exposed groups in female rats of the binge alcohol recovery model.	63
Figure 3.5.7	Immunolabeled humeral chondrocytes using the anti-Ki-67 antibody. Images are representative sections of the proximal and distal epiphyseal growth plates for the pair-fed control and alcohol-exposed groups in male rats of the binge alcohol recovery model.	64

List of tables:

Table	Description	Page
Table 2.1	Group allocation and administration	21
Table 2.2	Animal groupings	22
Table 2.3	Humeral osteometric description	22
Table 2.4	Scanning parameters	23
Table 2.5	Trabecular morphometric parameter description	24
Table 2.6	Parameters derived from the load displacement curve	25

Chapter 1

Introduction, Literature review, Aim and Objectives

1.1 Introduction:

Excessive alcohol consumption is a prominent problem in public health worldwide and it is now regarded as one of the leading causes for morbidity and mortality (Park & Kim, 2020; Gebeyehu & Srahbzu Biresaw, 2021). Beyond the long-term health consequences, alcohol abuse also plays a significant role in various forms of immediate harm like interpersonal violence, gender-based violence, road accidents and death (Morojele & Ramsoomar, 2016; Fontes Marx, M. *et al.*, 2021). Fontes Marx *et al.* (2021) reported that in South Africa, 50% of men and 20% of women consume alcohol. From this cohort, approximately 48% of men and 32% of women are binge drinkers. Alcohol consumption among South African youth raises more concern as approximately 32% of South African adolescents are defined as binge drinkers (Morojele & Ramsoomar, 2016; Mmereki *et al.,* 2022).

Binge drinking is the ingestion of alcohol in high volumes during a short period and it is proposed to precede chronic drinking (Park & Kim, 2020). While binge drinking may not directly correlate with alcohol dependence, it is still a dangerous activity predominantly associated with adolescents (ages 10-19) (Park & Kim, 2020). Adolescent binge drinking is often influenced by a combination of socioeconomic and psychosocial factors, such as the household environment and peer dynamics during social gatherings (Fontes Marx et al., 2021). Furthermore, Bosque-Prous *et al.* (2017) reported that adolescent binge drinking often transpires alongside other problematic behaviours including academic related issues.

The prevalence of adolescent binge drinking is unsettling as adolescence encompasses crucial growth and development, especially in terms of the skeletal system. Attaining peak bone mass during adolescence is essential for developing the biomechanical properties of the skeleton, such as strength and rigidity (Weaver, 2002). Research indicates that alcohol consumption can negatively impact skeletal health, leading to the hypothesis that adolescent binge drinking may harm bone development. Consequently, any failure to attain peak bone mass due to binge drinking could predispose adolescents to serious health issues later in life, such as osteoporosis (Weaver, 2002). Furthermore, it raises the question of whether alcohol abstinence can reverse any damage inflicted by binge drinking (Wezeman *et al.,* 1999; Lauing *et al.,* 2008).

Considering the above, this study examined the impact of binge drinking on bone structure (both external and internal) as well as bone strength and development, specifically focusing on

the adolescent humerus. Additionally, it explored the potential for recovery of the humerus following a period of alcohol abstinence after binge drinking.

To investigate the impact of binge drinking on the external structure of the adolescent humerus, we conducted humeral osteometry, which involved taking precise measurements and recording humeral weights. Following this, we used 3D micro-focus X-ray tomography (3D-μCT) to analyse the internal structure of the adolescent humerus, allowing for detailed examination of humeral morphometry. To assess humeral strength, we performed a three-point bending test to identify potential biomechanical changes resulting from binge drinking. Additionally, we evaluated humeral development using Haematoxylin and Eosin (H&E) staining and immunohistochemistry (IHC). H&E staining facilitated a qualitative assessment of the growth plates, particularly focusing on growth plate chondrocytes (cartilage cells), whose presence is crucial for subsequent bone cell development. IHC provided a quantitative measure of chondrocyte proliferation, using the anti-Ki-67 antibody as a marker, since the presence of Ki-67 protein is indicative of cell proliferation.

1.2 Literature review:

1.2.1 Binge drinking and alcohol use

Binge drinking is the consumption of ≥5 standard beverages for men and ≥4 beverages for women in a single occasion leading to a blood alcohol concentration of ≥80mg/dL (Gowin *et al*., 2021). According to studies, binge drinking is most common among people aged 15 to 49, with the highest incidence of occurrence among adolescents (Park & Kim, 2020). Griswold *et al.* (2018) reported increased per capita alcohol consumption in Sub-Saharan Africa, while the World Health Organisation (WHO) similarly noted that heavy episodic drinking in the region remains high (≥60%) (World Health Organisation, 2018).

Adolescent binge drinking remains a significant concern in South Africa, with consistently high prevalence rates over time and growing implications for socioeconomic settings. A five-year study by SACENDU (1997–2001) identified alcohol as the second most abused substance among adolescents in major regions, with binge drinking being the most common pattern (Parry *et al.,* 2004). A 2011 national survey found that 25% of youth engaged in binge drinking, with reports of children as young as 11 participating (Reddy *et al.,* 2013). Subsequent research noted increasing rates in rural areas (Chauke *et al.,* 2015), and by 2018, prevalence levels were

comparable to those in western countries such as the USA (Letsela *et al.,* 2018). In the Gauteng province alone, 70% of high school learners in 2022 reported that they engage in binge drinking (Changes Addiction Rehab, 2022). These previous studies highlight the prevalence of adolescent binge drinking and therefore indicate urgent need for focused research on adolescent binge drinking in South Africa.

Direct advertising of alcohol across various media platforms plays a significant role in promoting binge drinking among adolescents (Grube, 2004; Wilcox *et al.,* 2012). Such advertising fosters a positive perception of alcohol among young people, enticing them to make purchases (Smith & Foxcroft, 2009; Stautz *et al.,* 2016). In countries like South Africa, where youth represent a substantial segment of the population, they become a lucrative target market for alcohol advertisers (Letsela *et al.,* 2018). Furthermore, alcohol consumption is often linked to social rites of passage and pop culture, which can amplify excessive drinking due to peer pressure (Grube, 2004).

Social venues such as restaurants, bars, and pubs significantly contribute to excessive drinking through promotions like "happy hour," during which alcohol is sold at discounted prices to boost sales (Xu and Chaloupka, 2011). These promotions lead to increased average alcohol consumption per customer over a short period, effectively fostering binge drinking (Xu and Chaloupka, 2011). Such environments promote binge drinking behaviour, and for individuals who primarily purchase alcohol during these promotional periods, this can result in repeated episodes of heavy drinking, which are detrimental to their physical health. Although these establishments are intended for adults, adolescents are often present and consuming alcohol, as many venues lack strict measures to verify the legal drinking age of their patrons (Mathibe *et al.,* 2022). In rural communities, restrictions on alcohol sales are often minimal, allowing young children to purchase and consume alcohol more easily (Mathibe *et al.,* 2022). This increased availability of alcohol is particularly concerning for adolescents. Letsela *et al.* (2018) noted that binge drinking is prevalent among the youth, largely due to the proximity of liquor stores to schools in both rural and urban areas. Given the high rates of HIV, gender-based violence, risky sexual behaviour, and teenage pregnancy in South Africa (issues that are often linked to excessive drinking), greater access of alcoholic beverages toward adolescents is likely to exacerbate these problems (Letsela *et al.,* 2018).

1.2.2 Adolescence: Skeletal growth and development

Understanding the prevalence of adolescent binge drinking also entails understanding the potential impact alcohol poses on the adolescent body. This is because adolescence is marked by significant biological changes such as skeletal growth and development. Adolescence is a period of dramatic growth and development during which a juvenile is transformed into an adult. This period establishes the internal and external body required to sustain an individual for their lifetime (Weaver, 2002). A myriad of cellular processes occurs to optimize existing systems and external factors, such as lifestyle choices, directly impact adolescence. Poor lifestyle choices, such as binge drinking, detrimentally affect cellular processes (Weaver, 2002). Since adolescence can also be characterised by skeletal growth and development, it is fair to hypothesize the deleterious impact binge drinking poses on the skeleton. In humans, skeletal growth and development occur through two processes namely: endochondral ossification and intramembranous ossification. Bones including the humerus develop through endochondral ossification while others including some facial bones develop through intramembranous ossification (Mackie *et al.,* 2008; Ross and Pawlina, 2010). As this study sought to discover the impact of binge drinking on the adolescent humerus, it was imperative to primarily understand endochondral ossification.

In endochondral ossification, mesenchymal cells (multipotent stem cells) differentiate into chondroblasts that resultantly secrete cartilaginous matrix. Once surrounded by the cartilaginous matrix, chondroblasts transform and mature, becoming chondrocytes. These chondrocytes constitute hyaline cartilage, and hyaline cartilage behaves as a vague scaffold from which bone develops by structuring itself in the general form and size of the future bone (Mackie *et al.,* 2008; Smith and Goodman, 2009; Ross and Pawlina, 2010). The cartilage model possesses a diaphysis (shaft) connected to a proximal and distal epiphysis (ends of the bone) via a metaphysis (therefore it is the area between the diaphysis and epiphysis) (Ross and Pawlina, 2010).

Between the epiphysis and metaphysis in both proximal and distal regions, a growth plate exists containing multiple chondrocyte zones that result in the longitudinal growth of bone (referred to as interstitial growth) namely: the resting zone (RZ); proliferative zone (PZ); the hypertrophic zone (HZ); the zone of calcified cartilage and the zone of resorption. (Mackie *et al.,* 2008; Smith and Goodman, 2009; Ross and Pawlina, 2010). In the resting zone, chondrocytes replicate at low rates, behaving like stem cells. Growth hormone (GH) interacts

with these chondrocytes and drive them into a proliferative state (Nilsson *et al.,* 2005). In the proliferation zone, chondrocytes replicate at high rates, produce collagen (Types II and XI), and arrange themselves along the long axis of the bones to appear like columns (Nilsson *et al.,* 2005; Mackie *et al.,* 2008; Smith and Goodman, 2009). Eventually, proliferative chondrocytes mature and cease cell division to become hypertrophic chondrocytes. In the hypertrophic zone, chondrocytes are greatly enlarged and remain metabolically active. Not only do these chondrocytes continue to produce Type II and XI collagen but also vascular endothelial growth factor (VEGF) which stimulates vascular invasion. In the zone of calcified cartilage, hypertrophied chondrocytes degenerate and calcify then the cartilage is replaced by blood vessels and bone cells called osteoblasts (Nilsson *et al.,* 2005; Ross and Pawlina, 2010). Osteoblasts secrete bone matrix according to the form and size of the hyaline cartilage model. In the zone of resorption, the calcified cartilage is directly connected to the connective tissue of the bone marrow cavity. Blood vessels invade this region form spearheads leaving the calcified cartilage appearing as longitudinal spicules (Ross and Pawlina, 2010).

While the cartilage calcifies, osteogenesis takes place where bone cells called osteoblasts develop and secrete bone matrix which contains proteins to create bone tissue. Bone tissue gradually replaces the cartilage model which eventually ossifies primarily in the diaphysis and this area is called the primary ossification centre (Mackie *et al.,* 2008; Ross and Pawlina, 2010). Bone is fully formed when osteoblasts are entirely bordered by bone matrix, which at that stage are known as osteocytes (Mackie *et al.,* 2008; Smith and Goodman, 2009). Another type of bone cell called osteoclasts simultaneously develop but assist in degrading the cartilage scaffold for bone tissue to properly establish itself (Mackie *et al.,* 2008; Smith and Goodman, 2009; Ross and Pawlina, 2010). While interstitial growth takes place to increase bone length, appositional growth simultaneously occurs. Appositional growth is the proliferation of osteoblasts at the surface of the cartilage model which results in increased width and diameter of the model. Osteoclasts also reabsorb bone on the inner surface to ensure that the resulting bone is not too thick to allow for locomotion and for the bone to adapt to various stresses associated with muscle activity (Ross and Pawlina, 2010).

As an organism matures, their growth plates at the epiphyses will eventually ossify which will lead to a cessation of bone growth lengthwise (therefore interstitial growth ceases). Ossification associated with the growth plates (which occurs after the primary ossification centre has been

established) are the secondary ossification centres (Mackie *et al.,* 2008; Ross and Pawlina, 2010).

The skeleton is dynamic so even when bones fully develop, their cellular activity does not cease. Instead, the skeleton undergoes constant remodelling which allows them to adapt to changing mechanical demands over time (Arias *et al.,* 2018). Bone remodelling entails the replacement of low-performing bone (old osseous tissue) with new fully functional bone (new osseous tissue) through four stages, post a quiescence stage, namely: activation, resorption, formation and mineralisation (Langdahl *et al*., 2016; Arias *et al.,* 2018; Kenkre & Bassett, 2018). Osteoclasts are key for bone remodelling as they engulf and consume old osseous tissue, and foreign material, in response to specific stimuli which would include changing mechanical stresses experienced by the skeleton such as compression and shear forces (Mackie *et al.,* 2008; Smith and Goodman, 2009). Osteoblasts will then synthesize new osseous tissue and thereafter mature where they will then function to maintain the new osseous tissue as osteocytes until another cycle of remodelling (Mackie *et al.,* 2008; Smith and Goodman, 2009; Ross and Pawlina, 2010).

1.2.3 Biomechanics

As previously mentioned, attaining peak bone mass during adolescence is essential for developing the biomechanical properties of the skeleton (Abrams, 2003). Excessive alcohol consumption disrupts this process, resulting in weakened bones. Weakened bones are more prone to fractures hence increased fracture risk is associated with heavy drinking. Therefore, it is crucial to examine the biomechanical properties of bones in relation to binge drinking, since it is a form of excessive alcohol consumption.

Biomechanical testing involves subjecting biological materials to tensile, compressive, bending, or torsional forces to assess their rigidity, which is the resistance to deformation when experiencing an applied force. Moreover, biomechanical testing helps evaluate bone strength, which is the ability of a bone to withstand forces and not fracture (Alexandre *et al.,* 2024). One common biomechanical test is the three-point bending test, which has been used in some adolescent binge drinking studies (Hogan *et al.,* 1997; Lauing *et al.,* 2008). To further investigate bone strength, powerful yet non-destructive imaging techniques like Three-dimensional Micro-Focus X-ray Computed Tomography (3D-μCT) are used. These techniques allow researchers to visualize and analyse bone microstructure, in a three-dimensional manner,

providing insights into how morphological changes influence mechanical properties (Giesen *et al.,* 2001; Van Audekercke & Martens, 2018; Michimoto *et al.,* 2020).

Skeletal bones consist of two main components: cortical (compact) and trabecular (spongy) bone. Using 3D-µCT, researchers can examine how alcohol consumption alters the internal architecture of bones, shedding light on the observed effects on bone strength in mechanical tests. This combined approach of strength testing and imaging helps elucidate the relationship between structural changes and biomechanical performance.

Previously, cortical bone was primarily analysed to deduce the rigidity of bone as it is the area that gives bones the ability to withstand greater mechanical stress (Oftadeh *et al.,* 2015; Van Audekercke & Martens, 2018). Currently, literature incorporates trabecular bone analysis as it is equally important. Trabecular bone is the main area of bone responsible for weight-bearing in vertebral bodies (Oftadeh *et al.,* 2015). It is a porous substance composed of bioapatite (a carbonate-containing version of hydroxyapatite that forms the inorganic component of bone) (Li & Pasteris, 2014) and collagen located at the epiphyses and metaphysis of long bones, such as the humerus (Oftadeh *et al.,* 2015). Furthermore, trabecular tissue is an organised lattice of trabeculae which gives rise to a stiff but ductile structure within bone. This enables support for the soft, highly cellular bone marrow which fills the intertrabecular spaces. Trabecular content and architecture contribute to bone rigidity hence trabecular properties such as the thickness, number and spacing are some parameters used to determine the bone strength and can be quantified through 3D-µCT scanning (Oftadeh *et al.,* 2015). Trabecular structure and architecture are responsive to biomechanical forces and stresses. Their appearance and prominence in various areas within bone tissue depends on external forces. In areas of great stress, osteoblasts receive signals to produce new osseous tissue thereby increasing bone mass in those regions (Oftadeh *et al.,* 2015; Lynnerup et al., 2019). Trabeculae align themselves in the same direction of the force or stress to withstand it and become dense in those areas as a way to maintain their function for a long time (Oftadeh *et al.,* 2015; Lynnerup et al., 2019). Therefore, trabecular and (or) cortical bone analysis can help deduce bone strength (Giesen *et al.,* 2001; Van Audekercke & Martens, 2018; Michimoto *et al.,* 2020).

Literature reports on the skeletal harm brought about through adolescent binge drinking with a plethora of studies focused on the long bones due to their similar development. Sampson *et al.* (1996) reported reduced femoral and tibial bone density (more evidently in the tibiae) and reduced calcium presence (expressed as mg/g of bone) as a result of binge drinking. Thereafter,

it was illustrated that robust bone health greatly depends on adequate attainment of peak bone mass in adolescence specifically in cortical bone as it plays a direct role in strength and support (Hogan *et al.,* 1997). Hogan *et al.* (1997) observed a 46% increase in femoral cortical bone area but a reduction of endosteal bone formation (68%) and bone stiffness (26%). Despite a reduction of whole bone strength, the increase in cortical bone area suggests a level of compensation to maintain bone function despite exposure to toxicity (binge drinking). Föger-Samwald *et al.* (2018) similarly associated impairment and evident compensation to binge drinking when examining the femur, tibia and humerus. This was observed using prepubescent male pigs which, moreover, suggests that skeletal compensatory mechanisms resulting from binge alcoholic exposure may exist in various mammals including humans (Föger-Samweld *et al.*, 2018).

Abrams (2003) reported that the different bones constituting the skeleton reach peak mass at different times. This therefore suggests that different responses to alcohol exposure could be observed between different bones. Lauing *et al.* (2008) observed this phenomenon between tibiae and lumbar vertebrae and site-specific differences within each bone when examining the effect of binge drinking on these bones using a male rat model. Moreover, Lauing *et al.* (2008) included an abstinence group wherein these study animals were exposed to alcohol in a binge manner (just like the other alcohol fed groups) however a period of alcohol abstinence followed after the exposure period to observe possible bone recovery from binge alcohol exposure. It was noted that the lumbar vertebrae were resistant to recovery however the tibia showed slight recovery suggesting that bone recovery (and the likelihood thereof) varies between different bones (Lauing *et al.,* 2008). The similar findings across these studies (Sampson *et al.,* 1996; Hogan *et al.,* 1997; Abrams, 2003; Lauing *et al.,* 2008; Föger-Samweld *et al.*, 2018) illustrate the array of impacts binge drinking poses on the adolescent skeleton.

As a remarkable percentage of adolescents engage in binge drinking, extensive literature exists to understand its impact on skeletal health during this critical developmental period. However, existing literature commonly reports on certain bones (like the femur and tibia) more than other bones (like the humerus). Consequently, there is a disparity of available knowledge regarding each skeletal bone in terms of alcohol related pathology. Skeletal bones such as the tibia and femur are better understood compared to bones such as the humerus which is associated with fewer studies (Clark *et al.,* 2006; Ndou & Schepartz, 2015; Föger-Samweld *et al.,* 2018). The humerus is also an important bone and needs to be studied to better understand how its

functionality may be impaired through adolescent binge drinking. The humerus is a form of a long bone and it characterises the human brachium (arm) (Kumar *et al.,* 2022; Mostafa *et al.,* 2022). Because it characterises the human brachium, serious injuries related to this bone commonly include fractures and humeral fractures are common in young people (Anley et al., 2019). Since alcohol consumption is associated with increased fracture risk, adolescent binge drinking may increase humeral fracture risk. Research focussed on the humerus may result in effective strategies being developed to improve management of humeral fractures which may include improved operative measures (Anley et al., 2019). As it is a long bone, it is divided into three regions namely the proximal epiphysis, diaphysis (midshaft) and distal epiphysis. Proximally, the humeral head articulates with the glenoid fossa through the glenohumeral joint which, structurally, is a ball and socket joint (Sontou and Nchimi, 2023). Distally, the humeral capitulum articulates with the radial head while the humeral trochlear articulates with the ulna to form a part of the synovial joint (Pillemer and Pillemer, 2022). Even though humeral fractures may occur in any region, they commonly occur in the proximal region. Humeral research that highlights the morphology of each region to a cellular level may assist to understand this common occurrence and this knowledge may improve patient outcome in terms of injury management (Anley et al., 2019). The humerus serves as an attachment site for 13 muscles which aid elbow and hand movement and furthermore supports various tendons, ligaments and areas of the circulatory system (Kumar *et al.,* 2022; Mostafa *et al.,* 2022). Therefore, this bone is vital for locomotion of the arm and in some animals, like the rat, it is also a weight bearing bone. Humeral research may highlight how shoulder or elbow movement may be impacted should humeral pathology occur.

1.2.4 Alcohol metabolism and the resulting cellular impacts

Alcohol is metabolized in the liver, where it is initially transformed into acetaldehyde by the enzyme alcohol dehydrogenase (ADH) and then further metabolized into acetic acid by acetaldehyde dehydrogenase (ALDH). Acetic acid is then released into the circulatory system and eventually reaches bodily tissues where it is oxidised into water, carbon dioxide and fatty acids (Caballería, 2003). Alcohol metabolism in hepatocytes occurs primarily in the cytosol (via alcohol dehydrogenases), peroxisomes (through catalase activity), and the endoplasmic reticulum (via the microsomal ethanol oxidizing system converting alcohol to acetaldehyde) (Caballería, 2003). After alcohol is metabolised, it passes through the digestive system, is absorbed into the bloodstream, and enters various tissues. Lipids (such as fats and hormones)

are organic compounds insoluble in water but are soluble in alcohol. As human cell membranes are phospholipid bi-layers, alcohol is able to enter tissues which underlies why alcohol is able to permeate all bodily tissues even during moderate consumption (Molina and Nelson, 2018). Alcohol can disrupt cell membranes, reduce their integrity and increase fluidity and permeability, which impairs function (Toth *et al.,* 2014). Increased permeability allows a greater amount of alcohol into cells, leading to mitochondrial damage, elevated reactive oxygen species (ROS), and ultimately cytotoxicity and organ dysfunction (Toth *et al.,* 2014).Therefore, it is understood why excessive alcohol consumption, such as binge drinking, significantly raises the risk of organ dysfunction. (Molina and Nelson, 2018).

The human genome codes for several classes of alcohol dehydrogenase (ADH) which are located in different tissues such as the liver and stomach (Caballería, 2003). The functioning of the ADH classes located in the gastric mucosa of the stomach (classes 1, 3, 4 and 6) result in a phenomenon called first pass metabolism. This term describes the differential response between males and females resulting from alcohol consumption (Caballería, 2003). Males have more highly active forms of ADH present in their gastric mucosa compared to females resulting in a 30% reduction of alcohol absorption in males compared to females (Wilsnack *et al.,* 2018). Females become inebriated more quickly than males, explaining why men typically require more alcohol to reach similar levels of intoxication. This difference supports gender-specific definitions of binge drinking and shows why sexual dimorphism is an important factor to consider in alcohol research (Wilsnack *et al.,* 2018). First pass metabolism has also been used to explain the variations of alcohol response observed between different methods of alcohol administration most notably between oral and intravenous administration. Caballería (2003) reported similar serum alcohol levels in males and females when alcohol is administered intravenously. This contradicts the finding associated with oral administration as female serum alcohol levels were significantly higher than males (Caballería, 2003). Instead, Caballería (2003) agrees with Iwaniec & Turner (2013) who also reported different responses to alcohol in a Sprague Dawley rat model due to method of administration where the significant effect of alcohol was not observed through oral gavage (no significant changes in body weights and bone measurements) but was observed through intraperitoneal (IP) injections (significantly reduced body weights; reduced cancellous bone formation in tibiae suppressed periosteal bone formation).

Physiologically, excessive alcohol intake impacts bone development through a variety of pathways most notably through, suppression of bone formation; increased bone resorption; disruption of hormones key for bone development and nutrient deficiencies.

Alcohol disrupts bone homeostasis by simultaneously suppressing bone formation and promoting bone resorption. It enters chondrocytes by embedding its hydrocarbon tails into lipid bilayers, then damages organelles like mitochondria and the endoplasmic reticulum, triggering reactive oxygen species (ROS) release and cell death (Goldstein, 1986; Fan *et al.,* 2024). In osteoblasts, alcohol distorts membrane channels, disrupting signalling and inhibiting osteoprotegerin release. This allows Receptor Activator of NF-κB Ligand (RANKL) to bind Receptor Activator of NF-κB (RANK) on osteoclasts, activating bone resorption (De Leon-Oliva *et al.,* 2023). The resulting imbalance in the RANKL pathway favours bone loss, explaining the link between excessive alcohol use and reduced bone mass and density (De Leon-Oliva *et al.,* 2023).

Hormones such as growth hormone (GH); parathyroid hormone (PTH); and oestrogen are some of the commonly affected by excessive alcohol consumption and they are directly associated with skeletal development and growth. Growth hormone (GH), secreted by the pituitary gland at the base of the brain, stimulates the growth plate chondrocytes, promoting their proliferation, which is essential for longitudinal bone growth (Nilsson *et al.,* 2005). Moreover, it functions alongside Insulin Growth Factor 1 (IGF-1) to increase the rate of chondrogenesis once chondrocyte proliferation has begun. Dees and Skelley (1990) showed that alcohol attenuates GH functioning as they reported reduced levels of GH in alcohol consumers, most notably in females. Nilsson *et al.* (2005) showed that GH deficiency coincided with stunted limb growth. Given that GH is linked to the proliferation of growth plate chondrocytes (Nilsson *et al.,* 2005) and that alcohol has been shown to suppress GH activity (Dees and Skelley, 1990), these findings suggest that adolescent binge drinking may impair GH function and potentially hinder longitudinal growth.

Considering the impact of alcohol on GH and that the aforementioned studies (Sampson *et al.,* 1996; Hogan *et al.*, 1997; Lauing *et al.,* 2008; Föger-Samwald *et al.*, 2018) report structural changes in bones as a result of binge drinking, it was thus important to consider and assess chondrogenesis at the epiphyseal growth plate.

Parathyroid hormone (PTH) interacts with osteoblasts, stimulating their maturation into osteocytes. This process promotes bone formation, as the release of bone matrix occurs during osteoblast maturation. In addition, PTH facilitates bone resorption and remodelling by promoting osteoclast formation and subsequent calcium release, primarily through the inhibition of osteoprotegerin (Silva & Bilezikian, 2015). Related factors, such as parathyroid hormone-related protein (PTHrP) and Indian Hedgehog (IHH), further influence skeletal development by directly regulating endochondral ossification and enhancing chondrocyte differentiation and hypertrophy (Emons *et al.,* 2011). The dysfunction of these two factors results in distorted columnar arrangement of growth plate chondrocytes (Emons *et al.,* 2011). Moreover, early epiphyseal plate closure could occur as these factors encourage growth plate fusion (Maeda *et al.,* 2007). The transforming growth factor beta (TGF-β) superfamily performs multiple functions crucial for bone development especially during adolescence (Wozney 1989; Wu *et al.,* 2024). TGF-β molecules work in tandem with an intracellular mediator called Smad4 and it has been shown that Smad4 abolition results in distorted growth plate chondrocyte arrangement in rodent tibia (Sakou *et al.,* 1999; Shi and Massague, 2003; Zhang *et al.,* 2005). Mutated Smad4 results in reduced expression of Parathyroid related protein (PTHrP) and Indian Hedgehog (IHH) which also results in distorted growth plate chondrocyte appearance (Karp *et al.,* 2000). Emons *et al.* (2011) also associated distorted columnar chondrocyte arrangement with dysfunctional PTHrP and IHH. It is therefore possible that morphological analysis via staining, e.g. the H&E stain, may reveal these morphological changes.

Oestrogen has primarily been associated with female reproductive organs; however, it also helps develop and maintain non-reproductive organs, such as bone, in both males and females. Humans and rodents express estrogenic receptors in their bone cell membranes such as ESR1, ESR2 and GPER (Smith *et al.,* 2010). Proof that oestrogens impact male bone is that mutation of ESR1 in human males led to skeletal issues (Smith *et al.,* 2010). In rodents, deletion of ESR1 in osteocytes resulted in reduced trabecular bone volume as this resulted in decreased bone formation (Windahl *et al.,* 2013). Oestrogen prevents osteoblast apoptosis. Alcohol consumption is associated with reduced oestrogen levels in females, which can contribute to increased bone resorption and loss. This effect may be further exacerbated when alcohol exposure coincides with the ovarian or oestrus cycle, potentially prolonging the reduction in oestrogen levels. As a result, chondrocyte proliferation may decline due to a shortened lifespan of bone tissue cells. Block *et al.* (1993) reported decreased levels of oestrogen in adolescent

girls post moderate consumption of alcohol. If this study exposed females to alcohol in a binge manner, oestrogen levels may remain decreased for a longer period leading to a reduction of proliferative chondrocytes in females perhaps even post an abstinent period (Turner *et al.,* 1994). In contrast, some studies demonstrate that alcohol may raise oestrogen levels in males which may contribute more robust bone structure. Increased oestrogen in males is associated with enhanced bone cell production (Noirrit-Esclassan *et al.,* 2021), which may suggest increase in proliferating chondrocytes observed in their bones.

Alcohol consumption can adversely affect bone development by inducing nutrient deficiencies, particularly in vitamin D and calcium. The biologically active form of vitamin D, 1,25-dihydroxyvitamin D, plays a critical role in bone mass accrual during development by binding to and activating the vitamin D receptor (VDR) (Brumbaugh & Haussler, 1975). VDRs are expressed in various cell types throughout the body, including in the small intestine and kidneys, where they facilitate calcium absorption into the bloodstream (Bouillon et al., 2008). Once absorbed, calcium enters bone tissue and is incorporated into the bone matrix in the form of hydroxyapatite crystals, contributing to bone mineralization in a tightly regulated process (Li et al., 1998; Amling et al., 1999).

Calcium homeostasis is maintained through a feedback mechanism involving the parathyroid hormone (PTH). When serum calcium levels decline, PTH stimulates the release of calcium from bone stores to restore normal circulating levels (Li et al., 1998; Amling et al., 1999). In addition to calcium regulation, VDRs on chondrocytes promote the expression of fibroblast growth factor 23 (FGF23) in osteoblasts, which is essential for maintaining phosphate balance, a key component of hydroxyapatite (Masuyama et al., 2006). Disruption of phosphate homeostasis can impair bone mineralization and compromise skeletal integrity.

Excessive alcohol intake has been shown to impair VDR function, thereby reducing the efficiency of calcium absorption. As a result, insufficient calcium enters the bloodstream and is ultimately unavailable for incorporation into the bone matrix, leading to impaired mineralization. This mechanism contributes to the observation that chronic alcohol consumption is associated with decreased serum calcium levels and increased urinary calcium excretion (Naude et al., 2012). Overall, alcohol-induced disruption of vitamin D and calcium metabolism poses a significant risk to optimal bone development and skeletal health.

1.2.5 Sexual dimorphism

Males and females present differential responses to alcohol due to sexual dimorphism. Therefore, the impact of adolescent binge drinking on bone health may differ between the sexes. As previously stated, the alcohol dehydrogenases (ADHs) in the gastric mucosa of males are more active than in the females leading to easier inebriation for females (Wilsnack *et al.,* 2018). Moreover, hormones, (growth hormone (GH); oestrogen and parathyroid hormone (PTH)) exert their functioning differently between males and females hence the dysregulation manifests as different perturbations between males and females. Alcohol consumption has been shown to correlate with reduced oestrogen levels in females (Block *et al.*, 1993) and elevated oestrogen levels in males (Noirrit-Esclassan *et al.,* 2021). Since oestrogen plays a key role in bone formation and mineralization, these hormonal changes may lead to different alterations in bone parameters, including bone weight between the sexes. GH levels decline in both sexes but decline more in females (Dees and Skelley, 1990) which may alter growth plate chondrocyte proliferation. This alteration may manifest as a morphological change that can be observed through use of histological staining methods.

Binge drinking studies that show evidence of pathology seldomly incorporate both male and female models (Sampson *et al.,* 1996; Hogan *et al.,* 1997; Lauing *et al.,* 2008; Föger-Samweld *et al.*, 2018). Human proximal humeral growth plates generally open and fuse between ages 12-20, while distal growth plates close between ages 11-19 (Zoetis *et al.,* 2003). On average within these age ranges, female growth plates tend to fuse earlier than males (Kvist *et al.,* 2021). Moreover, proximal and distal growth plates do not concurrently close. This differential closure timing between proximal and distal growth plates contributes to the higher incidence of proximal humeral fractures (Lill and Josten, 2000). Resultantly, if binge drinking was proposed to affect the humeri (with specific reference to the chondrocytes in the growth plates) there could be differential effects due to sexual dimorphism. Clark *et al.* (2006) indicated that distinctions in humeral width and length exist between males and females and are established prior to puberty. This includes periosteal diameter which is greater in males than in females, so the effects of alcohol exposure (therefore, binge drinking) on the humerus may be more evident in females than males. The periosteal layer assists with healing of bone, thus if the layer is wider in males than females, male humeri are more likely to better compensate for alcohol exposure. This possibly suggests that increased trabecular numbers and increased bone mineral density may be observed in males compared to females (Clark *et al.,* 2006).

1.2.6 Animal models in science and alcohol administration techniques

To investigate the impact of adolescent binge drinking, the correct model needed to be chosen. Alcohol studies in humans are difficult as they require consenting participants. Moreover, for certain organs like bone, it is very difficult to obtain live samples especially if the focus group is adolescents. For these reasons, mammalian models have been used to study the impact of adolescent binge drinking on skeletal bones, especially rat species. Rat models are widely used because of the shorter experimental periods, reduced costs, compared to other animal models such as primates, and easier management due to their smaller weights (Sengupta, 2013; Föger-Samweld *et al.,* 2018). It is observed that the aforementioned studies that made use of this model (Sampson *et al.,* 1996; Hogan *et al.,* 1997; Clark *et al.,* 2006; Lauing *et al.,* 2008) possess similar and reproducible results. As the aims of these previous studies mirrored the purpose of the current study, it was only fitting that the current study would make use of the same animal model. Human and rat bone development occur through similar fashions (endochondral and intramembranous ossification) thus it was considered reliable to extrapolate the findings from the study animals and apply it to humans (Sengupta, 2013). In terms of the humerus, human and rat species are quite similar. Human proximal humeral growth plates generally open and fuse between ages 12-20, while distal growth plates close between ages 11-19. In rats, seven postnatal weeks equates to 14.5 human years. Their proximal humeral growth plates open and fuse during adulthood (between 52-181 weeks) while distal growth plates open and fuse from early adolescence to adulthood (4-23 weeks) (Zoetis *et al.,* 2003). Despite differences in weight-bearing roles, wherein the rat humerus is a weight bearing bone that helps maintain the position of the rat body while the human humerus does not directly help maintain the position of the body, there are similarities (basic humeral structure; both rat and human humeri articulate with scapula via glenohumeral joint and to ulna and radius via elbow joint; humeri; humeri in both species are homologous) between rat and human humeri. These similarities support the relevance of comparing human and rat models for research. Furthermore, this model allowed for bone histomorphometry and microarchitecture analysis which is not easily performed using human models (Föger-Samweld *et al.,* 2018).

In terms of alcohol administration, it is difficult to fully imitate the spectrum of alcohol's impact on humans in animal models, as animals do not abuse alcohol nor do they develop alcoholism (Ripley & Stephens, 2011). The impact of alcohol on bone metabolism in rodent studies is determined by both duration of exposure and peak blood alcohol concentration (Turner *et al.,*

2012). Techniques, such as total intragastric infusion; oral gavage; drinking water; intraperitoneal (IP) injections and liquid diets (French, 2001; Turner *et al.,* 1998; Lieber *et al.,* 1989), are used to achieve the desired peak concentration. Among these methods, intragastric infusion allows for precise nutrient delivery and the administration of high alcohol doses. While this method can induce pathology, it is laborious and highly invasive (Turner *et al.,* 2012). Providing alcohol through drinking water is the simplest approach, but it presents challenges in regulating both macro- and micronutrient levels across study groups. Furthermore, high alcohol concentrations may lead to alcohol intolerance in animals, potentially reducing fluid intake and causing dehydration (Turner *et al.,* 2012). For binge drinking models, oral gavage and intraperitoneal injections are the most commonly used methods (Turner *et al.,* 2012). While intraperitoneal injection is useful for short-duration studies, it may not accurately reproduce the physiological reactions seen with oral alcohol administration (Turner *et al.,* 2012). To effectively mimic binge drinking in adolescent rats, it is important to evaluate the route of administration, with oral methods being most representative of typical drinking patterns. Consequently, this study employed oral gavage, allowing for precise dosage control and closely imitating the binge drinking behaviours observed in humans.

Overall, the background research regarding binge drinking, adolescence and adolescent binge drinking established purpose and design of the study, which was to identify the impact of binge drinking on the developing adolescent humerus, through a Sprague Dawley rat model, and to observe possible recovery in the humerus after a period of alcohol abstinence.

1.3 Aims and objectives:

1.3.1 Aim

To examine the impacts of binge drinking on the developing humerus in adolescent Sprague Dawley rats along with potential humeral recovery after alcohol abstinence.

1.3.2 Objectives

1. To evaluate the impact of binge drinking on gross humeral properties, such as osteometric measurements, trabecular thickness, volume, spaces and volume fraction using 3-D micro focus X-ray computed tomography (3-D Micro-CT scanning).
2. To assess whether binge alcohol consumption decreases humeral strength thus increasing the risk of fractures by performing a 3-point bending test.
3. Haematoxylin and Eosin staining along with immunolabelling with the anti-ki67 antibody to qualitatively and quantitatively assess the effects that binge drinking may have on humeral growth and development, by observing the proliferation of epiphyseal growth plate chondrocytes.

Chapter 2

Methodology

2.1 Ethical Clearance

Ethical clearance for this study was obtained from the Animal Research Ethics Committee (AREC) of the University of the Witwatersrand. (Clearance number: 2020/11/02/C).

2.2 Study animals

The study included 48 adolescent Sprague Dawley rats (both males and females) aged 7 weeks (49 postnatal days) that weighed between 150-320g. These animals were among the 72 adolescent rats used in Dr. Bhika's Ph.D. research. The chosen age (49 postnatal days) corresponds to 14.5 human years (Sengupta, 2013) which represents the human adolescent period (ages 10-19). The feeding period of the animal study (i.e., the binge alcoholic feeding and the period of abstinence) was completed in 2022.

All the study animals were housed in 430mm (length) x 220mm (width) x 200mm (height) cages where 2 rats of the same sex were paired together in each cage. They were maintained under an environment free of most pathogens, which was temperature-controlled (26-28°C), and consisted of a 12-hour light/dark cycle to regulate their circadian rhythm. Furthermore, the animals received a standard diet of rat food and tap water ad libitum.

2.3 Group allocation and administration

As the aim consisted of two main components (the impact of binge drinking on the developing adolescent humerus and humeral recovery) two major groups (Group 1 & Group 2) were established for the study. Group 1 was the binge alcohol group (chronic binge consumption model), where the animals were exposed to alcohol for four weeks, while Group 2 was the recovery group (binge alcohol recovery model), where the animals were exposed to alcohol for four weeks followed by a 26-day abstinent period. Furthermore, each major group was divided into an alcohol-exposed (A) and a control (B) group resulting in a total of four groups (1A,1B,2A,2B) where each of the four groups comprised of n=12 rats (six males and six females). Table 2.1 below gives further details regarding the allocation and administration of each group.

Table 2.1: Group allocation and administration:

Group	Administration	Description
1A	4-week alcohol-exposed rats	Rats were administered alcohol for 4 weeks (3 days/week), every alternate day via oral gavage
1B	4-week pair-fed control rats	Rats in this group were given a caloric equivalent of maltose dextrin via oral gavage on the same days as Group 1A
2A	Binge-alcohol recovery rats	To test bone recovery from the effect of binge drinking, rats were exposed to alcohol for 28 days like Group 1A. They were then held for an additional 26 days without alcohol exposure prior to euthanasia (Lauing *et al.,* 2008)
2B	Binge-alcohol recovery pair-fed control rats	Rats were given maltose dextrin for 4 weeks as per the pair-fed control Group 1B. They were then held for an additional 26 days without being given maltose dextrin prior to euthanasia

The study animals were administered a 20% (vol/vol) alcohol solution at a dose of 3g/kg as a single dose through oral gavage because peak blood alcohol concentration (BAC) of 100mg/dL was achieved through this single alcohol dosage (Jeanblanc *et al.,* 2019). A single dose of alcohol was selected to inhibit withdrawal symptoms that may have occurred from administering high alcohol doses twice a day (Penland *et al.,* 2001).

An isocaloric equivalent of maltose dextrin from Sigma-Aldrich, via oral gavage, was given to the control animals. Alcohol/maltose dextrin was administered thrice a week (on every alternative day) and no further administration was done during the remaining 4 days of the week. Due to rodents metabolising alcohol faster than humans, a BAC of approximately 1g/L (100 mg/dL) was necessary for the binge drinking model. An 80 mg/dL concentration which is considered binge drinking in humans is not effective in rats (Jeanblanc *et al.,* 2019). To measure BAC, blood was collected from the tail vein one hour after treatment, when peak BAC was achieved (Livy *et al.,* 2003), and BAC was assessed using an Alcohol Colorimetric kit and the Anthos 2010 Microplate Absorbance Reader (wavelength 620nm). Parameters such as body weight and food intake were monitored to assess the health of the study animals.

2.4 Skeletal harvesting

The study animals were euthanised through a pentobarbital intraperitoneal injection at the end of experimental day 28 for groups 1A and 1B, and day 54 (28 days of treatment + 26 days of abstinence) for groups 2A and 2B. Thereafter, the animals were fully immersed in 10% neutral buffered formalin (refer to appendix) following an abdominal incision that was made to permit penetration of the fixative. The animals' humeri (96 in total) were meticulously dissected under a laminar flow hood and individually stored in sterile containers each containing 30 ml of 10% neutral buffered formalin. Table 2.2 indicates the respective groupings of the obtained humeri.

Table 2.2: Animal groupings

Group 1: Binge Alcohol Group	**Group 2: Abstinent group**
Rat 1-6 (Pair-fed Control Males)	Rat 1-6 (Pair-fed Control Males)
Rat 7-12 (Alcohol-exposed Males)	Rat 7-12 (Alcohol-exposed Males)
Rat 13-18 (Pair-fed Control Females)	Rat 13-18 (Pair-fed Control Females)
Rat 19-24 (Alcohol-exposed Females)	Rat 19-24 (Alcohol-exposed Females)

2.5 Bone weight and osteometric measurements

Post dissections, the humeri were weighed on a Radwag analytical scale and following that, a vernier calliper was used to measure the bicondylar breadth and maximum humeral length. Descriptions of these two osteometric parameters can be seen in the table below.

Table 2.3: Humeral osteometric description: (Adapted from Aydin Kabakci *et al.*, 2017)

Osteometric parameter	**Description**
Maximum humerus length (mm)	The distance between the highest point of the humeral head and the lowest point of the trochlea
Bicondylar breadth (mm)	Measures the mediolateral distance of the epicondyles

2.6 Three-dimensional Micro-Focus X-ray Computed Tomography (3D-µCT)

A Nikon Metrology XTH 225 LC X-ray dual source microtomograph was used for unilateral 3D-µCT analysis of the humeri at the Evolutionary Studies Institute (ESI), University of the

Witwatersrand. Micro CT images were taken of the left humeri for all groups and the μCT system which uses the manufacturer's Inspect-X software allowed for image reconstruction. VG studio max software, from Volume Graphics, was then used for image visualisation and analysis post reconstruction. Table 2.4 indicates the relevant scanning parameters below.

Table 2.4: Scanning parameters:

Parameter	Value
X-ray voltage	80kV
X-ray current	100μa
Filter	3mm aluminium
Scanning resolution	22μm
Tomographic rotation	360 degrees
Rotation step	1 degree
Frame averaging	4
Scan duration	8 minutes

2.7 Humeral osteometry and trabecular morphometry

VG Studio Max®3.2 software built-in calliper was utilised to determine various trabecular morphometric parameters in both the proximal and distal epiphysis, such as bone volume fraction (BV/TV), trabecular number (Tb.N), trabecular thickness (Tb.Th) and trabecular spaces (Tb.Sp). These parameters are described in table 2.5. VG Studio Max®3.2 is a reliable software that analyses computed tomography data through automated protocol. It uses features like sub voxel- accurate surface determination and interval-based modes for high-accuracy surface determination which reduces error rates.

Table 2.5: Trabecular morphometric parameter description: (Adapted from Bouxsein *et al.*, 2010)

Parameter	Description	Unit
Bone volume fraction ($\frac{BV}{TV}$)	Ratio representing bone volume to total volume of the region of interest	%
Trabecular number (Tb. N)	Measures mean number of trabeculae per unit length	mm^{-1}
Trabecular thickness (Tb. Th)	Mean thickness of trabeculae	mm
Trabecular spacing (Tb. Sp)	Mean distance between trabeculae	mm

For each the proximal and distal epiphysis, a region of interest (ROI) was isolated and assessed to obtain morphometric measurements (thus a representation of the humeral architecture). An area of bone inferior to the epiphyseal growth plate in the proximal epiphyses and an area of bone superior to the epiphyseal growth plate in the distal epiphyses.

2.8 Biomechanics: Three point bending test

The three-point bending test was performed to assess whether binge drinking decreased humeral robustness using a Shimadzu 3-point bending machine. In this test, a force was applied (in a mediolateral direction) to the midshaft of the left humeri (after they were used for Micro-CT scanning) while it was placed on two supporting bars which were 15 mm apart. Load displacement curves were resultantly produced at a constant speed of 5 mm/min until failure. The figure below is a visualisation of the three-point test that was performed on the left humeri during the study using the Shimadzu 3-point bending machine.



Figure 2.1: Three-point bending test using the Shimadzu 3-point bending machine (Figure provided by R.Rakgoathe)

The parameters describing various aspects of bone strength were then described from the displacement curve. Description of these parameters was key (Table 2.6) as they indicated if binge drinking increased the risk of fractures through decreased humeral robustness.

Table 2.6: Parameters derived from the load displacement curve (Adapted from MJ. Silva, 2016)

Parameters	Definition
Displacement	The vertical deviation from the horizontal plane necessary to fracture a bone
Maximum force	The force necessary to completely fracture (deform) a bone
Break force	The force necessary to fracture a bone
Yield point	The value of the load at which the load displacement curve deviates from linearity
Time	The duration of a bone resisting the force until failure
Energy to fracture	The total energy input necessary to fracture a bone which is depicted as the total area under the curve

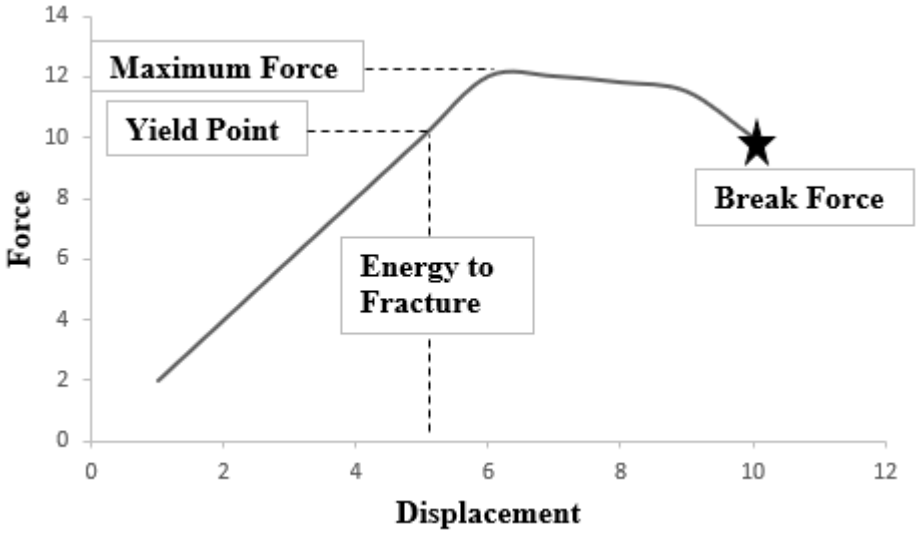


Figure 2.2: An illustration of a load displacement curve showing the various parameters describing bone strength

2.9 Tissue processing for histology and immunohistochemical techniques (IHC)

The formalin fixed right humeri were submerged in 14% w/v ethylenediaminetetraacetic acid (EDTA), pH =7.4 (refer to appendix), for decalcification (removal of calcium ions from bone to soften it) while housed in a Labcon incubator that possessed a platform shaker to allow continuous shaking for three weeks at 45°C. The EDTA was changed after seven days for the first week and thereafter, it was changed every four days. The specimens were examined after two weeks and four days to see if they had been completely decalcified using the Aribex NOMAD examiner portable x-ray system. Calcium presence gives rise to a white (radio opaque) appearance visualised in bones during x-ray scanning. Decalcification, however, causes the loss of this white appearance and the bone instead appears transparent (radiolucent) (Choi *et al.,* 2015). Visualising a radiolucent appearance of the humeri on the x-ray system therefore confirmed full decalcification. Thereafter, the humeri were cut into proximal (humeral head) and distal portions. Each proximal and distal portion were individually placed in tissue cassettes and labelled accordingly to identify the sex, animal number, group number and the specific portion of the humerus. All the cassettes were placed in a large container where they were submerged in 10% buffered formalin for 24 hours.

The tissue was processed through ascending grades of alcohol using the Thermo Scientific Citadel 2000 automatic tissue processor before embedding in paraffin wax. Serial sections were then cut with the Leica microtome at 5µm thickness in a longitudinal plane and placed on 3% silane coated slides (refer to appendix). Slides were coated with 3% silane for adherence of tissues during staining and immunohistochemistry procedures. The first section was stained with Haematoxylin and Eosin (H&E) to assess the morphology of the epiphyseal growth plate. Every second and third section were alternately immunolabeled with anti-Ki-67 antibody and its negative control, respectively, to evaluate the impact of binge drinking on the proliferation of epiphyseal growth plate chondrocytes. This process was repeated after discarding the first 20 sections, with each experiment conducted in duplicate for both the proximal and distal ends of the humeri. Ki-67 is a nuclear protein that is associated with proliferating vertebrate cells. As this protein is only expressed in proliferating cells (such as chondrocytes at the growth plates) it has therefore been used as a biomarker to detect cell proliferation (Zhang *et al.,* 2021). This is done through the development of antibodies raised against the Ki-67 protein, called the anti-Ki-67 antibody (Endl & Gerdes, 2000). The relevant bodily tissue, which in this case was the proximal and distal epiphysis of the humerus, was treated with the anti-Ki-67 antibody where it bound to the Ki-67 protein. The presence of Ki-67 was visualised and therefore cell proliferation (Zhang *et al.,* 2021). Using the anti-ki-67 antibody helped determine if binge drinking induces perturbations in chondrogenesis and consequentially overall growth.

2.10 Photography and quantification of chondrocytes

The Leica DM750, which is a light microscope fitted with an axiocam HRC digital camera, was used to obtain photomicrographs of stained slides which was thereafter transferred into Fiji Image-J 1.53 T software where the epiphyseal growth plate zones were delineated according to cell morphology. An in-built Image J software tool was employed to estimate the area of the respective epiphyseal growth plate zones. A manual counting method was used to quantify the H&E and Ki-67 protein-stained chondrocytes on the photomicrographs where the counting was done encompassing the entire proliferative zone of the epiphyseal growth plate. To test for repeatability and reliability, manual counting was repeated twice.

2.11 Measurement Reliability

The reliability of the results was assessed by employing the Lins Concordance Correlation Coefficient for the interobserver measurements. This test was used as it could assess both accuracy and precision of the interobserver measurements compared to other correlation coefficients that only measure precision. Performance of this technique entailed repeated measurement of 10% of the data (five times) by different observers (three) and run on Statistical Package for Social Services (SPSS) software. Values for pc range from -1 to 1 where a value close to 1 indicates a high degree of measurement similarity.

2.12 Data Analysis

Objective 1: Preliminary data such as humeral weight, maximum humeral length and bicondylar breadths were obtained in triplicate (one set of measurements and weights per day over the course of three days), organised onto Microsoft Excel 2023 (Microsoft Corporation). SPSS version 29 (IBM) software was then used to statistically analyse the raw data through Normality tests (such as the Shapiro Wilk test), T-tests and the Mann Whitney test (for non-parametric data). Interobserver measurements were taken of the preliminary data. The descriptive statistics of the data were conducted to determine the mean, standard deviation, mode, and median of the groups under analysis. In the results, the average values (mean) and standard deviation (SD) are reported as "mean ± SD" for each measurement. The afore-mentioned data was tested for normality using the Shapiro–Wilk test and when normal distribution was observed, parametric tests, e.g., paired T-test along with Levene's test for equality of variances were conducted to determine the intergroup variations. When normal distribution of data was not observed then the median values along with a non-parametric test, e.g., Man Whitney U test, was performed for analysis. The significance level was set at $p<0.05$. In both groups 1 and 2, comparisons were made between the pair-fed control and alcohol-exposed groups. Additionally, comparisons were made between the male and female groups to observe any differential effects of binge drinking due to sex.

Objective 1: Preliminary data obtained from 3D-µCT, that is the bone to total volume ratio (BV/TV); trabecular thickness (Tb.Th); trabecular number (Tb.N) and trabecular spacing (Tb.Sp), for both the proximal and distal epiphyses were organised onto Microsoft Excel 2023 (Microsoft Corporation). The descriptive statistics of the data were conducted to determine the mean, standard deviation, mode, and median of the groups under analysis. In the results, the

average values (mean) and standard deviation (SD) are reported as “mean ± SD” for each measurement. SPSS version 29 (IBM) software was then used to statistically analyse the raw data through Normality tests (such as the Shapiro Wilk test), T-tests and the Mann Whitney test (for non-parametric data). When normal distribution was observed, parametric tests, e.g., paired T-test along with Levene's test for equality of variances were conducted to determine the intergroup variations. If normal distribution of data was not observed then the median values along with a non-parametric test, e.g., Man Whitney U test, was performed for proper analysis. The significance level was set at $p<0.05$. In both groups 1 and 2, comparisons were made between the pair-fed control and alcohol-exposed groups for both the proximal and distal epiphyses. Additionally, comparisons were made between the male and female groups to observe any differential effects of binge drinking due to sex.

Objective 2: Preliminary data such as maximum force, maximum displacement, fracture time and break force were organised onto Microsoft Excel 2023 (Microsoft Corporation). SPSS version 29 (IBM) software was then used to statistically analyse the raw data through Normality tests (such as the Shapiro Wilk test), T-tests and the Mann Whitney test (for non-parametric data). The descriptive statistics of the data were conducted to determine the mean, standard deviation, mode, and median of the groups under analysis. In the results, the average values (mean) and standard deviation (SD) are reported as “mean ± SD” for each measurement. The afore-mentioned data was tested for normality through the Shapiro–Wilk test and when normal distribution was observed, parametric tests, e.g., paired T-test paired T-test along with Levene's test for equality of variances a were conducted to determine the intergroup variations. When normal distribution of data was not observed then the median values along with a non-parametric test, e.g., Man Whitney U test, was performed for proper analysis. The significance level was set at $p<0.05$. In both groups 1 and 2, comparisons were made between the pair-fed control and alcohol-exposed groups. Additionally, comparisons were made between the male and female groups to observe any differential effects of binge drinking due to sex.

Objective 3: Epiphyseal growth plate regions of Haematoxylin and Eosin (H&E) stained sections were assessed for changes in cell shapes, cell arrangements and zone visibility. In both groups 1 and 2, qualitative comparisons were made between the pair-fed control and alcohol-exposed groups for both the proximal and distal epiphyses. Additionally, qualitative comparisons were made between the male and female groups to observe any differential effects of binge drinking due to sex. Growth plates were described as “open” when an epiphyseal

growth plate was still visible at the time of qualitative assessment and when the majority of growth plates in a group were visible. Growth plates described as “closed” when an epiphyseal growth plate was completely fused at the time of qualitative assessment and when the majority of growth plates in a group were fused.

Objective 3: Preliminary data, that is the cell count of the proliferating chondrocytes in the growth plates for each animal, were obtained in duplicate (one set of measurements and weights per day over the course of two days), organised onto Microsoft Excel 2023 (Microsoft Corporation). SPSS version 29 (IBM) software was then used to statistically analyse the raw data through Normality tests (such as the Shapiro Wilk test), T-tests and the Mann Whitney test (for non-parametric data). The descriptive statistics of the data were conducted to determine the mean, standard deviation, mode, and median of the groups under analysis. In the results, the average values (mean) and standard deviation (SD) are reported as “mean ± SD” for each measurement. The afore-mentioned data was tested for normality through the Shapiro–Wilk test and when normal distribution was observed, parametric tests, e.g., paired T-test along with Levene's test for equality of variances were conducted to determine the intergroup variations. If normal distribution of data was not observed then the median values along with a non-parametric test, e.g., Man Whitney U test, was performed for proper analysis. The significance level was set at $p<0.05$. In both groups 1 and 2, comparisons were made between the pair-fed control and alcohol-exposed groups. Additionally, comparisons were made between the male and female groups to observe any differential effects of binge drinking due to sex. Variables considered to yield results included presence of growth plate, location and age. As growth plates may close at different times between sexes, if growth plates were absent due to closure, growth plate chondrocyte number were recorded as zero. In terms of location, the stained chondrocytes within all proliferative zones were accounted for in both sexes to ensure that the same area was analysed. In terms of age, it was essential to have age-matched males and females to show that they were developing in a similar fashion due to age.

Chapter 3

Results

3.1 Bone weight and osteometric measurements:

The associated results were considered reliable, as the Lins Concordance Correlation Coefficient (0.961) indicated a high degree of similarity between the recorded measurements and the interobserver measurements performed. Few significant changes were observed which were the female humeral weights and sex differences. Non-significant changes were predominantly observed between pair-fed control and alcohol-exposed groups. Levene's test for equality of variances showed that $p > 0.05$ therefore, similarity of variance in the associated data can be assumed.

3.1.1 Humeral weight:

Group 1:

Significant findings:

Significant differences were observed in the females and between the sexes. In the females, binge drinking significantly reduced humerus weight (alcohol-exposed humeri = 0.37g ± 0.02; pair-fed control humeri = 0.38g ± 0.01; $p = 0.045$). In the pair-fed control groups, male humeri (mean = 0.44g ± 0.15) were significantly heavier than female humeri (mean = 0.38g ± 0.01) ($p = 0.002$). Binge drinking did not alter this, as male humeri (mean = 0.50g ± 0.04) remained heavier than female humeri (mean = 0.37g ± 0.02) in the alcohol-exposed groups ($p<0.001$) (Fig. 3.1.1A).

Non-significant findings:

Within the male group, a non-significant rise of humeral weight resulting from alcohol exposure was observed (alcohol-exposed humeri = 0.50g ± 0.04; pair-fed control humeri = 0.44g ± 0.15; $p > 0.05$).

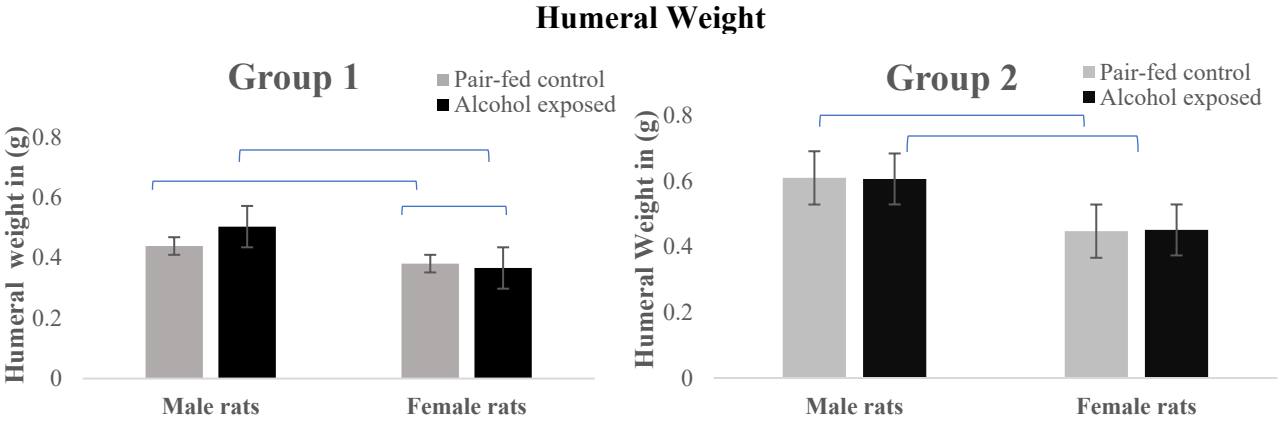
Group 2:

Significant findings:

The only significant results observed were sex differences. In the pair-fed control groups, male humeri (mean = 0.61mm ± 0.04) were significantly heavier than female humeri (mean = 0.48mm ± 0.04) ($p<0.001$). This observation was consistent in the alcohol-exposed groups between the male (mean = 0.61mm ± 0.04) and female humeri (mean = 0.45mm ± 0.02) ($p<0.001$) (Fig. 3.1.1B).

Non-significant findings:

Within the male and female groups non-significant changes were observed. In females, alcohol abstinence led to a non-significant weight reduction in alcohol-exposed humeri (mean = 0.45mm ± 0.02) compared to pair-fed control humeri (mean = 0.48mm ± 0.04) (Fig. 3.1.1B). In males, no difference was observed between alcohol-exposed (mean = 0.61mm ± 0.04) and pair-fed control humeri (mean = 0.61mm ± 0.04) ($p > 0.05$ for both males and females) (Fig. 3.1.1B).



(A) (B)

Figure 3.1.1: Humeral weight of the chronic binge consumption model (A) and the binge alcohol recovery model (B). The mean values for this parameter are represented for both pair-fed control and alcohol-exposed groups in male and female animals. Error bars represent the standard deviation. Significant differences are indicated by the connecting brackets.

3.1.2 Maximum humeral length:

Group 1:

Significant findings:

The only significant results observed were sex differences. In the pair-fed control groups, male humeri were significantly longer (mean = 25.57mm ± 8.08) than female humeri (mean = 25.25mm ± 0.13) ($p<0.001$). Similarly, in the alcohol-exposed groups, male humeri (mean = 27.50mm ± 0.76) were significantly longer than female humeri (mean = 24.78mm ± 0.58) ($p<0.001$) (Fig. 3.1.2A).

Non-significant findings:

Within male and female groups, binge drinking did not significantly impact humeral length. In females, humeral length was comparable between alcohol-exposed humeri (mean = 24.78mm ± 0.58) and pair-fed control humeri (mean = 25.25mm ± 0.13) (Fig. 3.1.2A). In males, the alcohol-exposed humeri (mean = 27.50mm ± 0.76) were slightly longer than the pair-fed control humeri (mean = 25.57mm ± 8.08) ($p > 0.05$ for both male and female groups) (Fig. 3.1.2A).

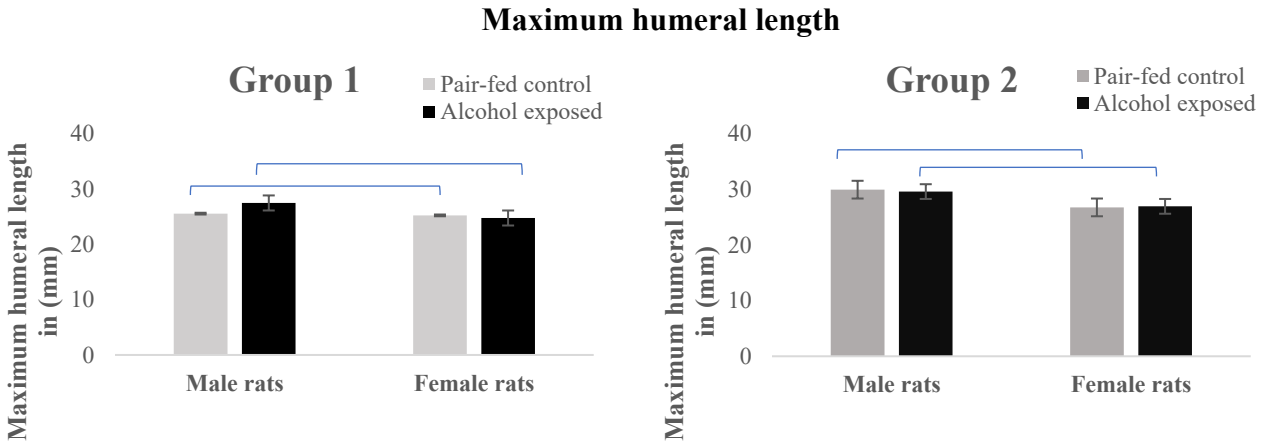
Group 2:

Significant findings:

The only significant results observed were sex differences. In both pair-fed control and alcohol-exposed groups, male humeri were significantly longer than female humeri (pair-fed control: males = 29.96mm ± 0.92, females = 26.78mm ± 0.48; alcohol-exposed: males = 26.96mm ± 0.41, females = 29.62mm ± 0.54) ($p < 0.001$ for both groups) (Fig. 3.1.2B).

Non-significant findings:

In females, alcohol abstinence showed no significant difference in humerus length between alcohol-exposed (mean = 26.96mm ± 0.41) and pair-fed control humeri (mean = 26.78mm ± 0.48). Similarly, in males, no significant differences were observed between alcohol-exposed (mean = 29.62mm ± 0.54) and pai-fed control humeri (mean = 29.96mm ± 0.92) ($p>0.05$ for both males and females) (Fig. 3.1.2B).



(A) (B)

Figure 3.1.2: Maximum humeral length of the chronic binge consumption model (A) and the binge alcohol recovery model (B). The mean values for this parameter are represented for both pair-fed control and alcohol-exposed groups in male and female animals. Error bars represent the standard deviation. Significant differences are indicated by the connecting brackets.

3.1.3 Bicondylar breadth:

Group 1:

Significant findings:

The only significant results observed were sex differences. In the pair-fed control group, female humeri had significantly larger breadths (mean = 6.82mm ± 0.11) than male humeri (mean = 6.76mm ± 2.14) ($p = 0.02$). In the alcohol-exposed group, male humeri had significantly larger breadths (mean = 7.47mm ± 0.17) than female humeri (mean = 6.69mm ± 0.28) ($p < 0.001$) (Fig. 3.1.3A).

Non-significant findings:

Within female and male groups, binge drinking did not adversely impact bicondylar breadth. There were non-significant changes observed within each sex group. In females, alcohol exposure led to a non-significant reduction in bicondylar breadth (alcohol-exposed: mean = 6.69mm ± 0.28; pair-fed control: mean = 6.82mm ± 0.11) (Fig. 3.1.3A). In males, binge drinking increased bicondylar breadth (alcohol-exposed: 7.47mm ± 0.17; pair-fed control: 6.76mm ± 2.14), though the difference was not significant ($p > 0.05$ for both females and males) (Fig. 3.1.3A).

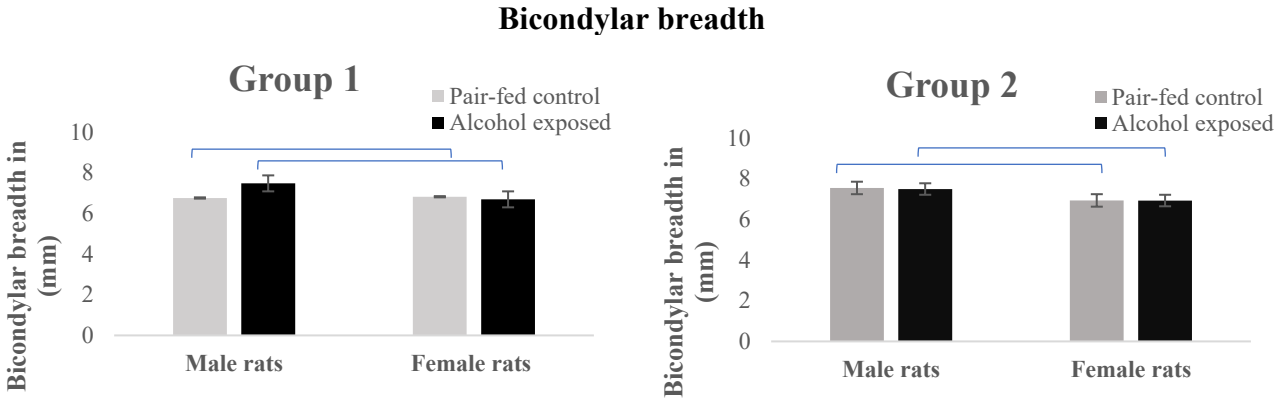
Group 2:

Significant findings:

When comparing the pair-fed control groups between sexes, the males had significantly larger breadths (mean = 7.55mm ± 0.22) than the females (mean = 6.93mm ± 0.28) ($p<0.001$). Similarly, in the alcohol-exposed groups, the males had significantly larger breadths (mean = 7.49mm ± 0.39) than the females (mean = 6.92mm ± 0.21) ($p<0.001$) (Fig. 3.1.3B).

Non-significant findings:

In females, alcohol abstinence showed no significant difference in bicondylar breadth between alcohol-exposed (mean = 6.92mm ± 0.21) and control humeri (mean = 6.93mm ± 0.28) (Fig. 3.1.3B). Similarly, in males, no difference was observed between alcohol-exposed (mean = 7.49mm ± 0.39) and control humeri (mean = 7.55mm ± 0.22) ($p > 0.05$ for both females and males) (Fig. 3.1.3B).



(A) (B)

Figure 3.1.3: Bicondylar breadth of the chronic binge consumption model (A) and the binge alcohol recovery model (B). The mean values for this parameter are represented for both pair-fed control and alcohol-exposed groups in male and female animals. Error bars represent the standard deviation. Significant differences are indicated by the connecting brackets.

3.2 Trabecular morphometry

The 3D-μCT data indicates only a few significant changes resulting from alcohol exposure in three of the four parameters (bone to total volume ratio (BV/TV); trabecular number (Tb.N) and trabecular spacing (Tb.Sp). The remaining results showcase the non-significant differences present across all the parameters. Levene's test for equality of variances showed that $p > 0.05$ therefore, similarity of variance in the associated data can be assumed.

3.2.1 Bone to total volume ratio (BV/TV):

Group 1:

Significant findings:

In the distal epiphyses, females had significantly higher BV/TV ratios (58.41% ± 0.04) compared to males (43.63% ± 0.21) ($p = 0.009$) (Fig. 3.2.1B).

Non-significant findings:

In female proximal epiphyses, binge drinking led to a non-significant decrease in BV/TV ratios (alcohol-exposed: 57.44% ± 0.06; pair-fed controls: 60.55% ± 0.07; $p > 0.05$) (Fig. 3.2.1A). In contrast, distal epiphyses showed a non-significant increase (alcohol-exposed: 60.38% ± 0.05; pair-fed controls: 58.41% ± 0.04; $p > 0.05$) (Fig. 3.2.1B).

In male proximal epiphyses, binge drinking led to a non-significant increase in BV/TV ratios (alcohol-exposed: 58.64% ± 0.05; controls: 46.93% ± 0.23; $p > 0.05$) (Fig. 3.2.1A). A similar trend was observed in the distal epiphyses (alcohol-exposed: 57.65% ± 0.06; controls: 43.63% ± 0.21; $p > 0.05$) (Fig. 3.2.1B).

In the proximal epiphyses, pair-fed control females had higher BV/TV ratios than males (60.55% ± 0.07 vs. 46.93% ± 0.23; $p = 0.310$). Among alcohol-exposed groups, males had slightly higher BV/TV than females (58.64% ± 0.05 vs. 57.44% ± 0.06). In the distal epiphyses, females showed slightly higher BV/TV than males (60.38% ± 0.05 vs. 57.65% ± 0.06). All differences were not statistically significant ($p > 0.05$) (Figures 3.2.1A and 3.2.1B).

Group 2:

Significant findings:

No significant results in binge alcohol recovery model for this parameter.

Non-significant findings:

In female proximal epiphyses, alcohol abstinence resulted in similar BV/TV ratios between alcohol-exposed (60.15% ± 0.04) and control humeri (60.95% ± 0.09; $p > 0.05$) (Fig. 3.2.1C). This pattern was also observed in the distal epiphyses (57.68% ± 0.04 vs. 59.16% ± 0.03; $p > 0.05$) (Fig. 3.2.1D).

In male proximal epiphyses, alcohol abstinence led to a non-significant increase in BV/TV ratios (61.24% ± 0.08 vs. 55.41% ± 0.05; $p > 0.05$) (Fig. 3.2.1C). In the distal epiphyses, BV/TV ratios were similar between alcohol-exposed and control humeri (58.90% ± 0.06 vs. 59.16% ± 0.03; $p > 0.05$) (Fig. 3.2.1D).

In the proximal epiphyses, pair-fed control females had slightly higher BV/TV ratios than males (60.95% ± 0.09 vs. 55.41% ± 0.05; $p > 0.05$). In the distal epiphyses, male and female BV/TV ratios were similar (59.16% ± 0.03 vs. 58.23% ± 0.06; $p > 0.05$). Among alcohol-exposed groups, BV/TV ratios were also comparable between males and females in both proximal (61.24% ± 0.08 vs. 60.15% ± 0.04; $p > 0.05$) and distal epiphyses (58.90% ± 0.06 vs. 57.68% ± 0.04; $p > 0.05$) (Figures 3.2.1C and 3.2.1D).

BV/TV:

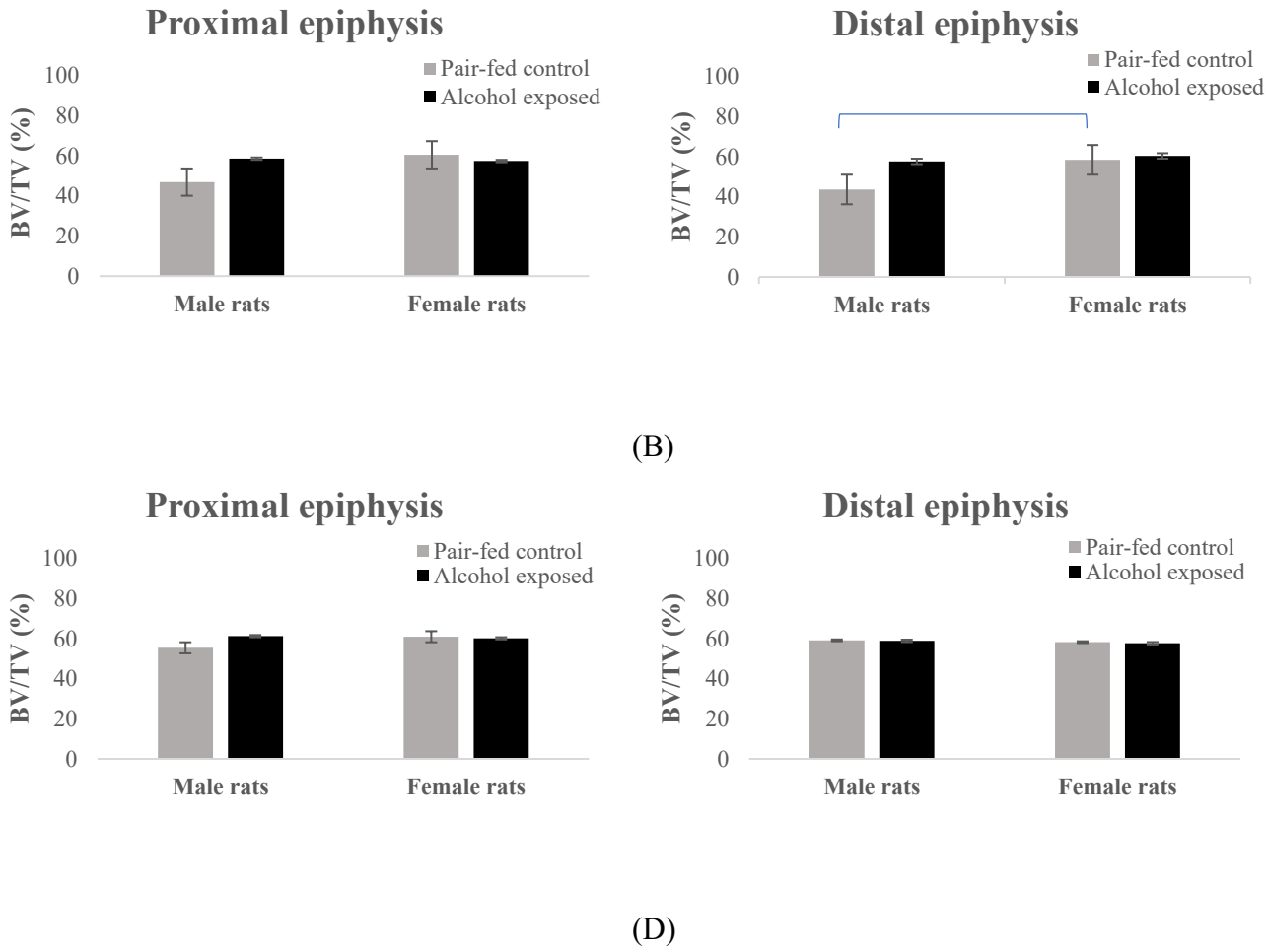


Figure 3.2.1: Humeral bone volume to total volume ratio (BV/TV) of the proximal and distal epiphyses for the chronic binge consumption model (A&B) and binge alcohol recovery model (C&D). The mean values for this parameter are represented for both pair-fed control and alcohol-exposed groups in male and female animals and the error bars represent the standard deviation. Significant differences are indicated by the connecting brackets.

3.2.2 Trabecular thickness (Tb.Th):

Group 1:

Significant findings:

No significant results for this parameter.

Non-significant findings:

In female animals, binge drinking had no significant effect on trabecular thickness. In the proximal epiphyses, Tb.Th was similar between alcohol-exposed (0.12 mm ± 0.02) and pair-

fed controls (0.13 mm ± 0.02; p > 0.05) (Fig. 3.2.2A). A similar result was observed in the distal epiphyses (0.14 mm ± 0.02 vs. 0.13 mm ± 0.01; p > 0.05) (Fig. 3.2.2B).

In male animals, binge drinking led to a non-significant increase in trabecular thickness. In the proximal epiphyses, Tb.Th was greater in alcohol-exposed humeri (0.11 mm ± 0.02) vs. pair-fed controls (0.09 mm ± 0.04) (p > 0.05) (Fig. 3.2.2A). In the distal epiphyses, values were 0.13 mm ± 0.01 vs. 0.10 mm ± 0.05, respectively (p > 0.05) (Fig. 3.2.2B).

In pair-fed controls, females had thicker trabeculae than males in both proximal (0.13 mm ± 0.02 vs. 0.09 mm ± 0.04; p = 0.05) and distal epiphyses (0.13 mm ± 0.01 vs. 0.10 mm ± 0.05; p > 0.05). In alcohol-exposed groups, Tb.Th was similar between females and males in both proximal (0.12 mm ± 0.02 vs. 0.11 mm ± 0.02; p > 0.05) and distal epiphyses (0.14 mm ± 0.02 vs. 0.13 mm ± 0.01; p > 0.05) (Figures 3.2.2A and 3.2.2B).

Group 2:
Significant findings:
No significant results for this parameter.

Non-significant findings:
In female proximal epiphyses, alcohol abstinence led to a non-significant reduction in Tb.Th (alcohol-exposed: 0.13 mm ± 0.01; control: 0.15 mm ± 0.03; p > 0.05) (Fig. 3.2.2C). In the distal epiphyses, Tb.Th was similar between groups (0.14 mm ± 0.02 vs. 0.15 mm ± 0.02; p > 0.05) (Fig. 3.2.2D).

In males, alcohol abstinence resulted in similar Tb.Th in both proximal (0.13 mm ± 0.02 vs. 0.13 mm ± 0.01; p > 0.05) (Fig. 3.2.2C) and distal epiphyses (0.15 mm ± 0.03 vs. 0.16 mm ± 0.01; p > 0.05) (Fig. 3.2.2D).

In pair-fed controls, females had slightly thicker trabeculae than males in the proximal epiphyses (0.15 mm ± 0.03 vs. 0.13 mm ± 0.01; p > 0.05), while distal Tb.Th was similar (0.15 mm ± 0.02 vs. 0.16 mm ± 0.01; p > 0.05). In alcohol-exposed groups, Tb.Th was comparable between females and males in both proximal (0.13 mm ± 0.01 vs. 0.13 mm ± 0.02; p > 0.05) and distal epiphyses (0.14 mm ± 0.02 vs. 0.15 mm ± 0.03; p > 0.05) (Figures 3.2.2C and 3.2.2D).

Tb.Th:

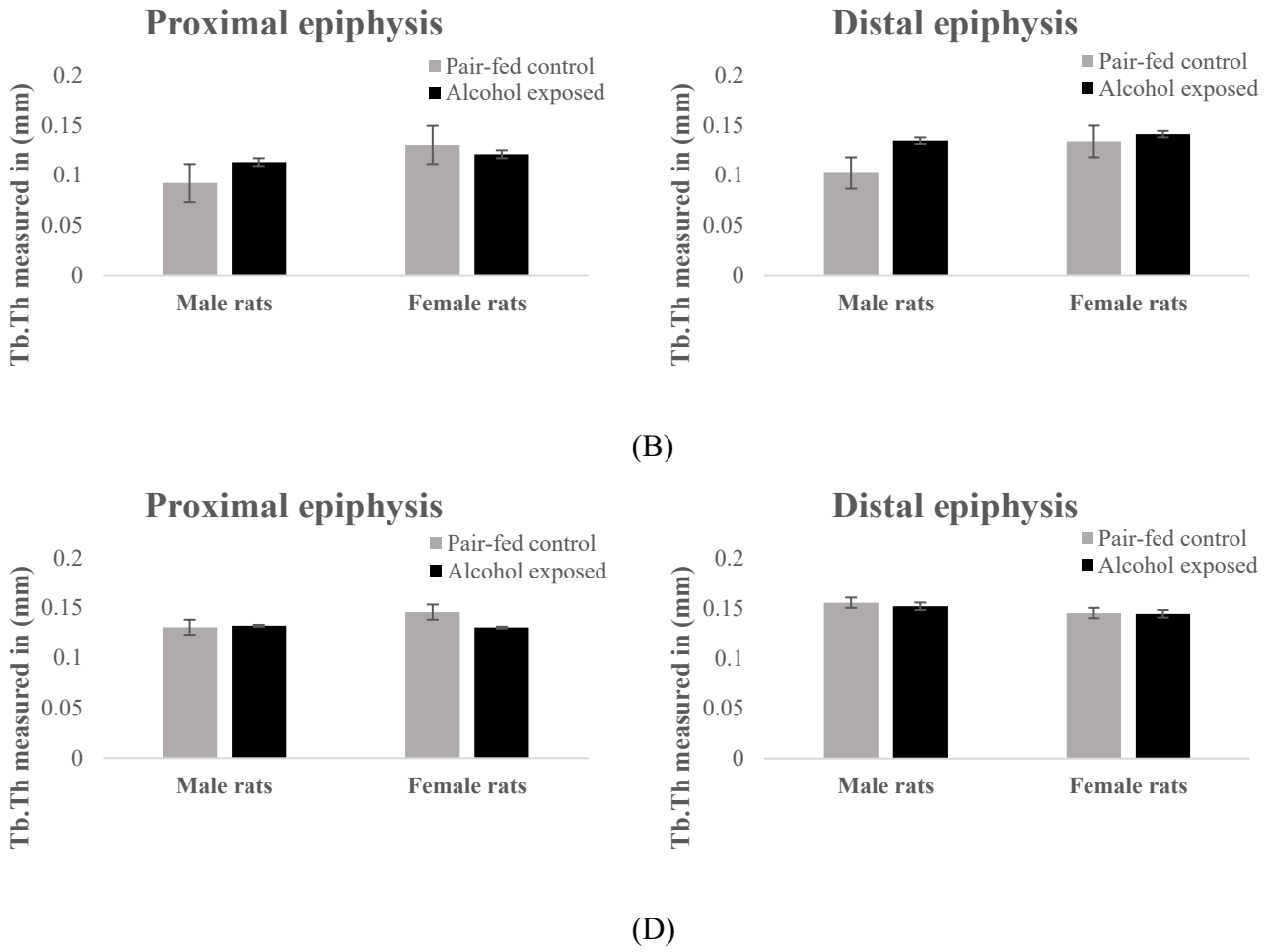


Figure 3.2.2: Humeral trabecular thickness of the proximal and distal epiphyses for the chronic binge consumption model (A&B) and binge alcohol recovery model (C&D). The mean values for this parameter are represented for both pair-fed control and alcohol-exposed groups in male and female animals and the error bars represent the standard deviation.

3.2.3 Trabecular Number (Tb.N):

Group 1:

Significant findings:

No significant results in this parameter for this group.

Non-significant findings:

In female proximal epiphyses, binge drinking led to a non-significant increase in trabecular number (Tb.N) (alcohol-exposed: 4.78 $mm^{-1} \pm 0.34$; control: 4.68 $mm^{-1} \pm 0.28$; $p > 0.05$) (Fig.

3.2.3A). A similar, non-significant difference was observed in the distal epiphyses (4.29 mm^{-1} ± 0.16 vs. 4.38 mm^{-1} ± 0.16; $p > 0.05$) (Fig. 3.2.3B).

In male proximal epiphyses, binge drinking led to a non-significant increase in Tb.N (alcohol-exposed: 5.40 mm^{-1} ± 1.22; control: 4.31 mm^{-1} ± 2.20; $p > 0.05$)) (Fig. 3.2.3A). Similar findings were observed in the distal epiphyses (4.31 mm^{-1} ± 0.45 vs. 3.57 mm^{-1} ± 1.76; $p > 0.05$) (Fig. 3.2.3B).

In pair-fed controls, males showed a non-significant reduction in Tb.N compared to females in both proximal (4.31 mm^{-1} ± 2.20 vs. 4.68 mm^{-1} ± 0.28) and distal epiphyses (3.57 mm^{-1} ± 1.76 vs. 4.38 mm^{-1} ± 0.16). In alcohol-exposed groups, males had higher Tb.N than females in the proximal (5.40 mm^{-1} ± 1.22 vs. 4.78 mm^{-1} ± 0.34) and similar values in the distal epiphyses (4.31 mm^{-1} ± 0.45 vs. 4.29 mm^{-1} ± 0.16), with all differences non-significant ($p > 0.05$) (Figures 3.2.3A and 3.2.3B).

Group 2:

Significant findings:

In male proximal epiphyses, alcohol abstinence significantly increased Tb.N, with alcohol-exposed humeri (4.66 mm^{-1} ± 0.30) showing higher values than controls (4.24 mm^{-1} ± 0.17; $p = 0.007$) (Fig. 3.2.3C).

Non-significant findings:

In female proximal epiphyses, alcohol abstinence led to a non-significant increase in Tb.N (alcohol-exposed: 4.63 mm^{-1} ± 0.23; control: 4.25 mm^{-1} ± 0.50; $p > 0.05$) (Fig. 3.2.3C). In the distal epiphyses, Tb.N was similar between groups (4.01 mm^{-1} ± 0.21 vs. 4.02 mm^{-1} ± 0.37; $p > 0.05$) (Fig. 3.2.3D).

In the male distal epiphyses, the alcohol-exposed (3.91mm^{-1} ± 0.27) and pair-fed control humeri (3.82mm^{-1} ± 0.20) presented comparable Tb.N ($p > 0.05$) (Fig. 3.2.3D).

In pair-fed controls, male and female Tb.N were similar in both proximal (4.24 mm^{-1} ± 0.17 vs. 4.25 mm^{-1} ± 0.50; $p > 0.05$) and distal epiphyses (3.82 mm^{-1} ± 0.20 vs. 4.02 mm^{-1} ± 0.37; $p > 0.05$). In alcohol-exposed groups, Tb.N was also similar between males (4.66 mm^{-1} ± 0.30)

and females (4.63 mm^{-1} ± 0.23) in the proximal ($p > 0.05$) and distal epiphyses (3.91 mm^{-1} ± 0.27 vs. 4.01 mm^{-1} ± 0.21; $p > 0.05$) (Fig. 3.2.3C and 3.2.3D).

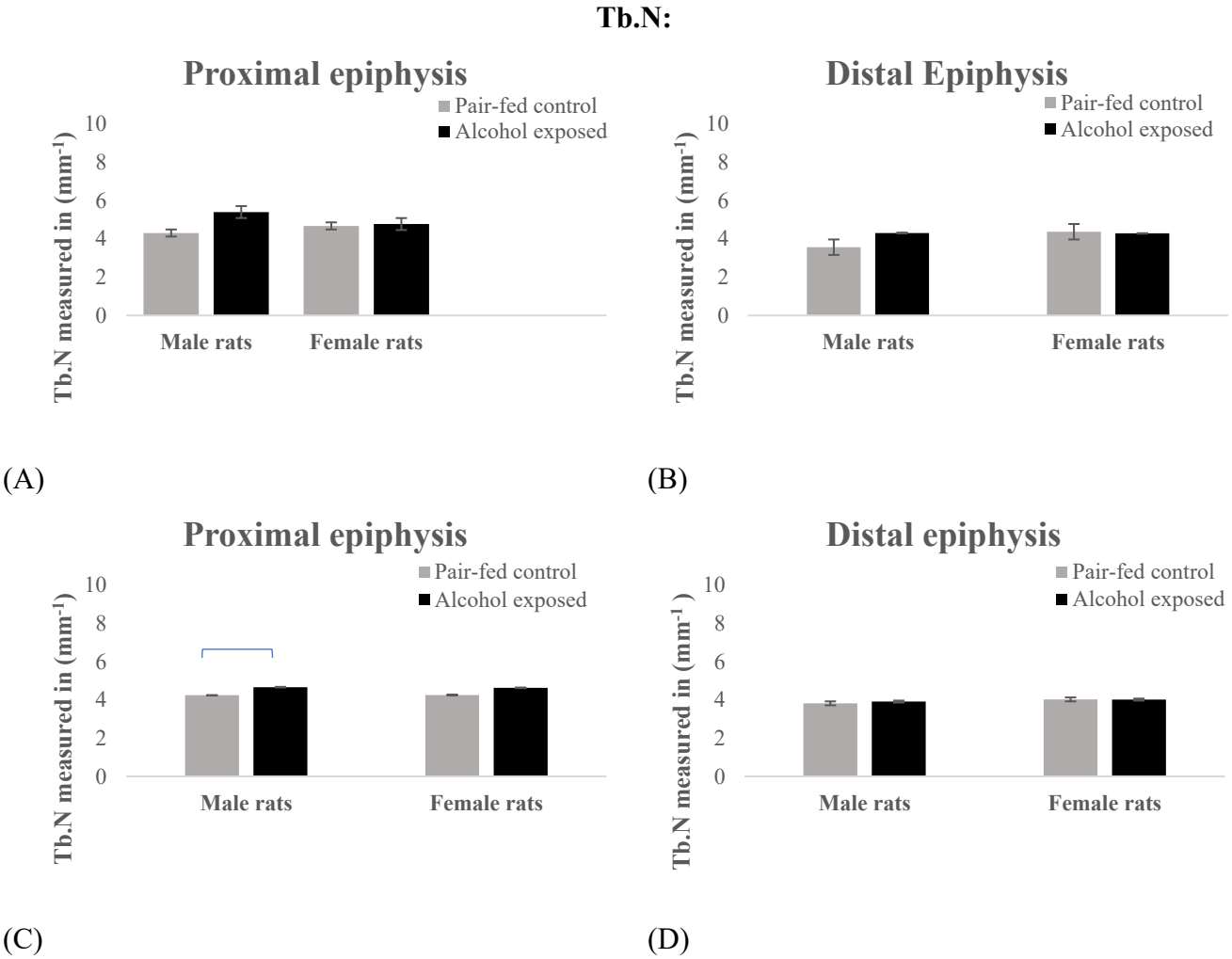


Figure 3.2.3: Humeral trabecular number of the proximal and distal epiphyses for the chronic binge consumption model (A&B) and binge alcohol recovery model (C&D). The mean values for this parameter are represented for both pair-fed control and alcohol-exposed groups in male and female animals and the error bars represent the standard deviation. Significant differences are indicated by the connecting brackets.

3.2.4 Trabecular Spacing (Tb.Sp):

Group 1:

Significant findings:

No significant results for this parameter in this group.

Non-significant findings:
In female epiphyses, binge drinking had no effect on trabecular spacing (Tb.Sp). In the proximal epiphyses, alcohol-exposed (0.09 mm ± 0.01) and control humeri (0.08 mm ± 0.01) were similar ($p > 0.05$) (Fig. 3.2.4A). The distal epiphyses also showed no difference (alcohol-exposed: 0.09 mm ± 0.01; control: 0.09 mm ± 0.01; $p > 0.05$) (Fig. 3.2.4B).

In male epiphyses, binge drinking had no effect on trabecular spacing (Tb.Sp). In the proximal epiphyses, alcohol-exposed (0.08 mm ± 0.02) and control humeri (0.07 mm ± 0.04) were similar ($p > 0.05$) (Fig.3.2.4A). The distal epiphyses showed no difference (alcohol-exposed: 0.10 mm ± 0.02; control: 0.09 mm ± 0.05; $p > 0.05$) (Fig. 3.2.4B).

In the pair-fed control groups, males (0.07 mm ± 0.04) and females (0.08 mm ± 0.01) exhibited similar Tb.Sp in the proximal epiphyses ($p > 0.05$). In the distal epiphyses, males (0.09 mm ± 0.05) and females (0.09 mm ± 0.01) showed similar Tb.Sp ($p = 0.065$). In the alcohol-exposed groups, Tb.Sp in males (0.08 mm ± 0.02) and females (0.09 mm ± 0.01) were similar in the proximal epiphyses ($p > 0.05$) and distal epiphyses (males: 0.10 mm ± 0.02; females: 0.09 mm ± 0.01; $p > 0.05$) (Figures 3.2.4A and 3.2.4B).

Group 2:
Significant findings:
Alcohol abstinence in males resulted in significantly smaller trabecular spaces in the proximal epiphyses. Alcohol-exposed humeri (0.08 mm ± 0.02) had reduced Tb.Sp compared to pair-fed control humeri (0.11 mm ± 0.02) ($p = 0.015$) (Fig. 3.2.4C).

Non-significant findings:
In the female animals, alcohol abstinence resulted in similar trabecular spacing (Tb.Sp) measurements between the alcohol-exposed (mean = 0.09mm ± 0.01) and pair-fed control humeri (mean = 0.09mm ± 0.02) ($p > 0.05$) in the proximal epiphyses (Fig. 3.2.4C). This finding was consistent in the distal epiphyses when comparing the alcohol-exposed (mean = 0.11mm ± 0.01) and pair-fed control humeri (mean = 0.11mm ± 0.02) ($p > 0.05$) (Fig. 3.2.4D).

In the male distal epiphyses however, the Tb.Sp was similar between the alcohol-exposed (mean = 0.10mm ± 0.01) and pair-fed control humeri (mean = 0.11mm ± 0.01), with no statistical difference ($p > 0.05$) (Fig. 3.2.4D).

In the pair-fed control groups, trabecular spacing (Tb.Sp) was similar between males (0.11 mm ± 0.02) and females (0.09 mm ± 0.02) in the proximal epiphyses ($p > 0.05$) and in the distal epiphyses (males: 0.11 mm ± 0.01, females: 0.11 mm ± 0.02) ($p > 0.05$). In the alcohol-exposed groups, Tb.Sp was also similar between males (0.08 mm ± 0.02) and females (0.09 mm ± 0.01) in the proximal epiphyses ($p > 0.05$) and in the distal epiphyses (males: 0.10 mm ± 0.01, females: 0.11 mm ± 0.01) ($p > 0.05$) (Figures 3.2.4C and 3.2.4D).

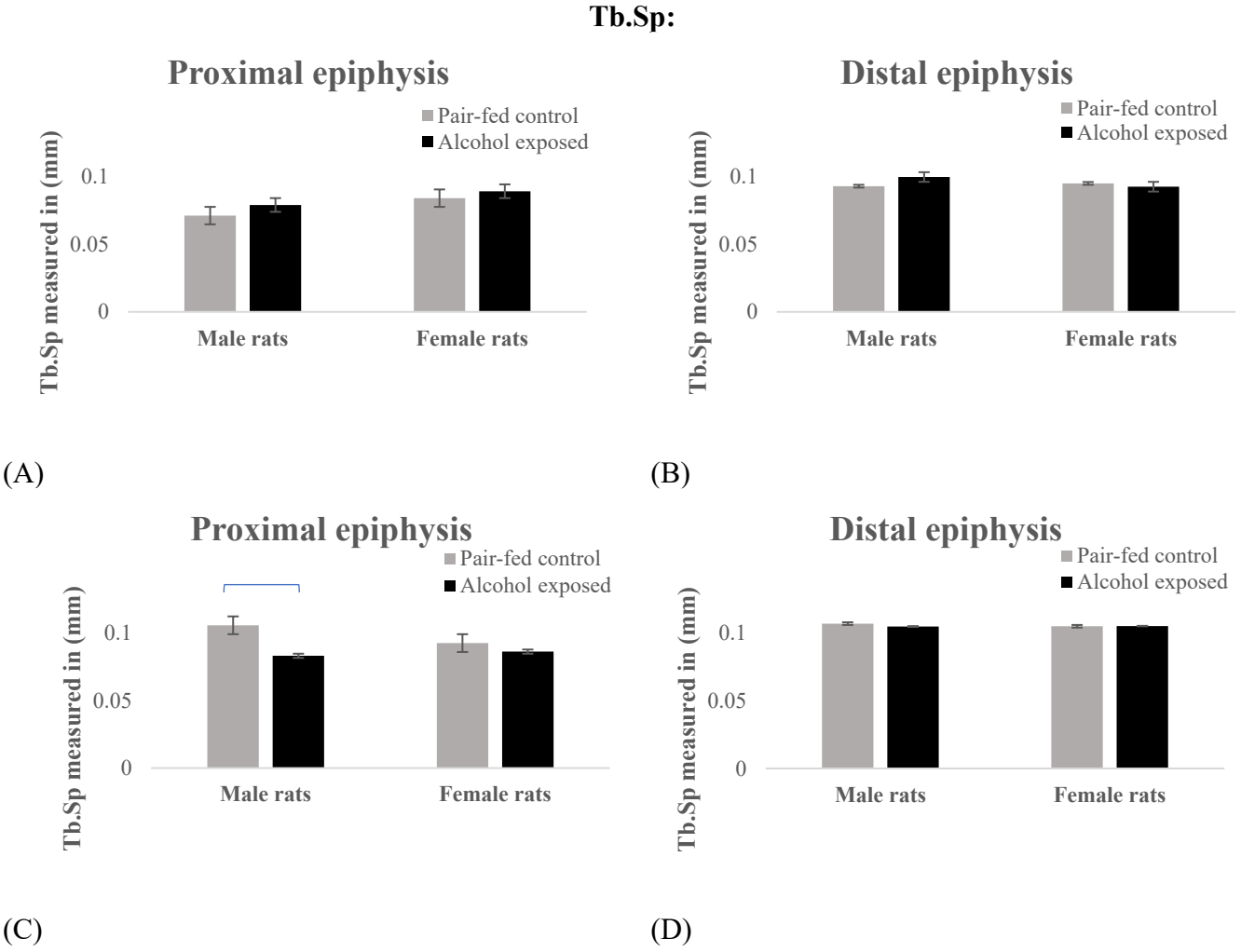


Figure 3.2.4: Humeral trabecular space of the proximal and distal epiphyses for the chronic binge consumption model (A&B) and binge alcohol recovery model (C&D). The mean values for this parameter are represented for both pair-fed control and alcohol-exposed groups in male and female animals and the error bars represent the standard deviation. Significant differences are indicated by connecting brackets.

3.3 Biomechanics: Three-point bending test

The results of biomechanical testing showed that an abstinent period post alcohol-exposure greatly reduced fracture times in female humeri. Moreover, biomechanical testing demonstrated that significant differences exist between male and female humeri. Non-significant differences were also observed within each parameter. Levene's test for equality of variances showed that $p > 0.05$ therefore, similarity of variance in the associated data can be assumed.

3.3.1 Maximum force:

Group 1:

Significant findings:

The only significant results observed were sex differences. Male humeri required more force to fracture than female humeri in both pair fed control (64.27N ± 5.33 vs. 44.83N ± 3.08, $p<0.001$) and alcohol-exposed groups (61.75N ± 7.99 vs. 42.66N ± 5.58, $p<0.001$) (Fig. 3.3.1A).

Non-significant findings:

Binge drinking did not significantly affect humeral strength. In females, alcohol-exposed humeri (42.66N ± 5.58) showed a non-significant decline compared to pair-fed controls (44.83N ± 3.08). Similarly, in males, alcohol-exposed humeri (61.75N ± 7.99) required less force than pair-fed controls (64.27N ± 5.33) ($p > 0.05$ for both male and female groups) (Fig. 3.3.1A).

Group 2:

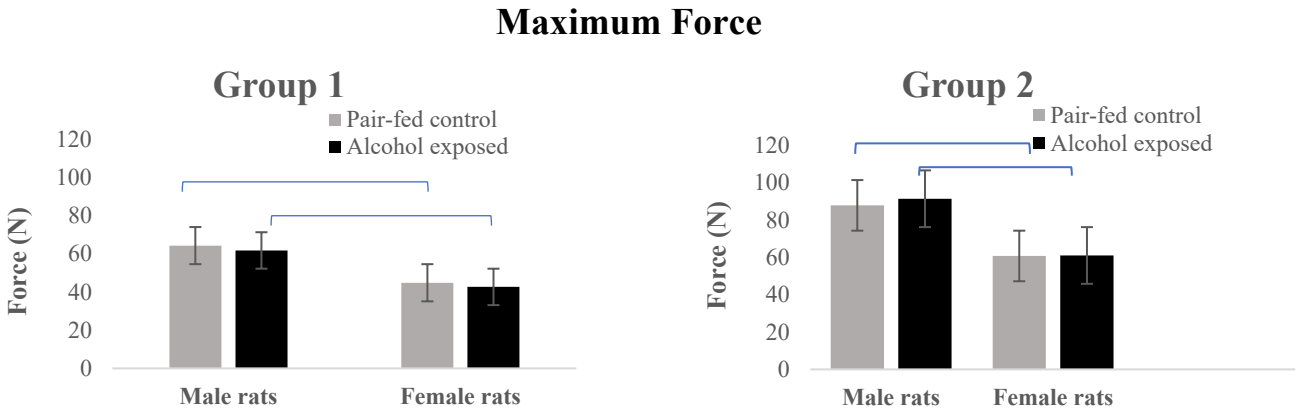
Significant findings:

The only significant results observed were sex differences. Male humeri required more force to fracture than female humeri in both pair fed control (87.94N ± 8.96 vs. 60.81N ± 10.21 $p<0.001$) and alcohol-exposed groups (91.49N ± 9.28 vs. 61.07N ± 3.22, $p<0.001$) (Fig. 3.3.1B).

Non-significant findings:

In females, alcohol abstinence showed no significant difference in fracture force between alcohol-exposed humeri (61.07N ± 3.22) and pair-fed controls (60.81N ± 10.21). In males, alcohol abstinence resulted in a non-significant increase in humeral rigidity, with alcohol-

exposed humeri (91.49N ± 9.28) requiring more force than pair-fed controls (87.94N ± 8.96, p > 0.05) (Fig. 3.3.1B).



(A) (B)

Figure 3.3.1: Maximum force of the chronic binge consumption model (A) and the binge alcohol recovery model (B). The mean values for this parameter are represented for both pair-fed control and alcohol-exposed groups in male and female animals. Error bars represent the standard deviation. Significant differences are indicated by the connecting brackets.

3.3.2 Maximum displacement:

Group 1:

Significant findings:

Binge drinking did not significantly impact the maximum displacement of the humeri. Therefore, there are no significant results for this parameter in this group.

Non-significant findings:

In females, displacement was similar between alcohol-exposed (0.84mm ± 0.19) and pair-fed control humeri (0.78mm ± 0.25). In males, a non-significant reduction in displacement was observed between alcohol-exposed (1.65mm ± 1.44) and pair-fed control humeri (1.87mm ± 1.68) ($p > 0.05$ for both female and male groups) (Fig. 3.3.2A). Male pair-fed control humeri (1.87mm ± 1.68) showed greater displacement than females (0.78mm ± 0.25), though non-significant ($p > 0.05$). A similar trend was observed in alcohol-exposed groups, with males (1.65mm ± 1.44) showing more displacement than females (0.84mm ± 0.19, $p > 0.05$) (Fig. 3.3.2A).

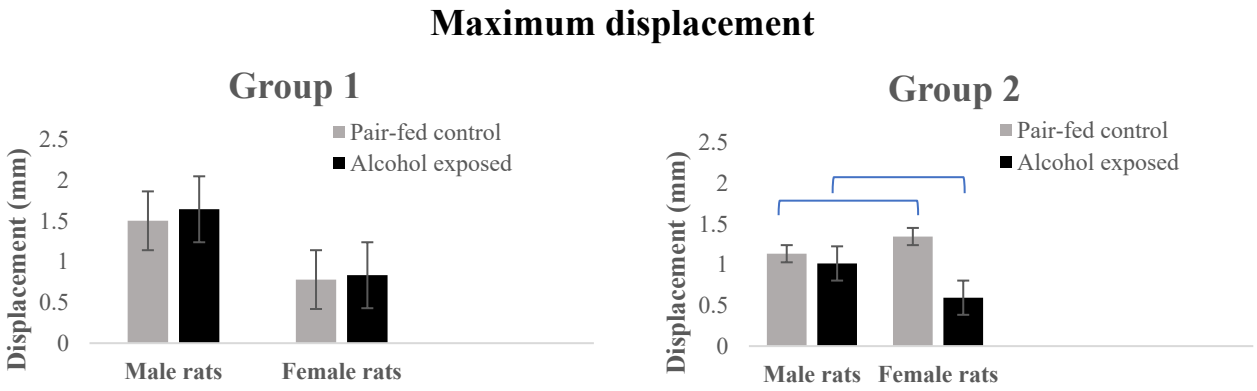
Group 2:

Significant findings:

The only significant results observed were sex differences. Male pair-fed control humeri (1.14mm ± 0.12) showed significantly greater displacement than female humeri (0.76mm ± 0.28, p = 0.007). This trend was consistent in alcohol-exposed groups, with male humeri (1.03mm ± 0.22) showing greater displacement than female humeri (0.56mm ± 0.08, p<0.001) (Fig. 3.3.2B).

Non-significant findings:

Alcohol abstinence showed non-significant effects on displacement in both female and male animals. In females, alcohol-exposed humeri (0.60mm ± 0.08) exhibited a slight reduction compared to pair-fed controls (0.76mm ± 0.28). In males, displacement values were similar between alcohol-exposed (1.02mm ± 0.22) and pair-fed control humeri (1.14mm ± 0.12) (p > 0.05 for both female and male groups).



(A) (B)

Figure 3.3.2: Maximum displacement of the chronic binge consumption model (A) and the binge alcohol recovery model (B). The mean values for this parameter are represented for both pair-fed controls and alcohol-exposed groups in male and female animals. Error bars represent the standard deviation. Significant differences are indicated by the connecting brackets.

3.3.3 Fracture time:

Group 1:

Significant findings:

Binge drinking did not significantly impact the fracture time of the humeri. Therefore, there are no significant results for this parameter in this group.

Non-significant findings:

Binge drinking had non-significant effects on fracture times in both female and male humeri. In females, alcohol-exposed humeri (16.70sec ± 3.89) took longer to fracture than pair-fed controls (15.62sec ± 4.91) (Fig. 3.3.3A). A similar trend was seen in males, with alcohol-exposed humeri (32.91sec ± 28.77) showing longer fracture times than pair-fed controls (30.08sec ± 33.60) ($p > 0.05$ for both female and male groups) (Fig. 3.3.3A). Between sexes, male humeri (30.08sec ± 33.60) required more time to fracture than female humeri (15.62sec ± 4.91) in the control group ($p > 0.05$), and in the alcohol-exposed group, male humeri (32.91sec ± 28.77) took longer than female humeri (16.70sec ± 3.89) ($p > 0.05$) (Fig. 3.3.3A).

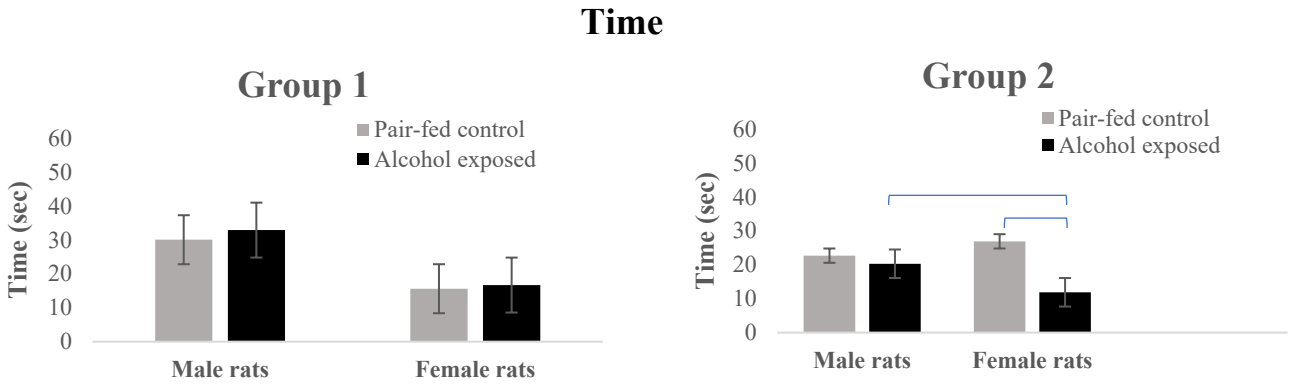
Group 2:

Significant findings:

In females, alcohol-exposed humeri (11.89sec ± 1.49) fractured more quickly than pair-fed control humeri (26.93sec ± 25.36) post alcohol abstinence ($p = 0.009$) (Fig. 3.3.3B). When comparing the sexes it was noted that in the alcohol-exposed groups, females presented shorter fracture times (11.89sec ± 1.49) than the males (20.31sec ± 4.45) that were statistically significant ($p<0.001$) (Fig. 3.3.3B).

Non-significant findings:

Alcohol abstinence had no significant impact on fracture times in males or between sexes. In males, fracture times between alcohol-exposed (20.31sec ± 4.45) and pair-fed control humeri (22.70sec ± 2.40) were not significant (Fig. 3.3.3B). Males also had shorter fracture times than females in the pair-fed control group (22.70sec ± 2.40 vs. 26.93sec ± 25.36) ($p > 0.05$ for both female and male groups) (Fig. 3.3.3B).



(A) (B)

Figure 3.3.3: Fracture time of the chronic binge consumption model (A) and the binge alcohol recovery model (B). The mean values for this parameter are represented for both pair-fed controls and alcohol-exposed groups in male and female animals. Error bars represent the standard deviation. Significant differences are indicated by the connecting brackets.

3.3.4 Break force:

Group 1:

Significant findings:

Significant sex differences were observed in break force. In the pair-fed control group, male humeri (61.10N ± 10.53) required significantly more force to fracture than female humeri (44.72N ± 3.06) ($p = 0.002$). A similar trend was found in the alcohol-exposed group, with male humeri (60.10N ± 8.17) requiring more force than female humeri (41.46N ± 5.18) ($p < 0.001$). (Fig. 3.3.4A).

Non-significant findings:

Binge drinking had non-significant effects on break force in both sexes. In females, alcohol-exposed humeri (41.46N ± 5.18) required slightly less force to fracture than pair-fed controls (44.72N ± 3.07) (Fig. 3.3.4A). In males, no significant difference was observed, with break force similar between alcohol-exposed (60.10N ± 8.17) and pair-fed control humeri (61.10N ± 10.53) ($p > 0.05$ for both female and male groups) (Fig. 3.3.4A).

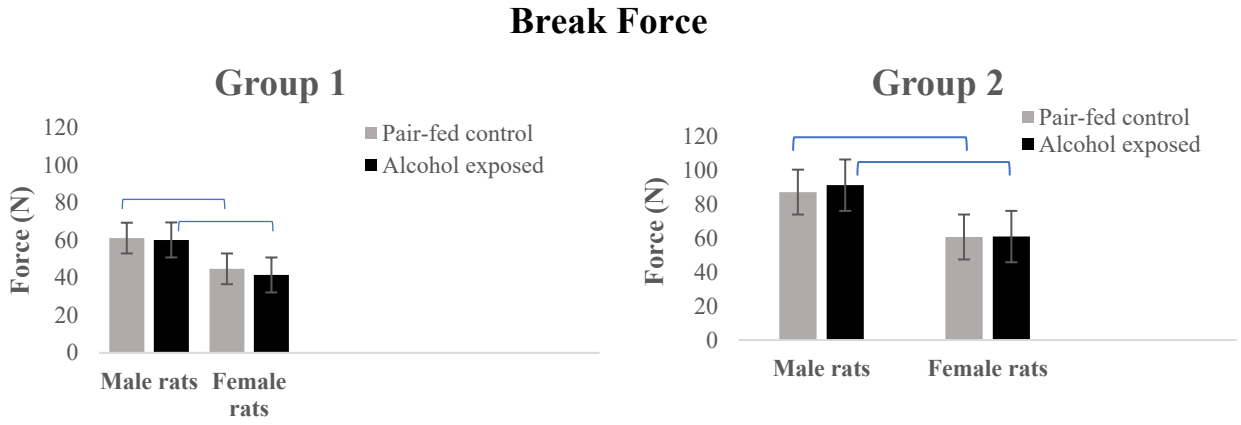
Group 2:

Significant findings:

Significant sex differences in break force were observed after alcohol abstinence. In the pair-fed control group, male humeri (87.32N ± 8.68) required significantly more force to fracture than female humeri (60.81N ± 10.21) ($p = 0.032$). Similarly, in the alcohol-exposed group, male humeri (91.40N ± 9.32) required more force than female humeri (61.07N ± 3.22) ($p < 0.001$) (Fig. 3.3.4B).

Non-significant findings:

Alcohol abstinence in females showed no significant difference in break force between alcohol-exposed (61.07N ± 3.22) and pair-fed control humeri (60.81N ± 10.21) (Fig. 3.3.4B). In males, alcohol abstinence resulted in a non-significant increase in break force, with alcohol-exposed humeri (91.40N ± 9.32) requiring more force than pair-fed controls (87.32N ± 8.68) ($p > 0.05$ for both female and male groups) (Fig. 3.3.4B).



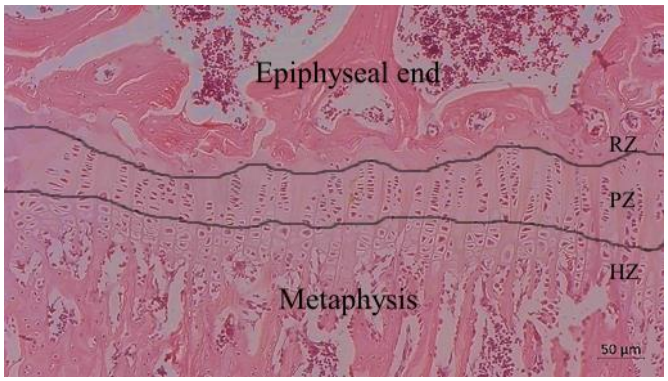
(A) (B)

Figure 3.3.4: Break force of the chronic binge consumption model (A) and the binge alcohol recovery model (B). The mean values for this parameter are represented for both pair-fed control and alcohol-exposed groups in male and female animals. Error bars represent the standard deviation. Significant differences are indicated by the connecting brackets.

3.4 Morphological assessment of the humeral epiphyseal growth plate through Haematoxylin and Eosin (H&E) staining:

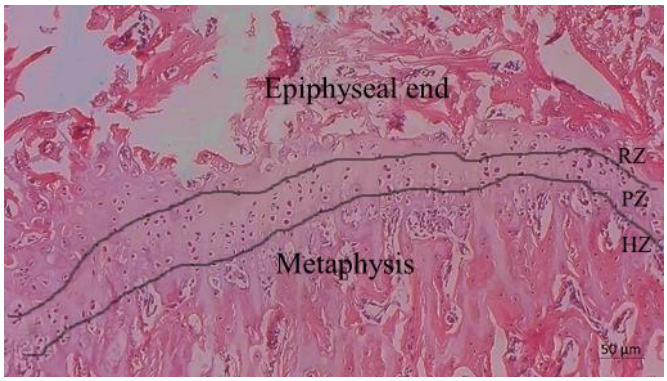
Photomicrographs of the stained tissue for all groups are provided including a reference image (Fig 3.4.1) for both the proximal and distal epiphysis to assist with the visual orientation of the photomicrographs. Proliferative zones have been manually highlighted for reference for the reader.

Proximal growth plate



(A)

Distal growth plate



(B)

Figure 3.4.1: Reference illustrations of the humeral proximal (A) and distal epiphysis (B) showing the growth plate chondrocyte zones in progressive order namely: the resting zone (RZ), proliferative zone (PZ) and hypertrophic zone (HZ).

Group 1:

In the female animals, alcohol exposure coincided with a disorganised appearance of the chondrocytes in the resting zone (RZ), proliferative zone (PZ) and hypertrophic zone (HZ) of the proximal growth plates (Fig. 3.4.2). The typical columnar arrangement of chondrocytes particularly in the proliferative zone (PZ), as seen in the pair-fed control group, appeared askew in the alcohol-exposed group. Moreover, the distinctions between the different zones were not as clear in the alcohol-exposed group when compared to the pair-fed control group. There was reduced visibility of the hypertrophic zone (HZ) as this zone was evidently smaller in size in the alcohol-exposed group than the pair-fed control group. In the distal growth plates, columnar chondrocyte arrangements were observed in the alcohol-exposed group which was a similar morphology to the growth plates of the pair-fed control group (Fig 3.4.2). Moreover, distinctions between the zones were evident thus all the zones were visible (Fig. 3.4.2).

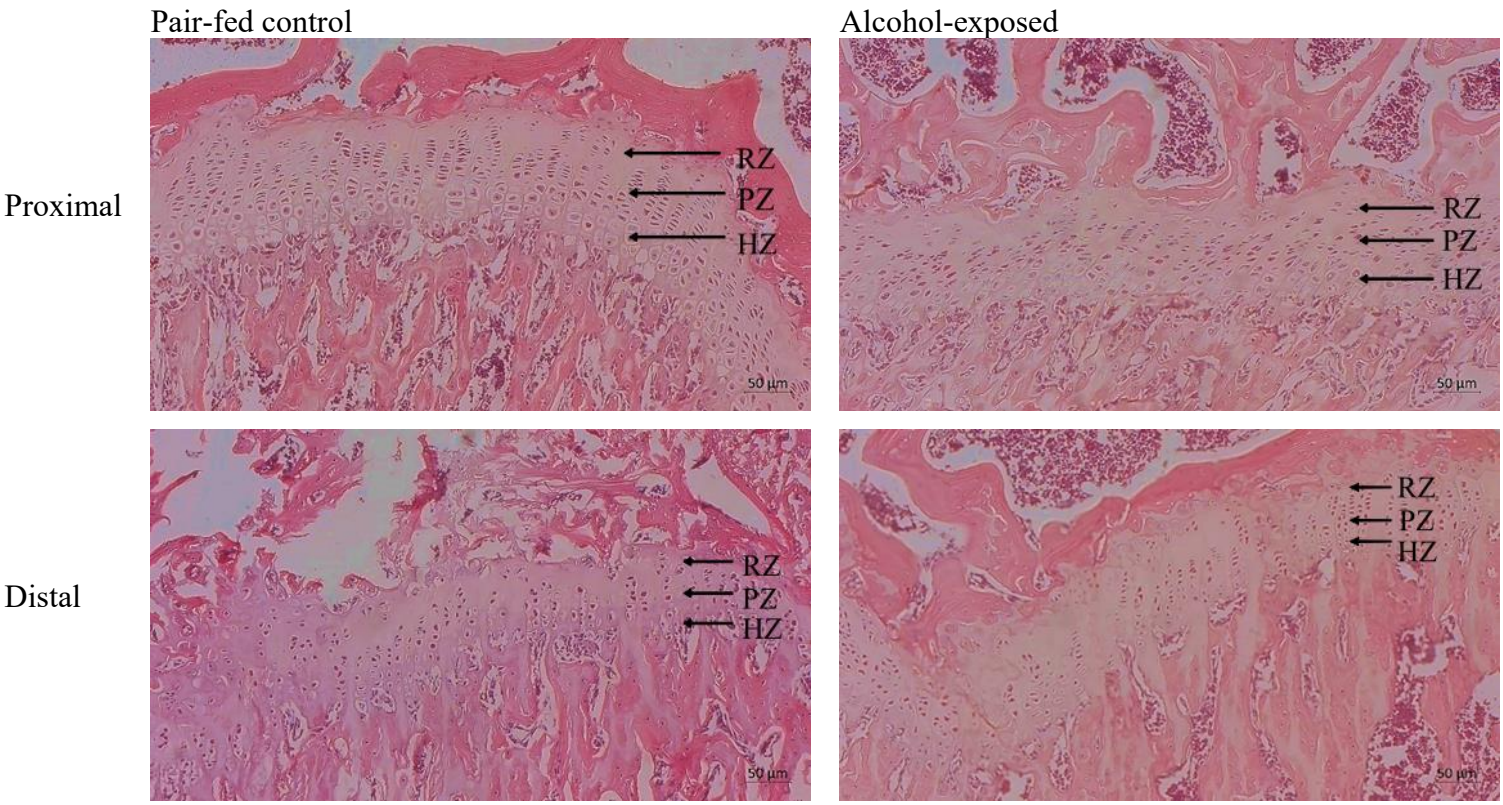


Figure 3.4.2: Haematoxylin and Eosin-stained sections of the proximal and distal epiphyseal growth plates of the humeri for the pair-fed control and alcohol-exposed groups in female rats of the chronic binge consumption model.

Regarding the male animals, alcohol exposure coincided with a columnar appearance of the chondrocytes in the resting zone (RZ), proliferative zone (PZ) and hypertrophic zone (HZ) of the proximal growth plates (Fig. 3.4.3). The typical columnar arrangement of chondrocytes, particularly in the proliferative zone (PZ), seen in the alcohol-exposed group mirrored that of the pair-fed control group. Moreover, the distinctions between the different zones were clear in the alcohol-exposed group, similar to the pair-fed control group, as the active zones were visible. In the distal extremities, growth plates were only observed in the alcohol-exposed group as they had already closed in the pair-fed control group (Fig. 3.4.3). Furthermore, in the distal growth plates of the alcohol-exposed group, the chondrocytes, for the most part, were arranged in columnar fashion. However, there were localised areas of disturbed chondrocyte arrangements, meaning that in certain areas, chondrocytes did not appear arranged in a columnar fashion (Fig. 3.4.3).

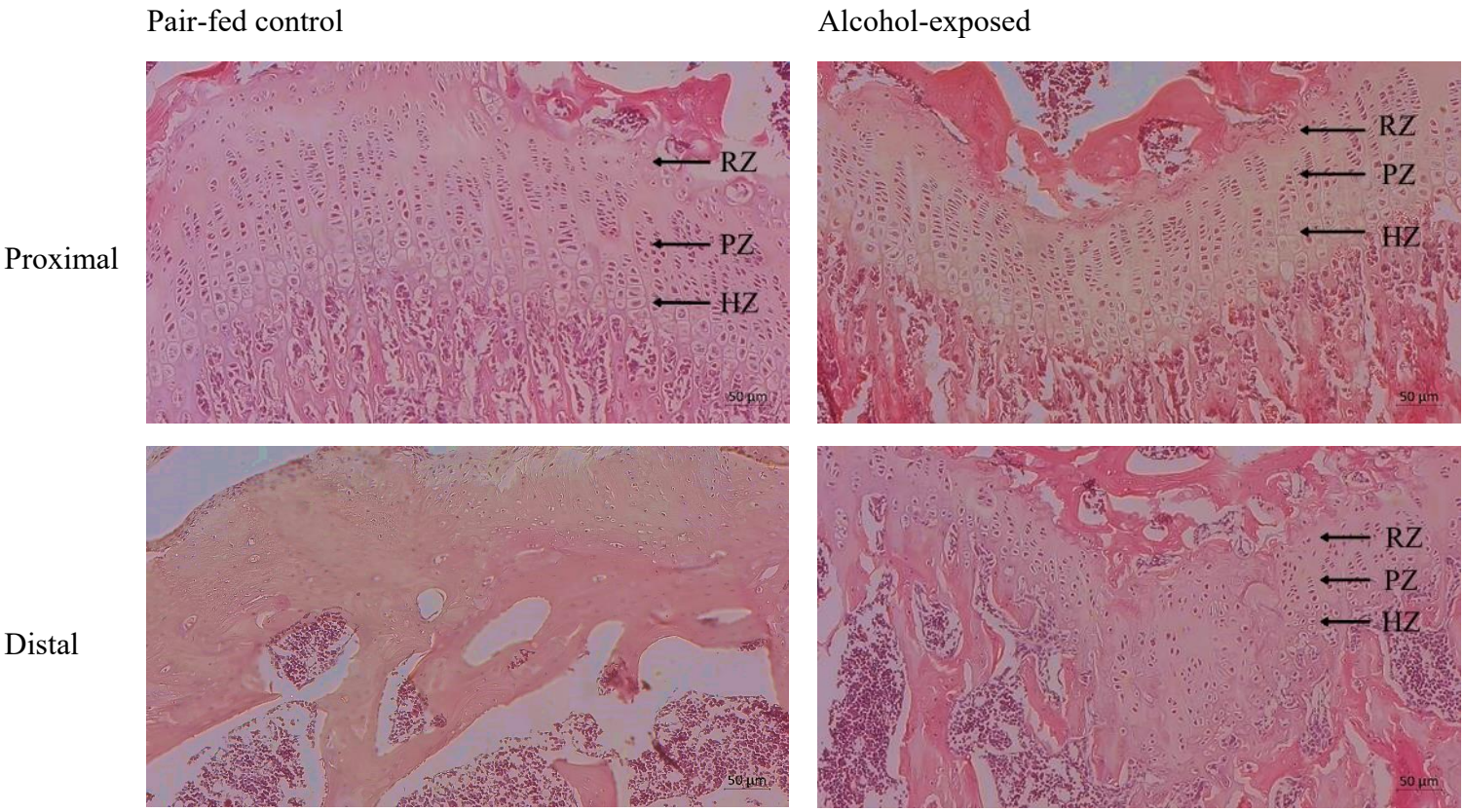


Figure 3.4.3: Haematoxylin and Eosin-stained sections of the proximal and distal epiphyseal growth plates of the humeri for the pair-fed control and alcohol-exposed groups in male rats of the chronic binge consumption model.

Comparisons between the females and the males reveal that alcohol exposure had differential impact between the sexes. Male growth plates visually presented an abundance of chondrocytes with extensive columnar arrangements (Fig. 3.4.3). Alcohol exposure did not disturb these columnar arrangements in the male epiphyseal growth plates, like it did in the female epiphyseal growth plates (Fig. 3.4.2) (Fig. 3.4.3). The active zones in male epiphyseal growth plates were well defined compared to the female epiphyseal growth plates and complete growth plate ossification was associated with the male animals as the male distal pair-fed controls no longer exhibited growth plates (Fig. 3.4.3) whereas female distal pair-fed control epiphyseal growth plates were still open (Fig. 3.4.2).

Group 2:

In the female animals, alcohol-exposed and pair-fed control groups presented similar morphology in the proximal extremity. The proliferative zone (PZ) chondrocytes were arranged in their typical columnar fashion and the hypertrophic zone (HZ) chondrocytes were visible. (Fig 3.4.4). The minor difference between these groups was that inter-lacunar ossification (ILO) was evident in the alcohol-exposed group than the pair-fed control group. Inter-lacunar ossification can be observed in the growth plates of rat long bones during endochondral ossification. In the distal extremity, closed growth plates were observed in both the pair-fed control (three out of three sections that remained intact post staining) and the alcohol-exposed groups (three out of three sections that remained intact post staining) (Fig. 3.4.4) . Consequently, no growth plate comparisons could be made for the distal extremity. The growth plates themselves were not as conspicuous as they were nearing complete ossification.

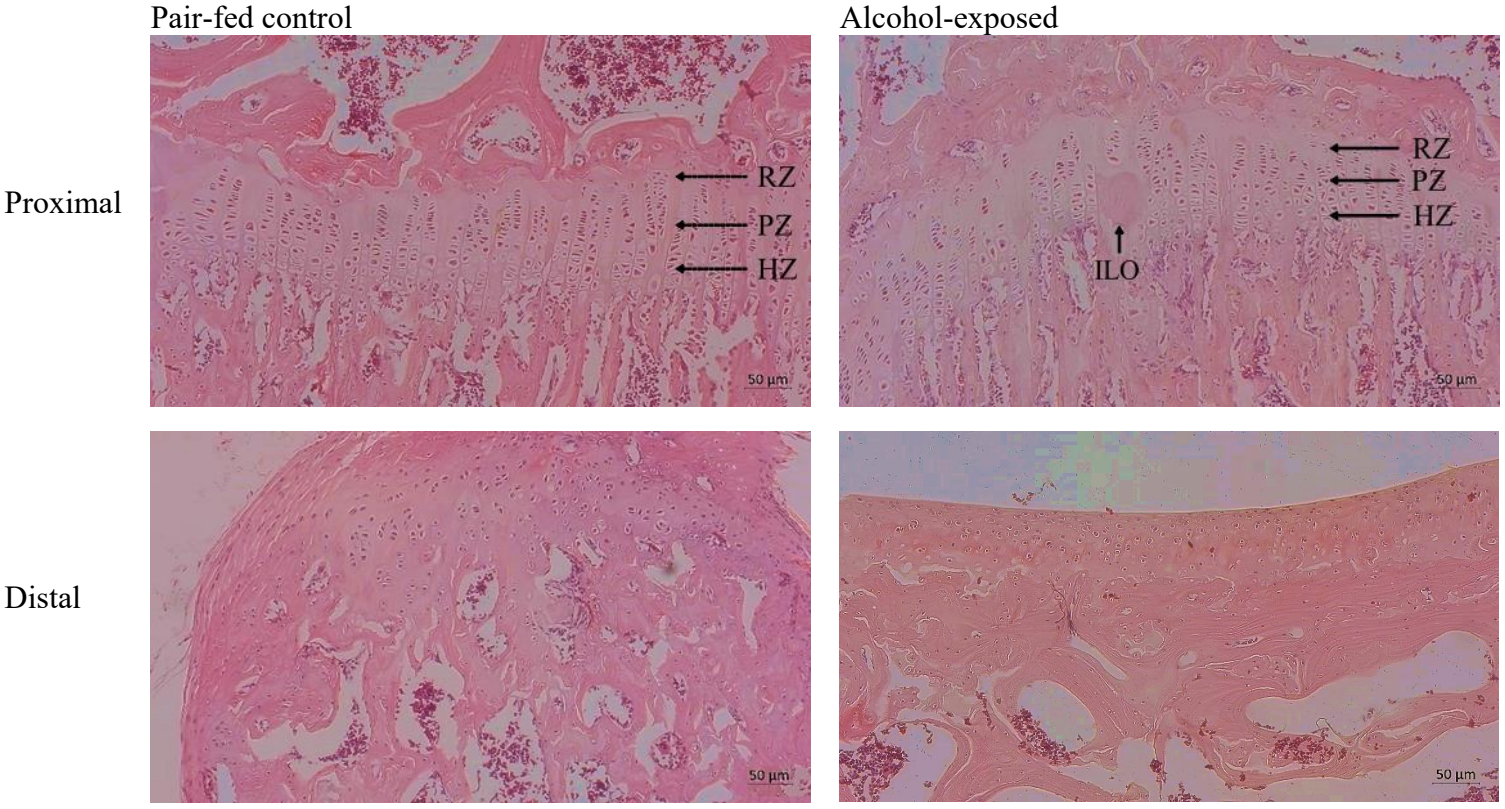


Figure 3.4.4: Haematoxylin and Eosin-stained sections of the proximal and distal epiphyseal growth plates of the humeri for the pair-fed control and alcohol-exposed groups in female rats of the binge alcohol recovery model.

With regards to the male animals, alcohol exposure followed by alcohol abstinence was presented as typical growth plate morphology in the proximal extremity. In the proximal

growth plates of the pair-fed control and alcohol-exposed groups, the proliferative zone (PZ) chondrocytes were arranged in a columnar fashion and the hypertrophic zone (HZ) chondrocytes were visible. (Fig. 3.4.5). In the distal extremity, the growth plates had closed in both the pair-fed control and alcohol-exposed groups thus the chondrocyte zones were no longer visible (Fig. 3.4.5).

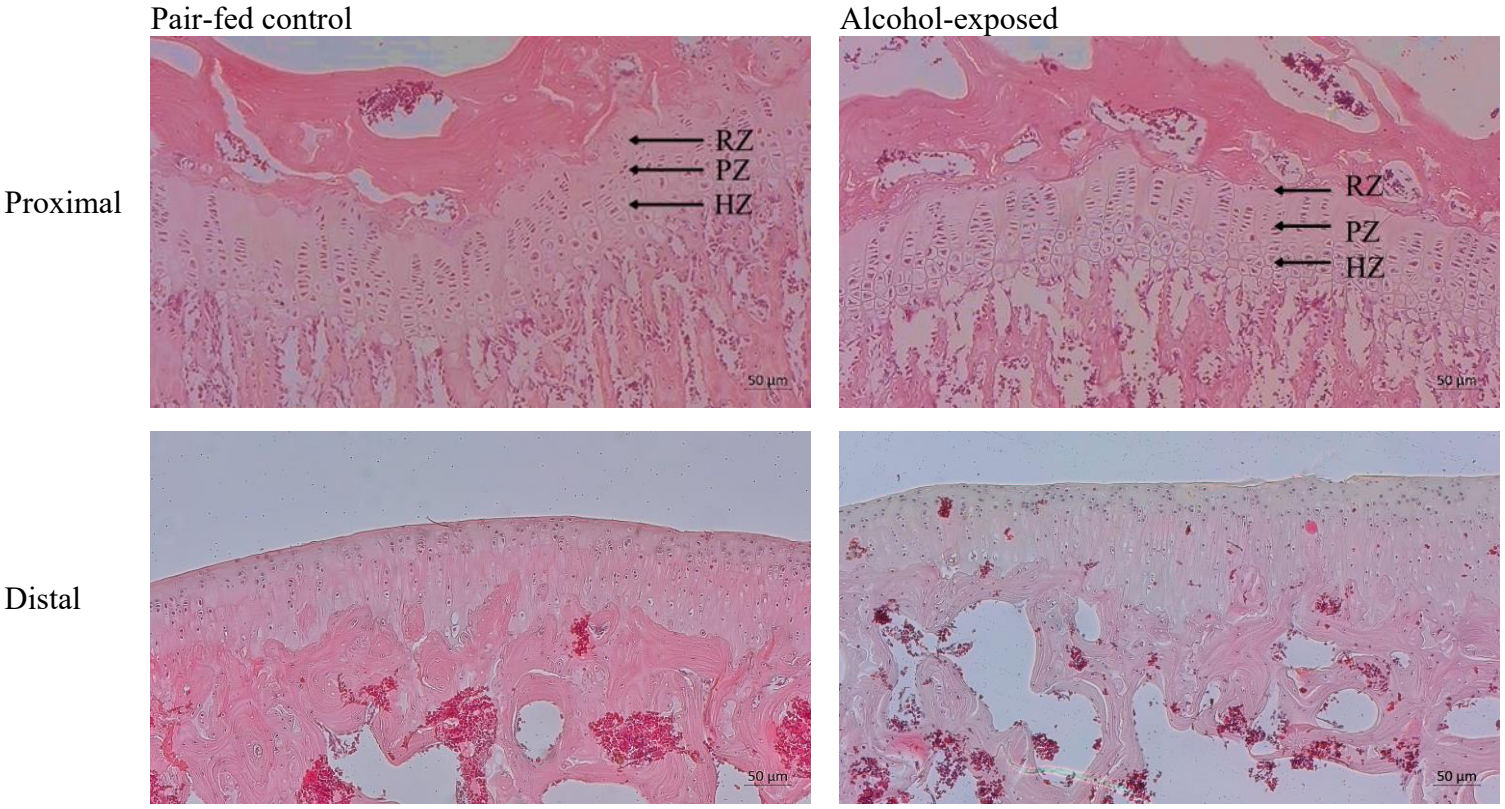


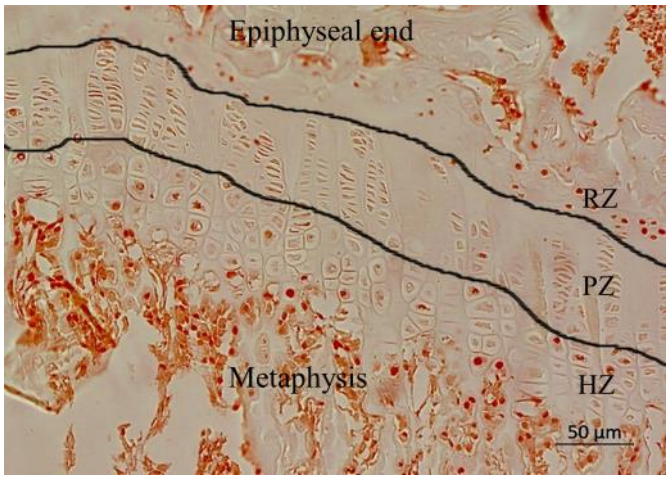
Figure 3.4.5: Haematoxylin and Eosin-stained sections of the proximal and distal epiphyseal growth plates of the humeri for the pair-fed control and alcohol-exposed groups in male rats of the binge alcohol recovery model.

Upon comparing the male and female animals in this group, it was firstly noted that the growth plates appeared of similar sizes. Neither sex showed an overt size difference over the other specifically in the proximal extremity. Furthermore, in the open growth plates, wherein the active zones were visible, alcohol exposure followed by alcohol abstinence resulted in clear distinctions between the different active zones in both males and females as the chondrocyte zones were well defined in both sexes. Finally, ossification was associated with both sexes as most of the distal growth plates had ossified.

3.5 Immunohistochemistry (IHC): Using the anti-Ki-67 antibody

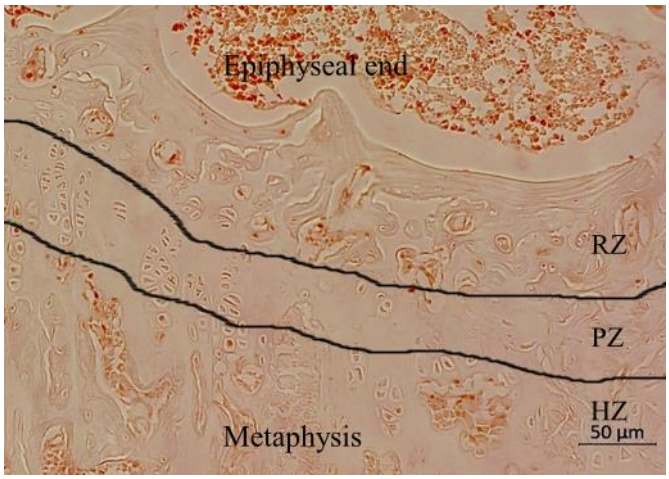
Levene's test for equality of variances showed that p> 0.05 therefore, similarity of variance in the associated data can be assumed. Photomicrographs of the stained tissue for all the groups are also provided including a reference image (Fig 3.5.1) for both the proximal and distal epiphysis to assist with visual orientation of the photomicrographs.

Proximal growth plate



(A)

Distal growth plate



(B)

Figure 3.5.1: Reference illustrations of the humeral proximal (A) and distal epiphysis (B) showing the active chondrocytes in the resting zone (RZ), proliferative zone (PZ) and hypertrophic zone (HZ).

Group 1:

Significant findings:

No significant results in this group.

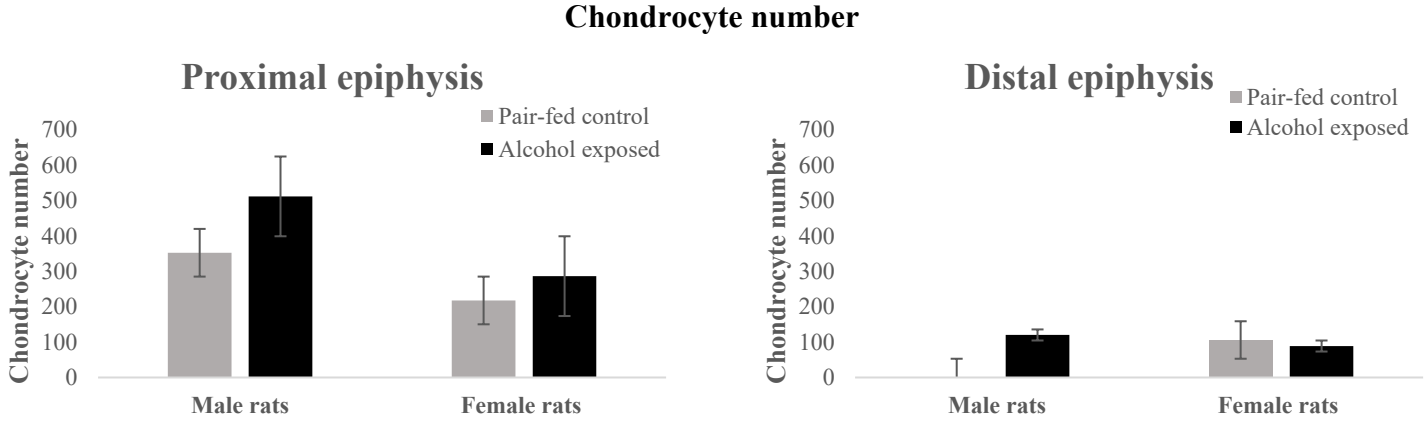
Non-significant findings:

A non-significant increase in chondrocyte proliferation in the female proximal growth plates was observed, with alcohol-exposed humeri showing more proliferating cells (286 ± 139.30) than pair-fed control group (217 ± 68.72) ($p > 0.05$) (Fig. 3.5.2A) (Fig. 3.5.3). In the distal growth plates, reduced chondrocyte proliferation was observed, with alcohol-exposed humeri (89 ± 50.20) showing fewer proliferating cells than pair-fed controls (106 ± 65) ($p > 0.05$) (Fig. 3.5.2B) (Fig.3.5.3).

In males, in a non-significant increase in chondrocyte proliferation was noted in the proximal growth plates, with alcohol-exposed humeri (512 ± 21.92) showing more proliferating cells than pair-fed controls (352 ± 105.95) ($p > 0.05$) (Fig. 3.5.2A) (Fig. 3.5.4). In the distal growth

plates, alcohol-exposed humeri were associated with open growth plates (two out of three growth plates); while pair-fed control humeri showed closed plates (all three growth plates), alcohol-exposed humeri remained open but were in the process of closing (mean = 120 ± 88.03) (Fig. 3.5.2B) (Fig. 3.5.4).

In the pair-fed control groups, males (352 ± 105.95) had more proliferating chondrocytes than females (217 ± 68.72) in the proximal growth plates, though the difference was not significant ($p = 0.069$). In the distal growth plates, males had closed plates (four out of six growth plates), while females showed a mix of open (four out of six growth plates) and closed plates (two out of six growth plates) (mean = 106 ± 65), with no significant difference ($p > 0.05$) (Fig. 3.5.2) (Fig. 3.5.3) (Fig. 3.5.4). In the alcohol-exposed groups, males (512 ± 21.92) had more proliferating chondrocytes than females (217 ± 68.72) in the proximal growth plates, but this was not significant ($p > 0.05$). A similar pattern was observed in the distal growth plates, with males (120 ± 88.03) having more proliferating chondrocytes than females (89 ± 50.20), but the difference was not significant ($p > 0.05$)) (Fig. 3.5.2) (Fig. 3.5.3) (Fig. 3.5.4).



(A) (B)

Figure 3.5.2: Chondrocyte numbers of the proximal epiphysis (A) and distal epiphysis (B) of the chronic binge consumption model. The mean values for this parameter are represented for both pair-fed control and alcohol-exposed groups in male and female animals and the error bars represent the standard deviation.

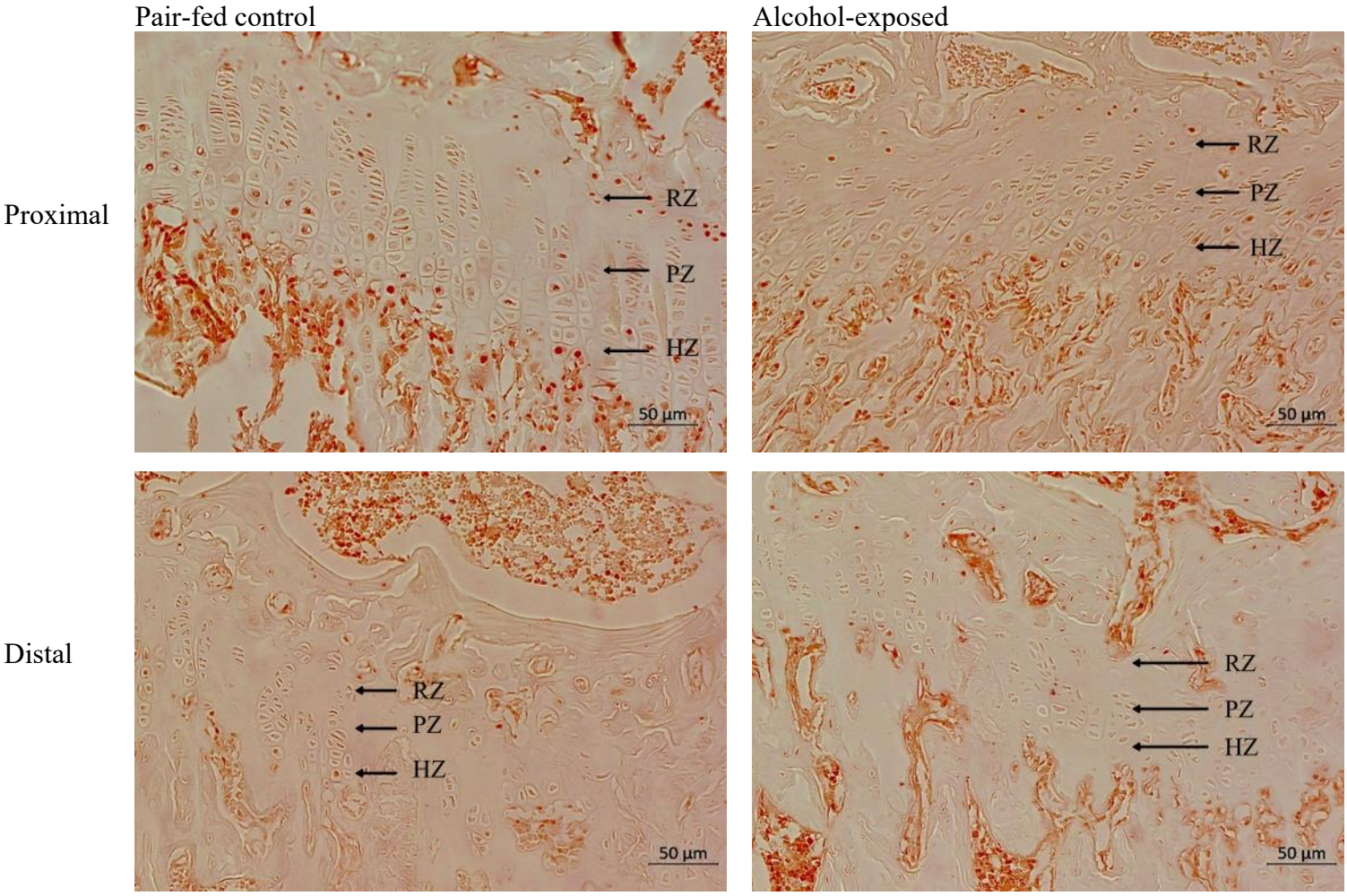


Figure 3.5.3: Immunolabeled humeral chondrocytes using the anti-Ki-67 antibody. Images are representative sections of the proximal and distal epiphyseal growth plates for the pair-fed control and alcohol-exposed groups in female rats of the chronic binge consumption model.

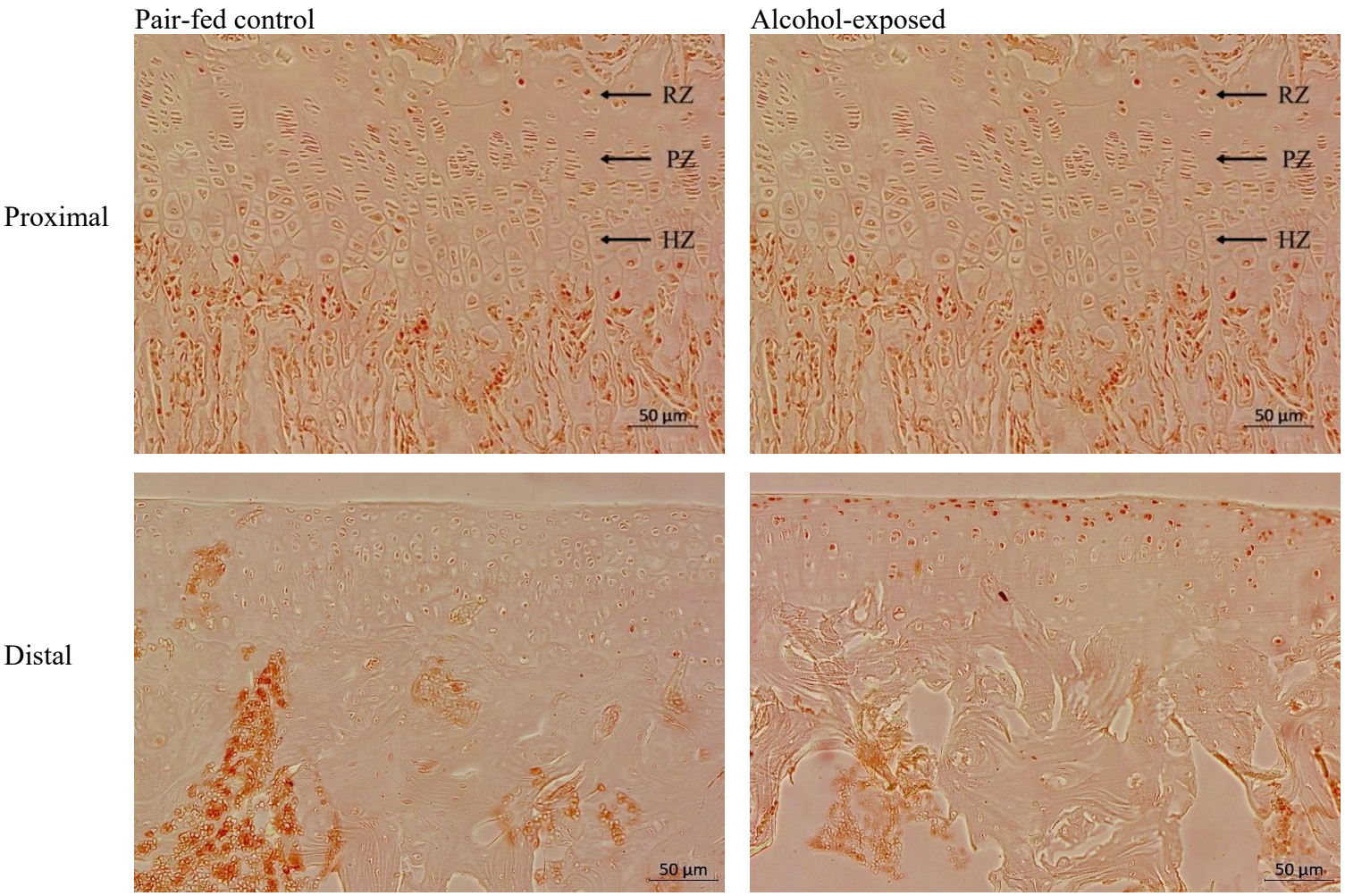


Figure 3.5.4: Immunolabeled humeral chondrocytes using the anti-Ki-67 antibody. Images are representative sections of the proximal and distal epiphyseal growth plates for the pair-fed control and alcohol-exposed groups in male rats of the chronic binge consumption model.

Group 2:

Significant findings:

In the pair-fed control groups, females (422 ± 77.81) had significantly more proliferating chondrocytes than males (191 ± 172.32) in the proximal growth plates ($p = 0.009$) (Fig. 3.5.5A) (Fig. 3.5.6) (Fig. 3.5.7).

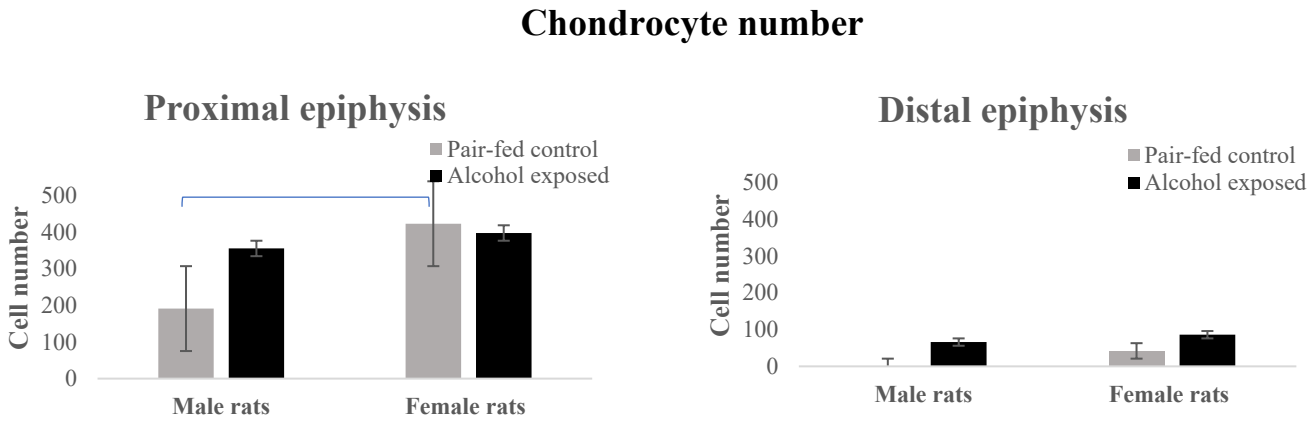
Non-significant findings:

A non-significant decrease in chondrocyte proliferation was seen in the female proximal growth plates, with alcohol-exposed humeri (397 ± 21.21) showing fewer proliferating cells than pair-fed controls (422 ± 77.81) ($p > 0.05$) (Fig. 3.5.5A) (Fig. 3.5.6). In the distal growth

plates, there were growth plate closures observed in most humeri (three out six growth plates that still remained intact for counting). In the few open plates (two out of six growth plates), alcohol-exposed humeri (86 ± 2.82) had more proliferating chondrocytes than the open plates of pair-fed controls (41 ± 2.12), though the difference was not significant ($p > 0.05$) (Fig. 3.5.5B) (Fig. 3.5.6).

In the male proximal growth plates, a non-significant increase in chondrocyte proliferation was noted, with alcohol-exposed humeri (355 ± 70.52) showing more proliferating cells than pair-fed controls (191 ± 172.32) ($p > 0.05$) (Fig.3.5.5A) (Fig. 3.5.7). In the distal regions, pair-fed control humeri had closed plates (all three sections), while alcohol-exposed humeri showed a few open plates (one out of three), nearing closure (mean = 66 ± 4.24) ($p = 0.101$).

In the distal growth plates, most male growth plates were closed (four out of six growth plates), whereas females had a mix of closed and open plates (three closed and two open growth plates), but the difference was not significant ($p > 0.05$) (Fig.3.5.5) (Fig. 3.5.6) (Fig. 3.5.7). In the alcohol-exposed groups, females (397 ± 21.21) had more proliferating chondrocytes than males (355 ± 70.52) in the proximal growth plates, though the difference was not significant ($p > 0.05$). A similar trend was observed in the distal growth plates, with females (86 ± 2.82) having more proliferating chondrocytes than males (66 ± 4.24), but this was also not significant ($p > 0.05$) (Fig. 3.5.5) (Fig. 3.5.6) (Fig. 3.5.7).



(A) (B)

Figure 3.5.5: Chondrocyte numbers of the proximal epiphysis (A) and distal epiphysis (B) of the binge alcohol recovery model. The mean values for this parameter are represented for both pair-fed control and alcohol-exposed groups in male and female animals and the error bars represent the standard deviation. Significant differences are indicated by connecting brackets.

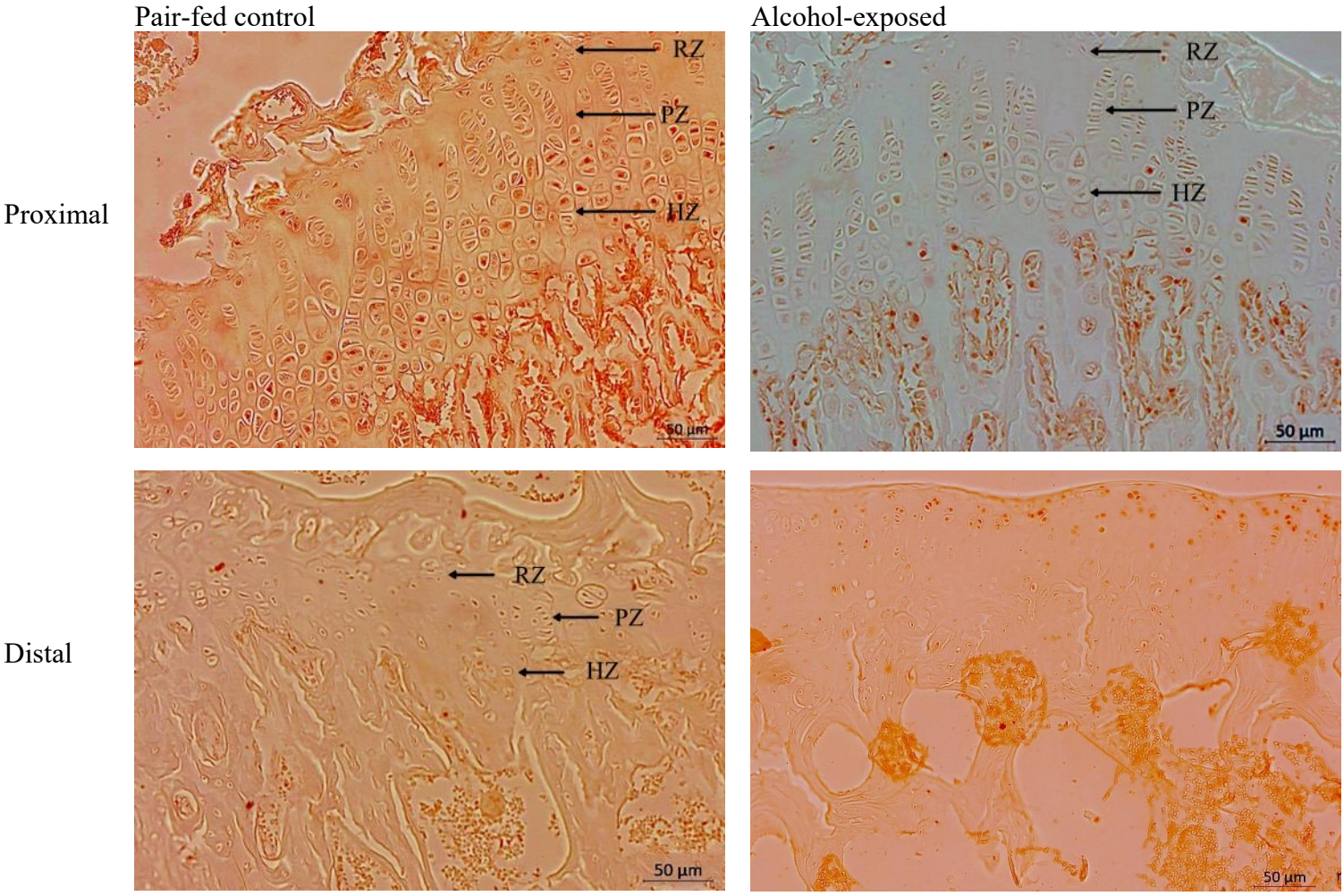


Figure 3.5.6: Immunolabeled humeral chondrocytes using the anti-Ki-67 antibody. Images are representative sections of the proximal and distal epiphyseal growth plates for the pair-fed control and alcohol-exposed groups in female rats of the binge alcohol recovery model.

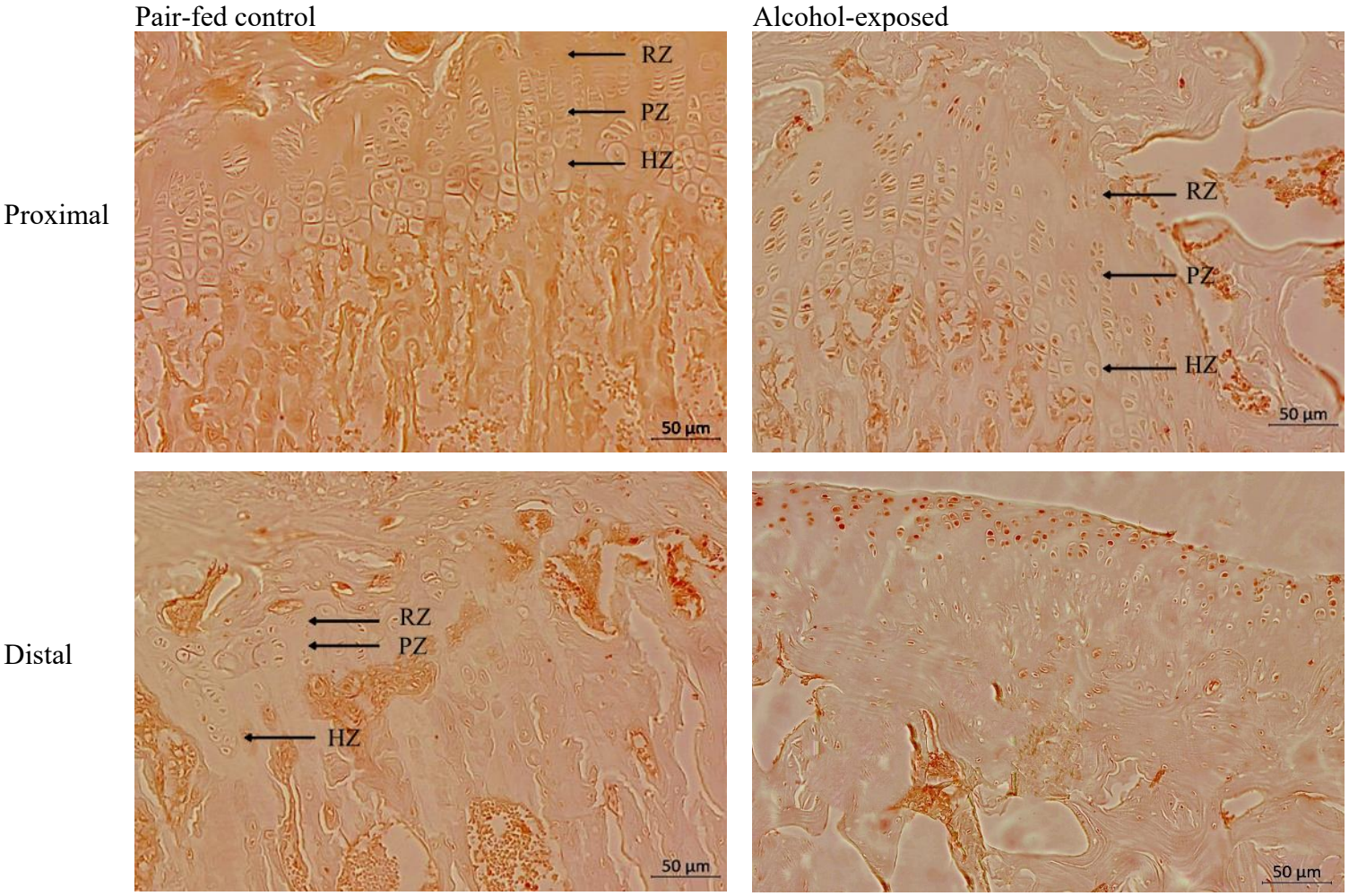


Figure 3.5.7: Immunolabeled humeral chondrocytes using the anti-Ki-67 antibody. Images are representative sections of the proximal and distal epiphyseal growth plates for the pair-fed control and alcohol-exposed groups in male rats of the binge alcohol recovery model.

In the current study, all proximal growth plates remained open, while the distal regions displayed a mix of open and closed growth plates. Notably, more animals in the binge alcohol recovery group exhibited closed distal growth plates, reflecting the older age of the animals in this model which was 15 weeks (7week age + 4-week alcohol-exposure + ~ 4-week abstinence period) compared to the animals ages in the chronic binge consumption model of 11 weeks (7-week age + 4-week alcohol exposure).

Chapter 4

Discussion and Conclusion

Discussion:

This study investigated the impact of adolescent binge drinking on the humerus using a Sprague Dawley rat model exposed to alcohol for four weeks, reflecting the adolescent association with binge drinking (Windle, 2003; Bosque-Prous *et al.,* 2017; Park & Kim, 2020; Fontes Marx *et al.,* 2021). This first group was termed the "chronic binge consumption model". Simultaneously, the recovery potential of the adolescent humerus was investigated through a period of alcohol abstinence, following the four-week alcohol exposure, to determine if the humerus could recover from the perturbations associated with binge drinking. This second group was termed "binge-alcohol recovery model". The objectives of the study were to evaluate the impact of binge drinking on gross humeral properties, assess whether binge drinking decreases humeral strength and assess the impact of binge drinking on humeral growth and development. Methods included osteometric analysis, 3D-μCT scanning, tensile testing, H&E staining, and immunohistochemistry.

Significant findings:

The overall results presented some significant findings in both groups. Some were specific to a particular sex while other findings were the results of comparisons performed between the sexes.

Regarding females, group 1 female humeral weights were significantly impacted by alcohol exposure as alcohol-exposed humeri weighed less on average than pair-fed control humeri. It has been previously reported that alcohol may disturb the bone remodelling process in females as it affects oestrogen functioning (Turner and Sibonga, 2001). Oestrogen plays a role in maintaining the life span of bone forming cells, such as osteoblasts, and reducing the life span of bone resorbing cells, which are osteoclasts. Moreover, alcohol consumption has been linked to decreased oestrogen levels in women (Turner and Sibonga, 2001; Khosla *et al.,* 2012). Consequentially when alcohol is consumed in young women, oestrogen levels have been observed to decline and the life span of osteoblasts decreases while that of osteoclasts increase encouraging bone resorption which can lead to decreased bone mass (Turner *et al.,* 1994). This could underlie why reduced humeral weights in females were observed. In the binge-alcohol recovery model, biomechanical testing revealed that alcohol-exposed female humeri were significantly easier to fracture even after a period of alcohol abstinence. Alcohol encourages bone resorption through decreased oestrogen levels which reduces bone mass accrual. This may underlie the increased fracture risk associated with binge drinking (Turner and Sibonga,

2001). Block *et al* (1993) reported reduced oestrogen levels two weeks after alcohol exposure in adolescent females after moderate alcohol consumption. The observed result in group 2 females suggests that binge drinking, like moderate alcohol exposure, may reduce oestrogen levels, with effects that persist over time (Block *et al.,* 1993).

Regarding males, assessment of trabecular morphometry showed that trabecular number (Tb.N) significantly increased and trabecular spacing (Tb.Sp) significantly decreased in the proximal epiphyses of group 2 humeri. Heavy alcohol consumption, such as binge drinking, correlates with reduced levels of testosterone in males as alcohol encourages the conversion of testosterone to oestrogen through a process termed aromatisation, which also has been observed in rat models (Gordon *et al.,* 1978, 1979). During aromatisation, testosterone and its precursor androstenedione are metabolised into oestrogens such as oestradiol and oestrone respectively hence increased oestrogen levels may be detected in binge-drinking males (Gordon *et al.,* 1978, 1979). Increased oestrogen in males is associated with enhanced bone cell production such as osteoblasts (Gordon *et al.,* 1979). The observations of Gordon *et al.* (1978, 1979) support the current findings regarding the observed changes and are suggestive of increasingly robust bone structure as a result of abstinence post an alcohol exposure period.

Regarding the sex differences observed, the findings demonstrated that sexual dimorphism plays a significant role in how males and females respond to alcohol exposure as male and female animals exhibited distinct differences in response to binge drinking.

In terms of osteometric measurements, males generally displayed greater weights, lengths, and bicondylar breadths compared to females in both study groups. Previous research by Clark *et al.* (2006) supports these findings, noting that sex differences in humeral morphology are established before puberty, with males exhibiting larger periosteal diameters resulting in wider and heavier humeri. In terms of trabecular morphometry, females displayed reduced bone volume (BV/TV) and trabecular number (Tb.N) along with greater thickness (Tb.Th) and spacing (Tb.Sp), in the proximal regions of the alcohol-exposed group than the males. Reduced bone volume (BV/TV) and trabecular number (Tb.N) could be indicative of decreased bone formation (Wezeman *et al.,* 2007) and the increased trabecular spacing (Tb.Sp) could point to greater bone porosity. Reduced oestrogen levels associated with alcohol consumption in females may underlie these findings (Turner and Sibonga, 2001; Khosla *et al.,* 2012). Moreover, females often experience lower oestrogen loestrusThe non-significant reduction in

chondrocyte proliferationevels post-ovulation, which may have coincided with their binge drinking cycles (Sato *et al.,* 2016). The oestrus cycle in female rats occurs between six to eight times a month as each cycle is between four and five days long. Each cycle consists of four stages namely: metestrus, dioestrus, proestrus and oestrus wherein dioestrus is when oestrogen levels are at their lowest (Emanuele *et al.*, 2002). Given the duration of alcohol exposure (four weeks), it is plausible that it coincided with the dioestrus stage, further contributing to the results observed in osteometric measurements and assessment of trabecular morphology.

In males however, moderate alcohol exposure in males not only leads to altered testosterone levels but also increased oestrogen levels through the aromatization of androgens, promoting bone growth (Purohit, 2000). The dosage of alcohol (20% (v/v)) may have been moderate for males as binge drinking is defined differently between sexes thus supporting humeral growth and recovery (Gowin *et al*., 2021). Male humeri demonstrated greater tensile strength, likely attributed to a larger periosteal diameter influenced by higher testosterone levels that promote periosteal expansion (Seeman, 2003; Clark *et al*., 2006). In females, oestrogen limits periosteal expansion leading to reduced periosteal diameter compared to males (Seeman, 2003). Since testosterone exerts its effects more in males than females during adolescence and oestrogen is a limiting factor in terms of periosteal diameter, this may underlie the tensile strength disparity observed between the sexes (Li & Fennessy, 2021). During biomechanical testing, female humeri exhibited significantly lower resistance to fractures than male humeri during biomechanical testing which correlates with the reduced BV/TV observed during Micro-CT analysis. These results may suggest a potential reduction of humeral strength in females following binge drinking, which might not fully recover during periods of abstinence and could possibly be associated with an increased risk of fracture. This finding aligns with White (2020), who reported that female tissues are more susceptible to the long-term impacts of alcohol.

The morphological changes in female humeri were pronounced compared to the males. More chondrocytes were visually apparent in the male growth plates compared to the female growth plates, a finding consistent with Hogan *et al. (*1997). In terms of chondrocyte arrangements, males did not exhibit much chondrocyte arrangement disorganisations. Notably, the growth plates of alcohol-exposed males were smaller, indicating potential disruption in growth hormone (GH) functioning, which is critical for skeletal growth (Shim, 2015). Zoetis *et al.* (2003) highlighted that female growth plates develop and close earlier than males but in the chronic binge consumption model closed growth plates were more prevalent in the male

animals. This could suggest a delayed closure of distal growth plates in females, (Zoetis *et al.,* 2003). In the binge alcohol recovery model, closed growth plates were more frequently observed in males, supporting the notion that male humeri recovered better than female humeri. The IHC analysis using anti-Ki-67 antibodies highlighted the differential responses to alcohol between sexes. In the chronic binge consumption model, female humeri displayed reduced chondrocyte numbers as a consequence of alcohol exposure, while male humeri exhibited an increase in chondrocyte numbers. However, in the binge alcohol recovery model, females had higher chondrocyte numbers than males, even though this difference was non-significant. This aligns with findings from Kalbfleisch *et al.* (1963) and Laitinen *et al.* (1991), who reported hypercalcemia, hypercalciuria and hypoparathyroidism in males resulting from excessive drinking, which therefore extends to binge drinking. These conditions stimulate increased PTH release to promote bone formation as a compensatory mechanism for the bone damage. This therefore suggests that excessive alcohol consumption, such as binge drinking, in males leads to compensatory mechanisms that promote bone formation, whereas the decline in female oestrogen levels leads to a decline in their bone mass and formation. Overall, the observations noted between the males and females illustrate the complex interactions between sexual dimorphism and alcohol consumption and how this interaction affects bone health.

Non-significant findings:

The non-significant results from both the chronic binge and binge alcohol recovery models indicate that 4-week adolescent binge drinking had minimal impact on male and female humeri for the most part, and abstinence afterward led to no significant recovery-related changes.

The chronic binge consumption model predominantly showed minor perturbations of four-week drinking on the adolescent humerus. The prevalence of non-significant changes may stem from factors such as alcohol dosage, administration method, exposure duration, diet, and restricted housing movement. This is because previous studies (Sampson *et al.,* 1996; Hogan *et al.*, 1997; Sampson *et al.,* 1999; Wezeman *et al.,* 1999 Wezeman *et al.,* 2000; Callaci *et al.,* 2004; Callaci *et al.,* 2006; Lauing *et al.,* 2008) contrastingly observed significant changes in bones as a consequence of binge drinking. Sampson *et al.* (1996) and Hogan *et al.* (1997) exposed female rats to alcohol for eight weeks via a modified Lieber de Carli diet (liquid diet comprising of 400 IU/l vitamin D; 1.3g/l of Calcium (Ca^{2+}); 1.75g/l of phosphorus and 8.1% v/v alcohol), which was the animals' sole source of nutrients and observed significant declines in femoral strength. Wezeman *et al.* (1999) employed the Lieber de Carli diet for eight weeks

(60 days) and observed significant femoral length and weight reductions in female rats associated with alcohol exposure. Wezeman *et al.* (2000) similarly employed the Lieber de Carli diet but for four weeks (28 days) and also observed significant femoral length and weight reductions in female rats associated with alcohol exposure. In the current study, the animals were subjected to a 20% (v/v) alcohol solution (3 g/kg) for three days per week for four weeks (28 days), via oral gavage, and a solid food diet of rat food pellets that consisted of grains and vegetable protein among other ingredients. Solid foods reduce the volume of alcohol absorbed into the circulatory system and thus reduce the volume of alcohol to which tissues could be exposed (Caballería, 2003). Therefore, the consumption of solid food in tandem with binge alcoholic exposure could have contributed to the predominantly non-significant humeral changes in both sexes for the chronic binge consumption model

Moreover, Iwaniec and Turner (2013) previously reported how oral gavage is not consistently associated with detrimental changes in bone compared to the Lieber de Carli diet and intraperitoneal (IP) injections in alcohol-related studies. Sampson *et al.* (1999) subjected female animals to a 5% alcohol solution (1.14 g/kg) via oral gavage two days per week for seven weeks and observed non-significant and few significant increases in bone length in tibiae and femora, respectively. Callaci *et al.* (2004) exposed male rats to 20% (v/v) alcohol for four consecutive days per week for three weeks via intraperitoneal (IP) injections and observed significant alterations in trabecular bone where parameters such as BV/TV were significantly reduced, which contrasts the current study as non-significant increases in BV/TV were observed in the male animals. Therefore, the method of alcohol administration, which was oral gavage in this study, could also be responsible for the results associated with the chronic binge consumption model. Additionally, the four-week exposure period may have been too short a period to observe significant alterations, as longer durations (Sampson *et al.,* 1996; Hogan *et al.,* 1997; Wezeman *et al.,* 1999; Wezeman *et al.,* 2000) have been associated with more substantial effects in response to alcohol. The results imply that the four-week period of the study may have been insufficient to detect notable changes in the microarchitecture of the humerus due to binge drinking.

Another reason for the results could be limited movement as the study animals were housed in cages. While the cages were of standard size to allow movement of animals, they lacked objects for play or exploration that could have encouraged more physical activity and therefore more mechanical loading of bone (Liu et al., 2022). This may have limited the biomechanical

stressors needed for bone remodelling and growth hence non-significant changes were observed.

Although the findings of the present study are predominantly non-significant, their value remains considerable within the context of alcohol research, particularly with regard to the physiological mechanisms involved in binge drinking. Despite the inherent limitations of animal models in fully replicating the complex human physiology (Ripley & Stephens, 2011), this study was designed to address critical factors that contribute to the effects of alcohol consumption. This includes the method of alcohol administration and solid food nutrition. These factors are frequently overlooked in some animal models but are essential for accurately approximating the human drinking experience.

Previous studies investigating binge drinking utilised alcohol liquid diets, such as the Lieber de Carli model (Sampson *et al.,* 1996; Hogan *et al.,* 1997; Wezeman *et al.,* 1999; Wezeman *et al.,* 2000). While these diets have their advantages in terms of controlling alcohol intake, they also present several notable drawbacks. Chief among these is their nutritional inadequacy, particularly when used as the sole source of nutrition over extended periods (Anji & Kumari, 2008). When animals are maintained on alcohol liquid diets, they can lose body weight. This is not fully reflective of human drinking patterns, where alcohol is typically consumed alongside solid food (Piano, 2001). The presence of solid food in the stomach can significantly alter the absorption dynamics of alcohol, delaying its entry into the bloodstream and modifying its subsequent metabolism in the liver (Horowitz *et al.,* 1989). This difference in absorption rates between animal models and humans may be a contributing factor to the observed discrepancies in findings across studies.

Moreover, the method of alcohol administration is a key consideration. In human consumption, alcohol passes through the digestive tract before entering the circulatory system, a process that is mirrored in this study through the use of oral gavage. This method ensures that alcohol undergoes some degree of gastric processing before being absorbed into the bloodstream (Bode & Bode, 2000). In contrast, some studies have employed intraperitoneal (IP) injections (Callaci et al., 2004; Callaci et al., 2006; Lauing et al., 2008), which bypass the digestive system entirely, allowing for more rapid absorption of alcohol directly into the bloodstream. This methodological difference can have significant implications for the physiological responses

observed in experimental animals, as the absence of digestive processing may lead to more pronounced and accelerated systemic effects (Iwaniec and Turner, 2013)

Given these methodological considerations, it is plausible that the non-significant findings of the current study reflect the inherent protective mechanisms associated with the natural course of food and alcohol consumption. The presence of solid food and the gastric processing of alcohol likely attenuate some of the physiological impacts observed in models that do not account for these factors. Thus, the results of this study, though non-significant, may suggest that these natural protective mechanisms offer a buffer against the more extreme effects of alcohol seen in other models that fail to replicate the complexity of human drinking patterns.

In terms of biomechanical testing, to date, no studies have used the three-point bending test to simultaneously examine the impact of adolescent binge drinking and the impact of alcohol abstinence on humeral strength. Previous studies that incorporated the three-point bending test for biomechanical analysis of the long bones primarily used the femur and tibia (Sampson *et al.,* 1996; Hogan *et al.* 1997; Lauing *et al.*, 2008; Föger-Samwald *et al.,* 2018). The limited studies that made use of the humerus aimed to determine the impact of medication on the bone (Frankle & Borrelli, 1990; Rundle *et al.,* 2014). Prodinger *et al.* (2018), however, performed the three-point bending test on the femur, tibia and humerus, using a rat model, to compare their response to tensile strength tests. Great similarity was observed in terms of their response, therefore suggesting that three-point bending tests performed in previous studies using the femora and tibia can be used to understand current bone strength tests examining the humeri (Prodinger *et al.*, 2018). In terms of tensile strength testing, four-week alcohol exposure did not significantly impair humeral strength, as minute differences existed between the alcohol-exposed and pair-fed control humeri for both males and females in the chronic binge consumption model. While the alcohol-exposed humeri were slightly easier to fracture than the pair-fed control humeri, the results contrast Hogan *et al.* (1997) and Callaci *et al.* (2004) who detail an evident reduction of bone compressive strength as a result of binge drinking. Differences in exposure time and alcohol administration between the studies could underlie these contrasting results. Alcohol exposure time in the Sampson *et al.* (1996) study was eight weeks via the Lieber-DeCarli diet in female rats and Callaci *et al.* (2004) exposed male rats to alcohol for three weeks via intraperitoneal injections (IP injections). Alcohol exposure via IP injections has resulted in considerable alterations in bone (Callaci *et al.,* 2004; Rai *et al.,* 2008)

which may underlie why significant changes were not observed in the current study as the oral gavage method was used for four weeks.

In terms of chondrocyte morphology, the histological findings presented appear similar to Miralles-Flores and Delgado-Baesa (1992) as they reported askew arrangement of columnar chondrocyte stacks and reduced hypertrophic regions yet their findings originate from 15-day-old female rat tibiae prenatally exposed to alcohol for four-weeks. Snow and Keiver (2007) contrastingly reported increased hypertrophic regions and reduced sizes of the resting and proliferative regions in the tibiae of 21-day old rat foetuses prenatally exposed to alcohol wherein the mothers were exposed to alcohol for six weeks. Both studies by Miralles-Flores and Delgado-Baesa and Snow and Keiver involved prenatal alcohol exposure and alcohol exposure via liquid diets compared to the post-natal alcohol exposure via oral gavage in this study. While these two previous studies focused on prenatal alcohol exposure and the current study focused on post-natal alcohol exposure, both types of studies indicate that alcohol exposure at different stages of youth may cause subtle changes in morphology of growth plate chondrocytes.

Additionally, the histological results of the current study imply that binge drinking could disrupt hormonal functioning associated with bone development, particularly the roles of growth hormone and TGF-β signalling pathways, which are critical during adolescence. The transforming growth factor beta (TGF-β) superfamily performs diverse functions crucial for bone development, especially during adolescence (Wozney, 1989; Wu *et al.,* 2024). TGF-β molecules work in tandem with an intracellular mediator called Smad4 (Sakou *et al.,* 1999; Shi and Massague, 2003; Zhang *et al.,* 2005). Smad4 forms part of the Smad family of intracellular mediators and alcohol has been shown to attenuate Smad functioning. Gerjevic *et al.* (2012) showed that alcohol attenuates Smad4 functioning. When alcohol is consumed, it is metabolised in the liver and it disrupts the function of a peptide hormone called Hepcidin, which is one of the key regulators of iron homeostasis (Pigeon *et al.,* 2001; Park *et al.,* 2001). Alcohol disrupts iron homeostasis by downregulating the production of Hepcidin and Smad4 mediates Hepcidin transcription in the nucleus. Excessive alcohol consumption, such as binge drinking, significantly attenuates Smad4 binding hence Hepcidin is downregulated (Harrison-Findlik *et al.,* 2006; Gerjevic *et al.*, 2012). Furthermore, Zhang *et al.* (2005) demonstrated that Smad4 abolition results in disorganised growth plate chondrocyte arrangement in rodent tibia (growth plate chondrocytes were not arranged in their typical columnar fashion). Attenuated

Smad4 functioning has also been associated with reduced expression of the genes responsible for encoding Parathyroid related protein (PTHrP) and Indian Hedgehog (IHH) which has previously resulted in disorganised growth plate chondrocyte appearance (Karp *et al.,* 2000). Emons *et al.* (2011) also observed that dysfunctional PTHrP and IHH correlates with disorganised columnar chondrocyte arrangement. Though the analysis of Smad4 functioning was not an objective of this study, the disorganisation of chondrocyte columns in the proximal female growth plates suggests that Smad4 functioning could have been attenuated to an extent. Smad4 is connected to oestrogen signalling pathways, as it behaves as a transcription corepressor, and oestrogen signalling pathways are some of the predominant pathways in the female body (Wu *et al.,* 2003). As previously explained, oestrogen functioning is affected by alcohol; therefore, this may underlie why disorganisation of the columnar chondrocyte arrangement was predominantly evident in female growth plates (Wu *et al.,* 2003). Moreover, as oral gavage was used to administer alcohol in the current study, four-week binge drinking may have attenuated Smad4 functioning, especially in the females.

Regarding chondrocyte proliferation, our findings disagree with Roper *et al.* (2016), who reported reductions of chondrocyte numbers in rodent tibia due to binge drinking, particularly in the proximal regions. Differentiation and development of mesenchymal stem cells into mature chondrocytes takes place during bone development and fracture healing. Roper *et al.* (2016) showed that binge alcoholic exposure attenuates endochondral ossification of the tibia, thus leading to reduced chondrocyte numbers. Even though tibiae and humeri both develop through endochondral ossification and possess a similar shape, wherein there is a diaphysis and two epiphyses, their growth plates have different fusion times (humeral growth plates fuse at earlier ages than tibia) and patterns. This may underlie the contrasting results in the studies and underlie why alcohol may respond differently between different bones. Moreover, Roper *et al.* (2016) employed IP injections of 20% (v/v) alcohol so the method of alcohol administration further underlies why their results differ from ours despite employing the same alcohol dosage. Excessive alcohol consumption increases the production of reactive oxidative species (ROS). ROS is important in endochondral ossification as it encourages chondrocyte hypertrophy, which proceeds into bone formation (Tsermpini *et al.,* 2022). When ROS is present in excess, it may cause DNA damage to cells. Due to the current study incorporating a solid food diet, the amount of alcohol that entered the humerus did not induce as much damage. This may explain why the current study observed an increase in chondrocyte numbers specifically in the

proximal regions. The distal regions observed a decline due to growth plate closure which is a sign of proper humeral development therefore no significant damage caused by binge drinking.

Focussing on the binge alcohol recovery model, the associated results showcased that alcohol-exposed humeri were, for the most part, comparable to pair-fed control humeri. Following alcohol abstinence, female rats showed comparable humeral lengths and bicondylar breadths, and a non-significant reduction in humeral weight compared to pair-fed control humeri. Males exhibited minimal differences across all osteometric measurements between alcohol-exposed and pair-fed control humeri in both groups. Micro-CT analysis also indicated, for the most part, that the alcohol-exposed humeri were similar to the pair-fed control humeri. Similarly, tensile strength testing predominantly showed non-significant changes between the alcohol-exposed and pair-fed control humeri. In terms of histological analysis, most proximal growth plates showed typical columnar chondrocyte arrangements, and many distal growth plates were closed in both sexes. Regarding chondrocyte proliferation, males exhibited a non-significant increase in proliferating chondrocytes in the proximal epiphyses while females showed a reduced number, though this was not significant.

The above-mentioned results differ from Sampson and Spears (1999) who did not observe similarity between alcohol-exposed and control tibiae and femora of four-week alcohol exposed female rats. Wezeman *et al.* (1999) reported a lack of recovery post an abstinent period in the femora and tibiae of male rats. Several factors may explain these discrepancies, particularly differences in study design. Sampson and Spears (1999) and Wezeman *et al.* (1999; 2000) utilized the Lieber de Carli diet as the sole nutrient source, whereas this study employed oral gavage along with standard rat pellets. Additionally, the Wezeman *et al.* (1999) involved longer alcohol exposure (60 days) followed by a 90-day abstinence, compared to the current study's four-week exposure and 26-day abstinence. The reduced exposure time in the current study may be why reduced perturbations were observed in the humeri. Another factor could be that Wezeman *et al.* (1999; 2000) studied the femur, whereas the current study focused on the humerus. Perhaps alcohol-related changes to bone are bone- and site-specific and may not have affected the humerus as much as the femur. Lauing *et al.* (2008) employed similar time periods as the current study regarding the feeding and abstinence periods and they noted similarity between alcohol-exposed and control samples similar to the current study, to which they reported it as recovery. They studied the tibiae and lumbar vertebrae of adolescent male Sprague Dawley rats. The study design and experimental conditions mirrored the current study

except that IP injections were the method of alcohol administration in their study as opposed to oral gavage in this study.

The non-significant reduction in chondrocyte proliferation in alcohol-exposed female humeri in this study may be linked to decreased oestrogen levels which are critical for bone physiology. This has been shown in both human and animal studies (Block *et al.*, 1993; Turner and Sibonga, 2001). It is therefore plausible that a non-significant reduction of proliferative chondrocytes observed in the females post an abstinent period could be attributed to this.

Furthermore, the interaction between alcohol and testosterone which results in increased oestrogen may explain the non-significant increase in proliferating chondrocytes observed in male humeri as increased oestrogen levels promote bone growth (Gordon *et al.,* 1978, 1979; Turner and Sibonga, 2001). Interestingly, while male distal epiphyses showed evidence of proliferating chondrocytes in alcohol-exposed humeri, the pair-fed control group exhibited closed growth plates. Conversely, in females, alcohol exposure appeared to coincide with increased chondrocyte numbers in distal growth plates. In both humans and rats, distal epiphyses typically close much earlier than proximal epiphyses. Human proximal humeral growth plates generally open and fuse between ages 12-20, while distal growth plates close between ages 11-19 (Zoetis *et al.,* 2003). On average within these age ranges, female growth plates tend to fuse earlier than males (Kvist *et al.,* 2021). The animals in this study were seven weeks old when they were exposed to alcohol for a four-week period. Therefore, they were 11 weeks old when exposure period ended. This period falls within the expected time period that the distal growth plates typically close. The binge alcohol recovery model highlights the complex interactions between alcohol and hormonal regulation of bone growth and recovery, emphasizing that further research to understand these mechanisms fully is essential.

Limitations:

The experimental design may be considered a sedentary model as the animals were housed in 430mm (length) x 220mm (width) x 200mm (height) cages where 2 rats of the same sex were paired together in each cage. While the cages were of standard size to allow movement of animals, they lacked objects for play or exploration that could have encouraged more physical activity and therefore more mechanical loading of bone (Liu et al., 2022). This may have limited the biomechanical stressors needed for bone remodelling and growth hence non-significant changes were observed. Secondly, the oral gavage technique requires physical

restraining of animals for alcohol administration. This often creates stress in the study animals leading to elevated heart rates and blood pressure which may impact the overall results (Arantes-Rodrigues *et al.,* 2012). Binge drinking differs between individuals concerning the frequency of the binge episodes and the duration of each episode. Even though the focus was adolescents, who generally drink on weekends (hence three-day alcohol exposure per week), heterogeneity of drinking habits still exists among adolescents (Chung *et al.,* 2018). Moreover, since binge drinking is defined differently between males and females according to alcohol intake (Gowin *et al.,* 2021), male animals should have received a higher dosage than the females because males require higher doses and not the same dosage to be defined as binge drinkers especially considering first pass metabolism (Caballería, 2003).

Conclusion:

Overall, the findings indicate that four weeks of binge alcohol exposure did not cause severe structural damage to the humeri in either sex, as most parameters showed minimal or no change across both models. The results of the binge alcohol recovery model suggest that recovery may be possible and that male humeri respond better to alcohol exposure than female humeri. However, significant alterations in select measures, such as reduced humeral weights in females (Group 1), delayed fracture times in females (Group 2), and changes in trabecular architecture in males (Group 2), suggest that binge drinking, while not overtly damaging, did exert measurable adverse effects. Additionally, the study may indicate that the humerus exhibits site-specific responses to alcohol, suggesting that recovery processes and structural integrity could vary between proximal and distal regions. These results also indicate few sex-specific responses, showing the nuanced reciprocity between alcohol and skeletal development. Moreover, the findings underscore the complex interactions between sex, alcohol, and bone health, advocating for tailored approaches to better comprehend the impact of alcohol on skeletal growth and recovery. This nuanced understanding is essential for informing clinical practices and developing targeted interventions.

Future studies could explore the impact of binge drinking on hormones that contribute to skeletal growth such as parathyroid hormone, growth hormone, testosterone and oestrogen as the associated findings align with several previous studies that report on the impact of alcohol on these hormones. Moreover, future studies can explore how binge drinking impacts different bone cell populations in adolescent growth plates. As growth plates contain different cartilage

cells and bone cells, it would be of great interest to observe possible changes in population numbers due to binge drinking.

Future studies could explore the impact of binge drinking on hormones that contribute to skeletal growth such as parathyroid hormone, growth hormone, testosterone and oestrogen.

References:

Abrams, S.A. (2003) ‘Normal acquisition and loss of Bone Mass’, *Hormone Research in Paediatrics*, 60(Suppl. 3), pp. 71–76.

Alexandre, N. *et al.* (2024) ‘Biomechanical basis of bone fracture and fracture osteosynthesis in small animals’, *Biomechanical Insights into Osteoporosis*, pp. 1-47.

Amling, M. *et al.* (1999) ‘Rescue of the skeletal phenotype of vitamin D receptor-ablated mice in the setting of normal mineral ion homeostasis: Formal histomorphometric and biomechanical analyses1’, *Endocrinology*, 140(11), pp. 4982–4987.

Anley, C. *et al.* (2019) ‘Proximal humerus fractures - part 1: Conservative management’, *SA Orthopaedic Journal*, 18(3).

Arantes-Rodrigues, R. *et al.* (2012) ‘The effects of repeated oral gavage on the health of male CD-1 mice’, *Lab Animal*, 41(5), pp. 129–134.

Arias, C.F. *et al.* (2018) ‘Bone Remodeling: A tissue-level process emerging from cell-level molecular algorithms’, *PLOS ONE*, 13(9), pp. 1-19.

Aydin Kabakci, A.D. *et al.* (2017) ‘An osteometric study on humerus’, *International Journal of Morphology*, 35(1), pp. 219–226.

Block, G.D. *et al.* (1993) ‘Effects on pubertal hormones by ethanol abuse in adolescents’, *Alcoholism: Clinical and Experimental Research*, 17(2), pp. 505.

Bosque-Prous, M. *et al.* (2017) ‘Adolescent alcohol use and parental and adolescent socioeconomic position in six European cities’, *BMC Public Health*, 17(1), pp. 1-10.

Bouillon, R. *et al.* (2008) ‘Vitamin D and human health: Lessons from vitamin D receptor null mice’, *Endocrine Reviews*, 29(6), pp. 726–776.

Bouxsein, M.L. *et al.* (2010) 'Guidelines for assessment of bone microstructure in rodents using micro–computed tomography', *Journal of Bone and Mineral Research*, 25(7), pp. 1468–1486.

Brumbaugh, P.F. and Haussler, M.R. (1975) 'Specific binding of 1alpha,25-dihydroxycholecalciferol to nuclear components of Chick Intestine.', *Journal of Biological Chemistry*, 250(4), pp. 1588–1594.

Caballería, J. (2003) 'Current concepts in alcohol metabolism', *Annals of Hepatology*, 2(2), pp. 60–68.

Callaci, J.J. *et al.* (2004) 'The effects of binge alcohol exposure on bone resorption and biomechanical and structural properties are offset by concurrent bisphosphonate treatment', *Alcoholism: Clinical and Experimental Research*, 28(1), pp. 182–191.

Callaci, J.J. *et al.* (2006) 'Binge alcohol treatment increases vertebral bone loss following ovariectomy: Compensation by intermittent parathyroid hormone', *Alcoholism: Clinical and Experimental Research*, 30(4), pp. 665–672.

Changes Addiction Rehab (2022) *4 scary facts about binge drinking in South Africa*, *Changes Addiction Rehab*. Available at: https://changesrehab.co.za/4-scary-facts-about-binge-drinking-in-south-africa/ (Accessed: February 24, 2023).

Chappard, D. *et al.* (1991) 'Alcoholic cirrhosis and osteoporosis in men: A light and scanning electron microscopy study', *Journal of Studies on Alcohol*, 52(3), pp. 269–274.

Chauke, T.M., Van der Heever, H. and Hoque, M.E. (2015) 'Alcohol use amongst learners in rural high school in South Africa', *African Journal of Primary Health Care and Family Medicine*, 7(1), pp. 1-6.

Choi, S. E., Hong, S.W. and Yoon, S.O. (2015) 'Proposal of an appropriate Decalcification method of bone marrow biopsy specimens in the era of expanding genetic molecular study', *Journal of Pathology and Translational Medicine*, 49(3), pp. 236–242.

Chung, T. *et al.* (2018) 'Adolescent binge drinking: Developmental context and opportunities for prevention', *Alcohol research: current reviews*, 39(1), pp. 5-15.

Clark, E.M., Ness, A.R. and Tobias, J.H. (2006) 'Gender differences in the ratio between humerus width and length are established prior to puberty', *Osteoporosis International*, 18(4), pp. 463–470.

Clarke, B. (2008) 'Normal bone anatomy and physiology', *Clinical Journal of the American Society of Nephrology*, 3(Supplement_3), pp. 131-139.

Dees, L. and Skelley, C.W. (1990) 'Effects of ethanol during the onset of female puberty', *Neuroendocrinology*, 51(1), pp. 64–69.

De Leon-Oliva, D. *et al.* (2023) 'The rank–Rankl–OPG system: A multifaceted regulator of homeostasis, immunity, and cancer', *Medicina*, 59(10), pp. 1752.

Emanuele, M.A., Wezeman, F. and Emanuele, N.V., (2002) 'Alcohol's effects on female reproductive function' *Alcohol Research & Health*, 26(4), pp. 274-281.

Emons, J. *et al.* (2011) 'Mechanisms of growth plate maturation and epiphyseal fusion', *Hormone Research in Paediatrics*, 75(6), pp. 383–391.

Endl, E. and Gerdes, J. (2000) 'The Ki-67 protein: Fascinating forms and an unknown function', *Experimental Cell Research*, 257(2), pp. 231–237.

Fan, F. *et al.* (2024) 'Mechanisms of chondrocyte regulated cell death in osteoarthritis: Focus on Ros-triggered ferroptosis, parthanatos, and oxeiptosis', *Biochemical and Biophysical Research Communications*, 705, pp. 149733.

Fontes Marx, M. *et al.* (2021) 'Assessing intertemporal socioeconomic inequalities in alcohol consumption in South Africa', *Frontiers in Public Health*, 9, pp. 1-10.

Frankle, M. and Borrelli, J. (1990) 'The effects of testosterone propionate and methenolone enanthate on the healing of humeral osteotomies in the Wistar rat', *Journal of Investigative Surgery*, 3(2), pp. 93–113.

French, S.W. (2001) 'Intragastric ethanol infusion model for cellular and molecular studies of alcoholic liver disease', *Journal of Biomedical Science*, 8(1), pp. 20–27.

Föger-Samwald, U. *et al.* (2018) 'Bone effects of binge alcohol drinking using prepubescent pigs as a model', *Alcoholism: Clinical and Experimental Research*, 42(11), pp. 2123–2135.

Gebeyehu, E.T. and Srahbzu Biresaw, M. (2021) 'Alcohol use and its associated factors among adolescents aged 15–19 years at Governmental High Schools of Aksum town, Tigray, Ethiopia, 2019: A cross-sectional study', *Journal of Addiction*, 2021, pp. 1–8.

Gerjevic, L.N. *et al.* (2012) 'Alcohol activates TGF-beta but inhibits BMP receptor-mediated Smad signaling and smad4 binding to hepcidin promoter in the liver', *International Journal of Hepatology*, 2012, pp. 1–11.

Giesen, E.B.W. *et al.* (2001) 'Mechanical properties of cancellous bone in the human mandibular condyle are anisotropic', *Journal of Biomechanics*, 34(6), pp. 799–803.

Global status report on alcohol and health (2018) *World Health Organization*. Available at: https://www.who.int/publications/i/item/9789241565639 (Accessed: 05 February 2024).

Goldstein, D.B. (1986) 'Effect of alcohol on cellular membranes', *Annals of Emergency Medicine*, 15(9), pp. 1013–1018.

Gordon, G.G. *et al.* (1979) 'The effect of alcohol ingestion on hepatic aromatase activity and plasma steroid hormones in the rat', *Metabolism*, 28(1), pp. 20–24.

Gordon, G.G., Southren, A.L. and Lieber, C.S. (1978) 'The effects of alcoholic liver disease and alcohol ingestion on sex hormone levels', *Alcoholism: Clinical and Experimental Research*, 2(3), pp. 259–263.

Gowin, J.L. *et al.* (2021) 'Characteristics associated with high-intensity binge drinking in alcohol use disorder', *Frontiers in Psychology*, 12, pp. 1-11.

Griswold, M.G. *et al.* (2018) 'Alcohol use and burden for 195 countries and territories, 1990–2016: A systematic analysis for the global burden of disease study 2016', *The Lancet*, 392(10152), pp. 1015–1035.

Grube, J.W., (2004) 'Alcohol in the media: Drinking portrayals alcohol advertising, and alcohol consumption among youth. National Research Council Committee on Developing a Strategy to Reduce and Prevent Underage Drinking, and the Board on Children, Youth, and Families. Reducing Underage Drinking: A Collective Responsibility'.

Harrison-Findik, D.D. *et al.* (2006) 'Alcohol metabolism-mediated oxidative stress down-regulates hepcidin transcription and leads to increased duodenal iron transporter expression', *Journal of Biological Chemistry*, 281(32), pp. 22974–22982.

Hogan, H.A. *et al.* (1997) 'Alcohol consumption by young actively growing rats: A study of cortical bone histomorphometry and mechanical properties', *Alcoholism: Clinical and Experimental Research*, 21(5), pp. 809–816.

Hogan, H.A., Groves, J.A. and Sampson, H.W. (1999) 'Long-term alcohol consumption in the rat affects femur cross-sectional geometry and bone tissue material properties', *Alcoholism: Clinical and Experimental Research*, 23(11), pp. 1825–1833.

Iwaniec, U.T. and Turner, R.T. (2013) 'Intraperitoneal injection of ethanol results in drastic changes in bone metabolism not observed when ethanol is administered by oral Gavage', *Alcoholism: Clinical and Experimental Research*, 37(8), pp. 1271–1277.

Jeanblanc, J. *et al.* (2019) 'Animal models of binge drinking, current challenges to improve face validity', *Neuroscience and Biobehavioral Reviews*, 106, pp. 112–121.

Kalbfleisch, J.M. *et al.* (1963) 'Effects of ethanol administration on urinary excretion of magnesium and other electrolytes in alcoholic and normal subjects*', *Journal of Clinical Investigation*, 42(9), pp. 1471–1475.

Karp, S.J. *et al.* (2000) '*Indian hedgehog* coordinates endochondral bone growth and morphogenesis via *parathyroid hormone related-protein*-dependent and -independent pathways', *Development*, 127(3), pp. 543–548.

Kenkre, J. and Bassett, J. (2018) 'The bone remodelling cycle', *Annals of Clinical Biochemistry: International Journal of Laboratory Medicine*, 55(3), pp. 308–327.

Khosla, S., Oursler, M.J. and Monroe, D.G. (2012) 'Estrogen and the Skeleton', *Trends in Endocrinology and Metabolism*, 23(11), pp. 576–581.

Kodama, J. *et al.* (2022) 'The role of hypertrophic chondrocytes in regulation of the cartilage-to-bone transition in fracture healing', *Bone Reports*, 17, pp. 1-9.

Kumar, S. *et al.* (2022) 'Morphometric study of the nutrient foramen of the humerus in the population of bihar', *Cureus* 14(12), pp. 1-6.

Kvist, O. *et al.* (2020) 'A cross-sectional magnetic resonance imaging study of factors influencing growth plate closure in adolescents and young adults', *Acta Paediatrica*, 110(4), pp. 1249–1256.

Laitinen, K. *et al.* (1991) 'Transient hypoparathyroidism during acute alcohol intoxication', *New England Journal of Medicine*, 324(11), pp. 721–727.

Langdahl, B., Ferrari, S. and Dempster, D.W. (2016) 'Bone Modeling and remodeling: Potential as therapeutic targets for the treatment of osteoporosis', *Therapeutic Advances in Musculoskeletal Disease*, 8(6), pp. 225–235.

Lauing, K. *et al.* (2008) 'Binge alcohol treatment of adolescent rats followed by alcohol abstinence is associated with site-specific differences in bone loss and incomplete recovery of Bone Mass and strength', *Alcohol*, 42(8), pp. 649–656.

Letsela, L. *et al.* (2018) 'Alcohol availability, marketing, and sexual health risk amongst urban and rural youth in South Africa', *AIDS and Behavior*, 23(1), pp. 175–189.

Li, C. and Fennessy, P. (2021) 'The periosteum: A simple tissue with many faces, with special reference to the antler-lineage periostea', *Biology Direct*, 16(1), pp. 1-18.

Li, Y.C. *et al.* (1998) 'Normalization of mineral ion homeostasis by dietary means prevents hyperparathyroidism, rickets, and osteomalacia, but not alopecia in vitamin D receptor-ablated mice1', *Endocrinology*, 139(10), pp. 4391–4396.

Li, Z. and Pasteris, J.D. (2014) 'Chemistry of Bone Mineral, based on the hypermineralized rostrum of the beaked whale Mesoplodon densirostris', American Mineralogist, 99(4), pp. 645–653.

Lieber, C.S., Decarli, L.M. and Sorrell, M.F. (1989) 'Experimental methods of ethanol administration', *Hepatology*, 10(4), pp. 501–510.

Lill, H. and Josten, C. (2000) 'Proximal and distal humeral fractures in the elderly', *Der Orthopäde*, 29(4), pp. 327–341.

Liu, P. *et al.* (2022) 'Effects of mechanical stress stimulation on function and expression mechanism of osteoblasts', *Frontiers in Bioengineering and Biotechnology*, 10.

Lynnerup, N., Klaus, H.D. and Buikstra, J.E. (2019) 'Fundamentals of Human Bone and Dental Biology', in. Tempe, Arizona: Academic Press, pp. 35–58.

Mackie, E.J. *et al.* (2008) 'Endochondral ossification: How cartilage is converted into bone in the developing skeleton', *The International Journal of Biochemistry and Cell Biology*, 40(1), pp. 46–62.

Maeda, Y. *et al.* (2007) 'Indian hedgehog produced by postnatal chondrocytes is essential for maintaining a growth plate and trabecular bone', *Proceedings of the National Academy of Sciences*, 104(15), pp. 6382–6387.

Masuyama, R. *et al.* (2006) 'Vitamin D receptor in chondrocytes promotes osteoclastogenesis and regulates FGF23 production in osteoblasts', *Journal of Clinical Investigation*, 116(12), pp. 3150–3159.

Mathibe, M., Cele, L. and Modjadji, P. (2022) 'Alcohol use among high school learners in the peri-urban areas, South Africa: A Descriptive Study on accessibility, motivations and effects', *Children*, 9(9), pp. 1342.

Michimoto, I. *et al.* (2020) *Effects of the cancellous bone structure in the skull on ultrasonic wave propagation*, pp. 1-12.

Miralles-Flores, C. and Delgado-Baeza, E. (1992) 'Histomorphometric analysis of the epiphyseal growth plate in rats after prenatal alcohol exposure', *Journal of Orthopaedic Research*, 10(3), pp. 325–336.

Mmereki, B. *et al.* (2022) 'Risk factors for alcohol use among adolescents: The context of Township High Schools in Tshwane, South Africa', *Frontiers in Public Health*, 10, pp. 1-13.

Mohamed, A.M., (2008) 'An overview of bone cells and their regulating factors of differentiation'. *The Malaysian journal of medical sciences: MJMS,* 15(1), pp. 4-12.

Molina, P.E. and Nelson, S. (2018) 'Binge drinking's effects on the body', *Alcohol research: current reviews*, *39*(1), pp. 99.

Morojele, N.K. and Ramsoomar, L. (2016) 'Addressing adolescent alcohol use in South Africa', *South African Medical Journal*, 106(6), pp. 551-553.

Naude, C. *et al.* (2012) 'Vitamin D and calcium status in South African adolescents with Alcohol Use Disorders', *Nutrients*, 4(8), pp. 1076–1094.

Ndou, R. and Schepartz, L.A. (2015) 'Morphometric characteristics of the humerus and ulna in limbs bearing the supratrochlear aperture (STA)', *The Anatomical Record*, 299(2), pp. 220–233.

Nilsson, O. *et al.* (2005) 'Endocrine regulation of the Growth Plate', *Hormone Research in Paediatrics*, 64(4), pp. 157–165.

Noirrit-Esclassan, E. *et al.* (2021) 'Critical role of estrogens on bone homeostasis in both male and female: From physiology to medical implications', *International Journal of Molecular Sciences*, 22(4), pp. 1568.

Oftadeh, R. *et al.* (2015) 'Biomechanics and mechanobiology of Trabecular Bone: A Review', *Journal of Biomechanical Engineering*, 137(1), pp. 1–15.

Park, C.H. *et al.* (2001) 'Hepcidin, a urinary antimicrobial peptide synthesized in the liver', *Journal of Biological Chemistry*, 276(11), pp. 7806–7810.

Park, S.H. and Kim, D.J. (2020) 'Global and regional impacts of alcohol use on public health: Emphasis on alcohol policies', *Clinical and Molecular Hepatology*, 26(4), pp. 652–661.

Parry, C.D.H. *et al.* (2004) 'Trends in adolescent alcohol and other drug use: Findings from three sentinel sites in South Africa (1997–2001)', *Journal of Adolescence*, 27(4), pp. 429–440.

Penland, S. *et al.* (2001) 'Effects of nicotine on ethanol dependence and brain damage', *Alcohol*, 24(1), pp. 45–54.

Pigeon, C. *et al.* (2001) 'A new mouse liver-specific gene, encoding a protein homologous to human antimicrobial peptide hepcidin, is overexpressed during iron overload', *Journal of Biological Chemistry*, 276(11), pp. 7811–7819.

Pillemer, R. (2021) 'Anatomy and Function of the Elbow', Handbook of Upper Extremity Examination: A Practical Guide, *Springer Nature*, pp. 125-131.

Pillemer, R. (2022) 'Anatomy and Function of the Elbow', Handbook of Upper Extremity Examination: A Practical Guide, *Springer Nature*, pp. 125-131.

Prodinger, P.M. *et al.* (2018) 'Whole bone testing in small animals: Systematic characterization of the mechanical properties of different rodent bones available for rat fracture models', *European Journal of Medical Research*, 23(1), pp. 1-11.

Prof. Sakou, T. *et al.* (1999) 'Localization of smads, the TGF-β family intracellular signaling components during endochondral ossification', *Journal of Bone and Mineral Research*, 14(7), pp. 1145–1152.

Purohit, V. (2000) 'Can alcohol promote aromatization of androgens to estrogens? A Review', *Alcohol*, 22(3), pp. 123–127.

Rai, D.V. *et al.* (2008) 'Acute and chronic dose of alcohol affect the load carrying capacity of long bone in rats', *Journal of Biomechanics*, 41(1), pp. 20–24.

Reddy, S.P., *et al.* (2013) 'Umthente uhlaba usamila: The 3rd South African national youth risk behaviour survey 2011', pp. 1-164.

Ripley, T.L. and Stephens, D.N. (2011) 'Critical thoughts on current rodent models for evaluating potential treatments of alcohol addiction and withdrawal', *British Journal of Pharmacology*, 164(4), pp. 1335–1356.

Roothaer, X. (2019) 'Multi-scale study of the mechanical behaviour of bearing and bone-bearing bones: towards personalization of FE human models' (Doctoral dissertation, Université Polytechnique Hauts-de-France).

Roper, P.M. *et al.* (2016) 'Alcohol-related deficient fracture healing is associated with activation of FoxO transcription factors in mice', *Journal of Orthopaedic Research*, 34(12), pp. 2106–2115.

Ross, M.H. and Pawlina, W. (2010) *Histology: a text and atlas*. 6th edn. Philadelphia: Lippincott Williams & Wilkins.

Rundle, C.H. *et al.* (2014) 'Direct lentiviral-cyclooxygenase 2 application to the tendon-bone interface promotes osteointegration and enhances return of the pull-out tensile strength of the tendon graft in a rat model of biceps tenodesis', *PLoS ONE*, 9(5), pp. 1-10.

Sampson, H.W. (1997) 'Alcohol, osteoporosis, and bone regulating hormones', *Alcoholism: Clinical and Experimental Research*, 21(3), pp. 400–403.

Sampson, H.W. and Spears, H. (1999) 'Osteopenia due to chronic alcohol consumption by young actively growing rats is not completely reversible', *Alcoholism: Clinical and Experimental Research*, 23(2), pp. 324–327.

Sampson, H.W. *et al.* (1996) 'Alcohol consumption inhibits bone growth and development in young actively growing rats', *Alcoholism: Clinical and Experimental Research*, 20(8), pp. 1375–1384.

Sampson, H.W. *et al.* (1999) 'Binge drinking and bone metabolism in a young actively growing rat model', *Alcoholism: Clinical and Experimental Research*, 23(7), pp. 1228–1231.

Seeman, E. (2003) 'Periosteal bone formation — a neglected determinant of bone strength', *New England Journal of Medicine*, 349(4), pp. 320–323.

Sengupta, P. (2013) 'The laboratory rat: Relating its age with human's'. *International Journal of Preventive Medicine*, 4(6), pp. 624-630.

Shi, Y. and Massagué, J. (2003) 'Mechanisms of TGF-β signaling from cell membrane to the nucleus', *Cell*, 113(6), pp. 685–700.

Shim, K.S. (2015) 'Pubertal growth and epiphyseal fusion', *Annals of Pediatric Endocrinology and Metabolism*, 20(1), pp. 8-12.

Silva, B.C. and Bilezikian, J.P. (2015) 'Parathyroid hormone: Anabolic and catabolic actions on the skeleton', *Current Opinion in Pharmacology*, 22, pp. 41–50.

Silva, M.J. (2016) 'Understanding three point bending outcomes', Washington DC: Washington University, pp. 1-4.

Smith, L.A. and Foxcroft, D.R. (2009) 'The effect of alcohol advertising, marketing and portrayal on drinking behaviour in young people: Systematic review of prospective cohort studies', *BMC Public Health*, 9(1), pp. 1-11.

Snow, M.E. and Keiver, K. (2007) 'Prenatal ethanol exposure disrupts the histological stages of fetal bone development', *Bone*, 41(2), pp. 181–187.

Sontou, R. and Nchimi, A. (2023) 'Abduction arthro-fluoroscopy in adhesive capsulitis of the shoulder', *Journal of the Belgian Society of Radiology*, 107(1), pp. 1-4.

Stautz, K. *et al.* (2016) 'Impact of alcohol-promoting and alcohol-warning advertisements on alcohol consumption, affect, and implicit cognition in heavy-drinking young adults: A laboratory-based Randomized Controlled trial', *British Journal of Health Psychology*, 22(1), pp. 128–150.

Susan Smith, M. (2009) 'H. Maurice Goodman: Basic Medical Endocrinology, 4th EDN', *Endocrine*, 35(2), pp. 131.

Tsermpini, E.E., Plemenitaš Ilješ, A. and Dolžan, V. (2022) 'Alcohol-induced oxidative stress and the role of antioxidants in alcohol use disorder: A systematic review', *Antioxidants*, 11(7), pp. 1374.

Turner, R.T., Evans, G.L. and Wakley, G.K. (1994) 'Reduced chondroclast differentiation results in increased cancellous bone volume in estrogen-treated growing rats.', *Endocrinology*, 134(1), pp. 461–466.

Turner, R.T., Spelsberg, T.C. and Riggs, B.L. (1994) 'Skeletal effects of estrogen', *Endocrine Reviews*, 15(3), pp. 275–300.

Turner, R.T. *et al.* (1998) 'Effects of ethanol on gene expression in rat bone: Transient dose-dependent changes in mrna levels for matrix proteins, skeletal growth factors, and cytokines are followed by reductions in Bone Formation', *Alcoholism: Clinical and Experimental Research*, 22(7), pp. 1591–1599.

Turner, R.T. and Sibonga, J.D., (2001) 'Effects of alcohol use and estrogen on bone'. *Alcohol research & health*, *25*(4), pp. 276-281.

Turner, R.T., Rosen, C.J. and Iwaniec, U.T. (2010) 'Effects of alcohol on skeletal response to growth hormone in hypophysectomized rats', *Bone*, 46(3), pp. 806–812.

Turner, R.T., Doran, E., and Iwaniec, U.T. (2012). Detrimental effects of alcohol on bone growth. *Osteogenesis*, pp. 57-82.

Tóth, M.E., Vígh, L. and Sántha, M. (2014) 'Alcohol stress, membranes, and chaperones', *Cell Stress and Chaperones*, 19(3), pp. 299–309.

Van Audekercke, R. and Martens, M. (2018) 'Mechanical properties of cancellous bone', *Natural and Living Biomaterials*, pp. 89–98.

Weaver, C.M. (2002) 'Adolescence the period of dramatic bone growth', *Endocrine*, 17(1), pp. 43–48.

Weise, M. *et al.* (2001) 'Effects of estrogen on growth plate senescence and epiphyseal fusion', *Proceedings of the National Academy of Sciences*, 98(12), pp. 6871–6876.

Wezeman, F.H. *et al.* (1999) 'Chronic alcohol consumption during male rat adolescence impairs skeletal development through effects on osteoblast gene expression, bone mineral density, and bone strength', *Alcoholism: Clinical and Experimental Research*, 23(9), pp. 1534-1542.

Wezeman, F.H. *et al.* (2000) 'Alendronate administration and skeletal response during chronic alcohol intake in the adolescent male rat', *Journal of Bone and Mineral Research*, 15(10), pp. 2033–2041.

Wezeman, F.H. *et al.* (2007) 'Vitamin D and ibandronate prevent cancellous bone loss associated with binge alcohol treatment in male rats', *Bone*, 41(4), pp. 639–645.

White, A. (2020) 'Gender differences in the epidemiology of alcohol use and related harms in the United States', *Alcohol Research: Current Reviews*, 40(2), pp. 1-13.

Wilcox, G.B., Kacy Kim, K. and Schulz, H.M. (2012) 'Liquor advertising and consumption in the United States: 1971-2008', *International Journal of Advertising*, 31(4), pp. 819–834.

Wilsnack, R.W. *et al.* (2018) 'Gender differences in binge drinking: Prevalence, predictors, and consequences' *Alcohol research: current reviews*, 39(1), pp. 57-76.

Windahl, S.H. *et al.* (2013) 'Estrogen receptor-α in osteocytes is important for trabecular bone formation in male mice', *Proceedings of the National Academy of Sciences*, 110(6), pp. 2294–2299.

Windle, M. (2003) 'Alcohol use among adolescents and young adults', *Alcohol research and health,* 27(1), pp. 79-85.

Wozney, J.M. (1989) 'Bone morphogenetic proteins', *Progress in Growth Factor Research*, 1(4), pp. 267–280.

Wu, L. *et al.* (2003) 'SMAD4 as a transcription corepressor for estrogen receptor α', *Journal of Biological Chemistry*, 278(17), pp. 15192–15200.

Wu, M. *et al.* (2024) 'The roles and regulatory mechanisms of TGF-β and BMP signaling in bone and cartilage development, homeostasis and disease', *Cell Research*, 34(2), pp. 101–123.

Xu, X. and Chaloupka, F.J., (2011) 'The effects of prices on alcohol use and its consequences', *Alcohol Research and Health*, 34(2), pp. 236-245.

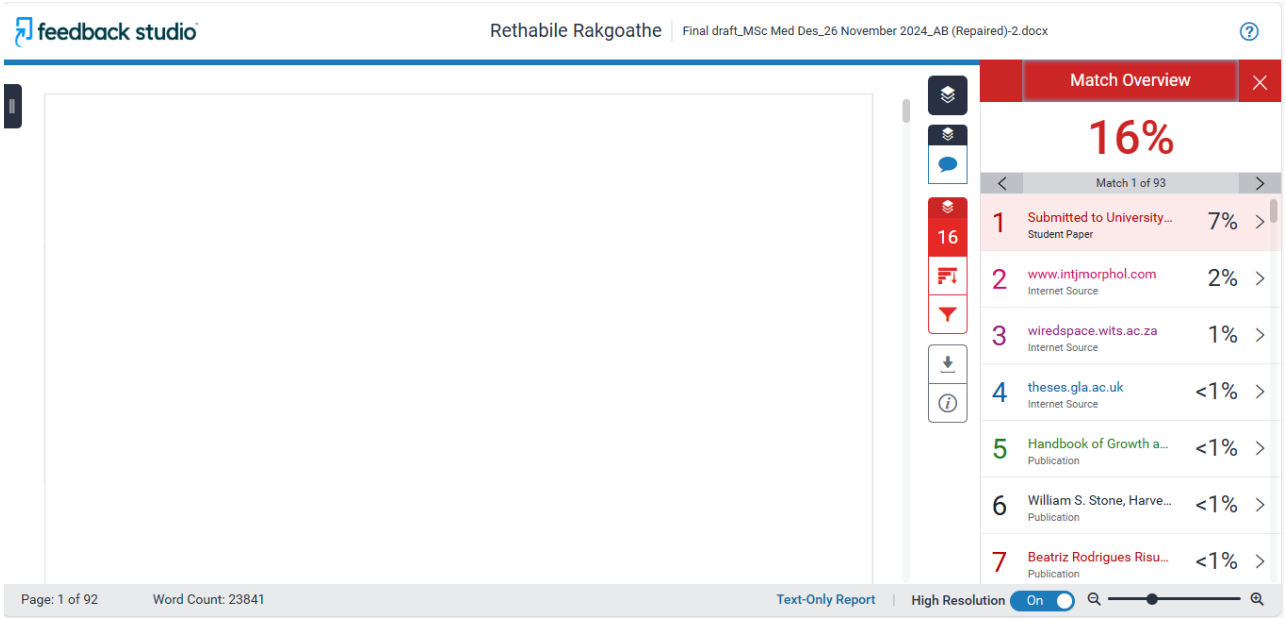
Zhang, A. *et al.* (2021) 'The role of ki67 in evaluating neoadjuvant endocrine therapy of hormone receptor-positive breast cancer', *Frontiers in Endocrinology*, 12, pp. 1-7.

Zhang, J. *et al.* (2005) 'SMAD4 is required for the normal organization of the cartilage growth plate', *Developmental Biology*, 284(2), pp. 311–322.

Zoetis, T. *et al.* (2003) 'Species comparison of postnatal bone growth and development', *Birth Defects Research Part B: Developmental and Reproductive Toxicology*, 68(2), pp. 86–110.

Appendix:

Appendix 1: Turnitin report and Similarity index letter



UNIVERSITY OF THE WITWATERSRAND, JOHANNESBURG | FACULTY OF HEALTH SCIENCES | Anatomical Sciences

To whom it may concern,

Student Rethabile Rakgoathe's MSc thesis with the title: "*The impact of binge alcohol consumption on the developing humerus of adolescent Sprague Dawley rats",* has a similarity index of 16%. This is due to the fact that numerous students have researched topics in a similar field, and Turnitin has picked up similarities in her materials and methods, which are very standardized. We are thus happy with her similarity index, as there are limited changes that she could make in this area.

Kind regards,





Dr Akaashni Bhika
14/01/2025

Dr Illke Malungo
14/01/2025

School of Anatomical Sciences
7 York Rd, Parktown, 2193, South Africa, Private Bag 3, WITS 2050
Tel: +27 11 717 2405/2305 | www.wits.ac.za/anatomicalsciences/

Appendix 2: Ethical Clearance certificate

AREC 2022 AM&E

Please note that only electronically completed applications will be accepted.

UNIVERSITY OF THE WITWATERSRAND, JOHANNESBURG
ANIMAL RESEARCH ETHICS COMMITTEE

registered as Animal Research Ethics Committee (AREC) with the South African National Health Research Ethics Council (NHREC) of the National Dept. of Health, ***reg. no. AREC -101210-002***

APPLICATION FOR ADAPTATIONS OR MODIFICATIONS AND EXTENSIONS TO EXPERIMENTS

a. Principal Investigator (PI) Name: Dr Akaashni Bhika

b. School / Department: School of Anatomical Sciences.

c. Email Address: akaashni.bhika@wits.ac.za

d. Experiment to be modified / extended **AREC NO**

Original AREC Clearance Certificate Number	**2020**	**11**	**02/C**
Clearance Certificate Expiry date	**4 Mar 2023**		
Number of previous AM&Es			4

e. Project Title:

The effect of binge-alcohol consumption on the development of adolescent Sprague Dawley rat mandibles

		No.	**Species**
f.	Number and species of animals originally approved	72	*Sprague-Dawley rats*
g.	Number of additional animals previously approved on AM&Es	8	*Sprague-Dawley rats*
i.	Number of animals used and currently involved in the study to date	80	**Animal study has been completed**

j. Specific details of Adaptations/Modification/ Extension:

May I please apply for an extension to continue collecting data on the harvested bones, as my PhD has not yet been completed (All work at WARF has been completed and data is currently being collected).

k. Motivation for Adaptations/Modification/ Extension:

Data on the harvested bones is still being collected. This data is necessary for me to complete my PhD.

Date: 26/01/2023 PI Signature:



UNIVERSITY OF THE WITWATERSRAND, JOHANNESBURG

AREC 2022 AM&E

RECOMMENDATIONS:

Approval for the extension of ethics until **31 March 2025**. Please note any further extension must be applied to prior to the revised expiry date.

Date:27 January 2023 Signature:



Deputy Chair, AREC

Appendix 3: Reagents Used:

- 3-Aminoprpyl triethoxy silane (CAS NO. 919-30-2 , Sigma Aldrich., Germany)
- Acetic acid (glacial) (Saarchem 1021020LC., RSA)
- Acetone (SAAR1022040LC, Merck Chemicals (Pty.) Ltd., RSA)
- Chloroform (CAS NO. 67-66-3, Associated Chemical Enterprise, RSA
- Chlorate hydrate (CAS NO. 302-17-0, Sigma Aldrich, Germany)
- Citric Acid (19150 41, Riedel-de Haën AG, Germany)
- Disodium hydrogen orthophosphate anhydrate (CAS NO. 7558-79-4, Associated Chemicals Enterprise, RSA)
- Entellen (HX 088232, Merck RGA, Germany)
- Eosin yellowish (SAAR2186000DC, Merck Chemicals (Pty.) Ltd., RSA)
- Erythrosin (Saarchem)
- Ethylenediamine tetraacetic acid (CAS NO. 60-00-4, Associated Chemicals Enterprise, RSA)
- Formaldehyde (Associated Chemicals Enterprise., RSA)
- Hydrochloric acid 1% (HCl) (Associated Chemicals Enterprise., RSA)
- Hydrogen peroxide (Catalog. 1037024, Merck (Pty.) Ltd., RSA)
- Magnesium Sulphate (CAS NO. 231-298-2, Associated Chemical Enterprises, RSA)
- Mayer's solution (SAAR2422001LC, Merck Chemicals (Pty.) Ltd., RSA)
- Potassium Alum (CAS NO. 7784-24-9, Associated Chemical Enterprises, RSA)
- Potassium chloride (CAS NO. 7447-40-7, Associated Chemicals Enterprise, RSA)
- Potassium dihydrogen orthophosphate (CAS NO. 7778-77-0, Associated Chemicals Enterprise, RSA)
- Rabbit Specific HPR/DAB (ABC) detection IHC kit (Ab64256 Abcam)
- Sodium chloride (CAS NO. 7647-14-5, Associated Chemical Enterprise, RSA)
- Sodium hydrogen carbonate (CAS NO. 582-28-20, Saarchem (Pty.) Ltd., RSA)
- Sodium hydroxide (CAS NO. 1310-73-2, Associated Chemicals Enterprise, RSA)
- Sodium Iodate (The lab Depot, Inc)
- Strept-Avidin HRP (Ab64269 Abcam)
- Tri Sodium citrate (di-hydrate) (CAS NO. 6132-04-3, Associated Chemicals Enterprise, RSA)
- Tween 20 (616-45-00KF, Saarchem, RSA)
- Wax (Merck Chemicals (Pty.) Ltd., RSA)
- Xylene (CAS NO. 108-38-3, Associated Chemicals Enterprise, , RSA)

Appendix 4: Equipment used:

- Automatic tissue processor (Shandon, Citadel 1000)
- Cassettes (Merck Chemicals (Pty.) Ltd, RSA)
- Digital Vernier caliper (series 530)
- Embedding table (Miles Scientific, serial number 31602-554)
- ESCO Laboratory fume hood (Model: EFA-4UDW-8. SN: 2011-60070)
- Incubator (Model-508-2U, Labcon shaker)
- Microfocus computed tomography (µCT) X-ray machine (NIKON XTH 225/320 LC)
- Microscope (axioscope) (Model Axiocom HRC, identification number 105- 041756)
- Microscope Slides (3000F-02-1009, Lasec, RSA)
- Microtome (Leica RM 2125RM, Fabr. Nr. 07390329)
- Moulds (Merck Chemicals (Pty.) Ltd., RSA)
- Water bath (Model number 416, SN: SE 9455)
- Weighing scales: (Model- KERN EW600-2M, Germany) (Model- SARTORIUS GMBH, Germany)

Appendix 5: Software used:

- Fiji Image-J 1.53 T software
- IBM SPSS version 29.0.2.0 (20)
- Microsoft Excel 2023 (Microsoft Corporation)
- Volume Graphics Studio (VGS) software Axiovision (AXIOVs) version 4.7.2.0

Appendix 6: Appendix 6: Calculation of the Alcohol (Alcohol 20%) dosage administered.

Dose = 3g/kg body weight

Alcohol density = 0.789g/ml

We need to calculate volume

•

$Volume = massdensity$

$= 3g 0.789gml/$

= 3.8ml

•Therefore, the dosage = 3.8ml/kg body weight

Appendix 7: Calculation of the Maltose dextrin (isocaloric) dosage administered.

- Calculate the caloric equivalent of the alcohol dosage administered.

1g of alcohol = 7kCal

3g of alcohol = 21kCal

20 % Alcohol was used, therefore; 3g.20% alcohol = 20% of 21kCal

= **4.2kCal** to match

1g Maltose dextrin = **3.89kCal** =$4.2kCal 3.89kCal/x\ 1g\ Maltose\ dextrin$
= 1.08g Maltose dextrin for caloric equivalence

Dissolve 1.08g Maltose dextrin in 4ml distilled water to make 27% Maltose dextrin solution.
1.08g MD in 4ml distilled water = 4.2kCal/4ml

= 1.05kCal/ml

- Calculate Maltose dextrin isocaloric dosage in **ml/kg** body weight

=$4.2kCalkg 1.05kCalmlx 1$

= **4ml/kg** body weight

Appendix 8: Preparation of 10% Neutral Buffered Formalin (1L):

1. Measure 100ml of Formaldehyde (37% - 40%)
2. Add 900ml of distilled Water
3. Add 0.35g of Sodium dihydrogen phosphate (anhydrous)
4. Add 0.65g of Disodium hydrogen phosphate (anhydrous)

Appendix 9: Measuring trabecular morphometry of humerus using VG studio software:

1. File
2. Import (import stack)
3. Directory > drive (location of your files)> folder> select folder < Click next
4. Specify resolution (copy all axis on xTekCT file)
5. Histogram
6. Calibration (enlarge size)
7. Define background
8. Define material
9. Contrast
10. Separation (if you have 2 specimens in a single file)
11. Object < register object < simple registration < align it (to your desired orientation) < finish.
12. Make sure the view is on "Scene"
13. Extraction 8.1 Select< rectangle shape < Extract ROI
14. Once extracted, make sure the background is uniform

    For trabecular morphometry:
15. Surface determination
16. Move the background far left
17. Move the material far right
18. Adjust the Iso-value so that you perfectly outline the bone material (spaces in the trabeculae should be outlined perfectly to enhance accuracy)
19. Click Finish
20. Get reading on the Morphometry "page"
21. Select Advanced (Classic)
22. Right click the ROI on the right tab
23. Select properties on the pop-up tab
24. Click "update" (all parameters)
25. Obtain reading on the Morphometry "page"

Appendix 10: EDTA solution (14%) for bone decalcification:

1. Dissolve 14g of EDTA in 100ml distilled water (pH 7.4).
2. Add ±16g of Sodium Hydroxide pellets to help dissolve EDTA
3. pH the EDTA solution to 7.
4. Incubate the tissue in 14% EDTA for 7 days at 45°C with continuous but gentle agitation.
5. After every 3-4 days, replace the 14% EDTA with a fresh supply.
6. Regularly check if specimens are pliable to ensure complete decalcification.
7. When the tissue is pliable (complete decalcification), wash specimens in running tap water for 10 mins.

Appendix 11: Silane coated slides:

3% APES solution:

1. Measure out 194ml of Acetone
2. Add 6ml of 3-Aminopropytriethoxysilane (APES)

Coating of slides:

1. Immerse slides in 3% APES solution for 30mins
2. Rinse the slides (10 dips) in acetone
3. Repeat step 2
4. Rinse the slides (10 dips) in distilled water
5. Leave to dry overnight at 37°C

Store slides at 4°C for ± 2 months

Appendix 12: Tissue processing using the Thermo Scientific Citadel 2000 automatic tissue processor:

1. 10% neutral buffered formalin (4hrs)
2. 70% alcohol (1hr)
3. 95% alcohol (2hrs)
4. 95% alcohol (2hrs)
5. 95% alcohol (2hrs)
6. 95% alcohol (2hrs)
7. 100% alcohol (2hrs)
8. 100% alcohol (2hrs)
9. 100% alcohol (2hrs)
10. Chloroform (2hrs)
11. Chloroform (2hrs)
12. Wax (2hrs)
13. Wax (2hrs)

Tissue embedding using paraffin wax:

1. Switch on the tissue embedding station to heat both the wax and metal moulds and to freeze the cooling section.
2. Once melted, carefully pour some wax into the metal mould. Use forceps to hold the mould in place as it is heated.
3. Use forceps to delicately place the specimen inside the metal mould. Ensure that the surface of the bone (proximal and distal ends) faces the bottom of the mould.
4. Pour more wax to embed the tissue being careful not to pour directly on the specimen to avoid any displacement.
5. Cover the mould with a plastic cassette. The cassette should be labelled to verify specimen type and number.
6. Carefully place the metal mould on the cooling section of the embedding station
7. Leave the mould on the ice for 30min to let the wax block solidify.

Appendix 13: Haematoxylin and Eosin staining (solutions):

Haematoxylin solution (1000ml):

1. Haematoxylin 1g
2. Aluminium potassium sulphate (Potassium alum) 50g
3. Sodium iodate 0.2g
4. Citric acid 1g
5. Chlorate hydrate 50g
6. Allow haematoxylin, aluminium potassium sulphate and sodium iodate to dissolve overnight.
7. Add chloral hydrate and citric acid.
8. Boil solution for 5 minutes and then allow to cool.

Eosin solution (1000ml):

1. Measure 1000mls of distilled water
2. Add 8g of stock eosin.
3. Add 2g of erythron.
4. Stir using a magnetic stirrer until fully dissolved.

Scott's tap water solution (100ml):

1. Sodium hydrogen carbonate 2g
2. Magnesium sulphate 20g
3. Distilled water 1000ml

Dissolve the salts in the water and store in stock solutions at room temperature.

Haematoxylin and Eosin Staining for Bone

Hydration

1. Deparaffinize sections in xylene for 10 minutes
2. Deparaffinize sections in xylene for 10 minutes
3. Immerse in 100% alcohol for 1 minute
4. Immerse in 100% alcohol for 1 minute
5. Immerse in 95% alcohol for 1 minute
6. Immerse in 70% alcohol for 1 minute
7. Wash in water for 1 minute

Nuclear Staining

1. Stain with Meyer's haematoxylin for 20 minutes
2. Wash in running tap water for 5 minutes
3. Differentiate in 1% acid alcohol (2 dips)
4. Wash in running tap water for 5 minutes
5. Stain with Meyer's haematoxylin for 5 minutes
6. Wash in running tap water for 5 minutes
7. Stain in Scott's tap water for 5 minutes
8. Wash in running tap water for 10 minutes

Cytoplasm Staining

1. Stain in Eosin for 2 minutes
2. Rinse in tap water

Dehydration and Mounting

1. Immerse in 70% alcohol for 1 minute
2. Immerse in 95% alcohol for 1 minute
3. Immerse in 100% alcohol for 1 minute x 2
4. Immerse in xylene for 10 minutes x 2
5. Mount in Entellan

Results

Nuclei: Blue-black

Muscle fibres: deep pink red

Cytoplasm: Varying shades of pink

Appendix 14: Immunohistochemistry:

Solutions to be made:

1. **10mM Sodium citrate buffer pH 6 + 0.05% Tween 20:**

Tri Sodium citrate (di-hydrate)	2.9g
Distilled Water	1000ml

   Mix to dissolve sodium citrate and adjust pH to 6 with 1M HCl

2. **1M Phosphate buffer pH 7.4:**

NaCl	16g
Na_2HPO_4	3.5g
KCl	0.4g
KH_2PO_4	0.4g
Distilled Water	2000ml

3. **DAB Working solution:**

   In a bijou bottle:

   1mg DAB

   2ml Tris HCl (50 Drops substrate & 1 Drop Chromogen)

   In a separate tube add: (Solution B)

   29µl Cold distilled water

   1µl hydrogen peroxide

   Add 20µl of Solution B to DAB working solution

Immunohistochemistry (IHC) Kit method:

Day 1:

1. Deparaffinize sections in xylene for 10 minutes
2. Deparaffinize sections in xylene for 10 minutes
3. Immerse in 100% alcohol for 1 minute
4. Immerse in 100% alcohol for 1 minute
5. Immerse in 95% alcohol for 1 minute
6. Immerse in 70% alcohol for 1 minute
7. Wash in running water for 5 minutes
8. Place sections in Citrate buffer pH 6 at 60°C in a water bath for 2 hours for antigen retrieval
9. Allow to cool at room temperature for 20 minutes
10. Rinse in PBS for 5 minutes
11. Rinse in PBS for 5 minutes
12. Rinse in PBS for 5 minutes
13. Block endogenous peroxidase with 1% H2O2 in methanol for 30 minutes
14. Rinse in PBS for 5 minutes
15. Rinse in PBS for 5 minutes
16. Rinse in PBS for 5 minutes
17. Incubate with Protein Block for 20 minutes
18. Incubate with Primary Antibody (Ki67) at 4°C overnight

Day 2:

1. Allow sections to reach room temperature for 30 minutes (minimum)
2. Wash in PBS for 5 minutes
3. Wash in PBS for 5 minutes
4. Wash in PBS for 5 minutes
5. Wash in PBS for 5 minutes
6. Incubate with biotinylated secondary antibody for 10 minutes
7. Wash in PBS for 5 minutes
8. Wash in PBS for 5 minutes
9. Wash in PBS for 5 minutes

10. Wash in PBS for 5 minutes
11. Incubate with Strept Avidin HRP for 10 minutes
12. Wash in PBS for 5 minutes
13. Wash in PBS for 5 minutes
14. Wash in PBS for 5 minutes
15. Wash in PBS for 5 minutes
16. Incubate with DAB solution for 30 minutes
17. Rinse in running tap water for 5 minutes
18. Immerse in 70% alcohol for 1 minute
19. Immerse in 95% alcohol for 1 minute
20. Immerse in 100% alcohol for 1 minute
21. Immerse in 100% alcohol for 1 minute
22. Immerse in xylene for 10 minutes
23. Immerse in xylene for 10 minutes

Results:

Nuclei of proliferating cells: orange/brown

Nuclei of non-proliferating cells: clear

Cytoplasm: Clear